INS and GPS integration

Casper Ebbesen Schultz

Kgs. Lyngby 2006
IMM-M.Sc-2006-60

Technical University of Denmark
Informatics and Mathematical Modelling
Building 321, DK-2800 Lyngby, Denmark
Phone +45 45253351, Fax +45 45882673
reception@imm.dtu.dk
www.imm.dtu.dk

ISSN 1601-233X

Abstract

The Global Positioning System (GPS) has been commonly used throughout the last couple of decades as a navigation system, that provide both military and private users, with accurate information about there position. The system has been implemented in a long range of different things such as car and boat navigation systems, cell phones and high precise geodetic surveying equipment. However as the GPS signal is an electromagnetic signal, it can be blocked by mountains, dense forests and areas with high buildings. Hence GPS will not provide a continuous and reliable position all the time. On the other hand Inertial Navigation System (INS) is an autonomous, all-weather navigation system that can provide continuous information of position, velocity and attitude regardless of the surroundings. However the performance of INS deteriorates with time due to the inertial sensors performance.

The integration of GPS and INS is an efficient way of limit the INS derived position, velocity and attitude errors by using the GPS measurements as update to the position and velocity whenever it is available. Further the INS can be used to identify and correct GPS carrier phase cycle slips. This dissertation therefore analyzes different integration methods of GPS and INS in order to increase the position, velocity and attitude accuracy especially during and after GPS data outage.

The results from the analysis showed that the use of integrated INS and GPS solutions during partial or complete GPS data outage can provide a significant improvement compared to the stand alone use of the INS system. Further the time to fix ambiguity after a GPS data outage can be minimized significantly using INS and different integration methods.

I would like to thank my supervisor Anna B.O. Jensen for support and guidance during this dissertation and other geomatics related projects throughout the last couple of years of study. Further a thank to all other members of the geoinformatic section at the department of Informatics and Mathematical

Modelling (IMM), Technical University of Denmark (DTU) that have helped with other projects and courses during my university studies.

A special thank will also go to the people from the PLAN group at the Department of Geomatics Engineering, University of Calgary, Canada that I spend 3½ month together with during the winter and spring of 2006. Especially Dr. Gérard Lachapelle that made it possible for me to get a temporary place in the PLAN group and use there SAINT™ software, Dr. Mark Petovello that helped during processing with the SAINT™ software and Saurabh Godha that provided me with a data set for processing and helped my answering all kinds of question related to the data set. Last but not least a great thank to all the people from CCIT room 309. We had some great time together and I hope we will see each other again in the future.

This dissertation has been done in both Canada (at University of Calgary, Alberta) and Denmark (Technical University of Denmark, Lyngby) from medio January 2006 to medio July 2006, with one month of planned vacation in between. The work load corresponds to 30 ECTS-points.

14th of July 2006
Lyngby, Denmark

Casper Ebbesen Schultz, s001897

Danish summary

Global Positioning System (GPS) har været vidt brugt de sidste par årtier som et navigations system, der let kan give information om ens position. Det er blevet implementeret i en lang række forskellige systemer f.eks. bil og båd navigation, mobiltelefoner og høj præcisions geodætisk landmåling. Men da GPS signalet er et elektromagnetisk signal vil det kunne blokeres a bjerge, tæt skov og områder med høje bygninger. GPS vil derfor ikke altid kunne give vedvarende og pålidelige positioner. Inertial Navigation System (INS) vil derimod i alt slags vejr og uanset sine omgivelser give konstante information om ens position, hastighed og orientering. Problemet med INS er dog at fejl meget hurtigt forøges pga. sensorernes fejl og måden navigations parametrene beregnes på.

Integration af henholdsvis GPS og INS er en effektiv måde at begrænse fejl fra INS på positionen, hastigheden og orienteringen, da den så ofte som muligt bruger GPS positionen til at opdatere positionen og hastigheden. Endvidere kan INS informationerne bruges til at identificere cycle slip i GPS målingerne. Dette projekt omhandler derfor en analyse af forskellige måder til integration af GPS og INS data i håbet om at øge præcisionen på ens position, hastighed og orientering specielt i situationer hvor der er eller har været afbrydelse af GPS signalet.

Resultatet fra analysen viser at brugen af integrerede INS og GPS data kan forbedre nøjagtigheden af positionen, hastigheden og orienteringen betydeligt sammenlignet med de tilsvarende ved udelukkende at bruge INS data. Endvidere kan tiden fra et GPS udfalds ophør og til ambiguiteten er bestemt som heltal mindskes signifikant ved at bruge forskellige integrations metoder.

Jeg vil takke min vejleder Anna B.O. Jensen for støtte og vejledning gennem dette og andre geoinformatik relaterede projekter gennem de sidste par års studier. Endvidere vil jeg også takke alle fra geoinformatik sektionen på instituttet Informatik og Matematisk Modellering (IMM), Danmarks Tekniske

Universitet (DTU) der har hjulpet med andre projekter eller undervist i kurser indenfor geoinformatikken gennem mine studieår.

En speciel tak skal også gå til folk fra PLAN gruppen ved Department of Geomatics Engineering, University of Calgary, Canada som jeg brugte 3½ måned sammen med i vinteren og foråret 2006. Speciel tak til Dr. Gérard Lachapelle som gav mig muligheden for at få en midlertidig plads i hans PLAN gruppe og bruge deres SAINT™ program, Dr. Mark Petovello der hjalp mig ved kørslerne med SAINT™ og Saurabh Godha der skaffede mig data til kørslerne og hjalp med besvarelser af alverdens spørgsmål i relation hertil. Sidst men ikke mindst vil jeg gerne takke alle dem fra rum 309 på CCIT. Vi havde en fantastisk tid sammen og jeg håber vi vil få genset hinanden i fremtiden.

Dette projekt er blevet til i både Canada (på University of Calgary, Alberta) og Danmark (Danmarks Tekniske Universitet, Lyngby) fra medio januar 2006 til medio juli 2006, med en måneds ferie indimellem. Projektet svarer til en arbejdsmængde på 30 ECTS-point.

Rapporten er udarbejdet på engelsk.

Table of Contents

Notation

Symbols

Depending on the literature and research area the same variable can use different symbols and the same symbol can mean different things! In order to ease the readers understanding of this dissertation the most relevant symbols used are listed below sorted by their alphabet.

Starting with a small Latin letter

a	… acceleration vector
	… semi-major axis of the reference ellipsoid
b_x	… accelerometer bias in the x^{th} axis
c	… speed of light in vacuum
d_x	… gyroscope bias in the x^{th} axis
d_{orb}	… orbital error
d_{ion}	… ionospheric error
d_{trop}	… tropospheric error
d_{noise}	… noise error (e.g. multipath)
dt	… satellite clock error
dT	… receiver clock error
e	… linear eccentricity of the reference ellipsoid
f	… specific force vector
g	… gravitation vector
h	… ellipsoidal height
p	… code pseudorange measurement
q	… quaternion
r	… position vector

s_x … accelerometer scale factor in the x^{th} axis

t … time

v … velocity vector

v_f … velocity due to specific force

w … process noise

x … state vector

z … observation vector

Starting with a capital Latin letter

F … dynamic matrix

G … noise coefficient matrix

… shaping matrix

I … identity matrix

H … design matrix

K … Kalman gain matrix

M … radius of curvature in meridian

N … radius of curvature in prime vertical

… carrier phase ambiguity

$N(a,b)$ … normal distribution with mean "a" and standard deviation "b"

P … error covariance matrix

R … radius of the Earth

… measurement noise covariance matrix

R_a … rotation matrix about a^{th} axis (R_1 = X-axis, R_2 = Y-axis and R_3 = Z-axis)

R_b^a … rotation matrix from frame "b" to frame "a"

Starting with a small Greek letter

α … wander angle / reciprocal of the correlation time

β … reciprocal of the correlation time

γ … normal gravity vector

$\delta(\bullet)$ … error of quantity $(\bullet)$

ε … misalignment error

η … pitch

… measurement noise

λ … geodetic longitude

… wavelength

ν … innovation sequence

… orthogonal vector to the specific force vector and the angular rate vector

ξ … roll

ρ … geometric (true) range between receiver and satellite

σ … standard deviation

τ … correlation time

φ … geodetic latitude

ψ … azimuth

ω_e … Earth rotation rate (= 15.04 deg/hr = $7.29 \cdot 10^{-5}$ rad/s)

ω_{bc}^{a} … angular velocity vector of frame “c”, relative to frame “b” and expressed in frame “a”

Starting with a capital Greek letter

$\Delta(\bullet)$ … increment of quantity $(\bullet)$

… difference between quantity $(\bullet)$

$\Delta\theta_{bc}^{a}$ … angular increments vector of frame “c”, relative to frame “b” and expressed in frame “a”

ϕ … carrier phase measurement

… transition matrix

$\dot{\phi}$ … Doppler range rate measurement

Ω_{bc}^{a} … skew symmetric form of the angular velocity vector ω_{bc}^{a}

Other signs

ℓ … lever arm

∇ … outlier or blunder vector

$(\bullet)^a$ … quantity $(\bullet)$ in frame "a"

$(\bullet)_n$ … quantity $(\bullet)$ at the n^{th} epoch

$(\bullet)^*$ … nominal value of quantity $(\bullet)$

$\overline{(\bullet)}$ … average of quantity $(\bullet)$

$\dot{(\bullet)}$ … time derivative quantity $(\bullet)$

$\hat{(\bullet)}$ … estimated (computed) values quantity $(\bullet)$

$\tilde{(\bullet)}$ … measurement of quantity $(\bullet)$

$(\bullet)^-$ … quantity $(\bullet)$ before update

$(\bullet)^+$ … quantity $(\bullet)$ after update

$(\bullet)(t)$ … quantity $(\bullet)$ as a function of time

$\frac{\partial}{\partial(\bullet)}$ … partial derivative with respect to $(\bullet)$

Acronyms

The acronyms are fully described the first time they are mentioned from chapter 2 and forward. The following times only the acronyms are used. The following acronyms listed in alphabetical order are used in this dissertation.

AS … Anti-Spoofing

C/A … Coarse-Acquisition

CUPT … Coordinate Update

DGPS … Differential GPS

DoD … Department of Defense

DOP … Dilution Of Precision

DR … Dead Reckoning

ECEF	… Earth-Centered-Earth-Fixed
EKF	… Extended Kalman Filter
GPS	… Global Positioning System
GNSS	… Global Navigation Satellite System
IMU	… Inertial Measurement Unit
INS	… Inertial Navigation System
ISA	… Inertial Sensor Assembly
LAMBDA	… Least Square Ambiguity Decorrelation Adjustment
LKF	… Linearized Kalman Filter
MEMS	… Micro Electro-Mechanical System
PDOP	… Position Dilution Of Precision
PRN	… Pseudo-Random Noise
RMS	… Root Mean Square
SA	… Selective Availability
SHU	… Small Heading Uncertainty
TEC	… Total Electron Content
UTC	… Universal Coordinated Time
WGS84	… World Geodetic System 1984
WL	… Widelane
ZUPT	… Zero Velocity Update

1 Introduction

Integrated INS and GPS systems are not a new phenomenon, but have been used the last couple of decade to a wide span of different systems. Ship, aircraft and submarine navigations systems are just some of the most common applications (Petovello, 2003). Most of the applications will strive for the following two characteristics:

1. Continuous and reliable navigation determination (most often position, velocity and attitude)
2. Acceptable accuracy level and the possibility to keep the accuracy over time

INS can provide the continuous and reliable navigation determination, but their errors are increasing over time due to the integration algorithm they use. In stead GPS can be used as an aiding system in order to minimize the errors over time by updating the position and velocity as often as possible (Godha, 2006). The main reason for integrating INS and GPS is therefore done in order to get a system that can achieve both of the above mentioned characteristics.

The accuracy needed can vary a lot between each application. Navigation systems for autonomous car and aircraft may require sub-metre level accuracy while others like car navigation systems only needs 10-30 meter of accuracy in order to achieve its goal (Godha, 2006). Most of the accuracy is determined by the equipment used in the INS and GPS. Especially the performance from different inertial sensors can vary a lot and low-cost INS systems may result in errors up to many hundreds of meters (and even thousands of meters!) in just a few minutes of stand alone mode (El-Sheimy, 2006).

This dissertation investigates the basics behind INS and GPS integration, and implements it in a software program. Results from the software program are then used to determine the performance of different integration techniques and the impact of changing some specific user parameters.

1.1 Dissertation objectives

The main objective of this dissertation was to analyze the performance of integrated INS and GPS data. In order to integrate the INS and GPS data a program was developed in MATLAB. The program turned out to have a hidden and unfound bug in the mechanization equations, so in order to perform the analysis another program was used.

In order to understand the analysis of integrated INS and GPS data a comprehensive description of the two systems underlying theory is described first. The emphasis is put on the INS where GPS mainly is described in order to understand the limitations of the system and the reason for the integrating. This is followed by a description of different estimation techniques that are used in different integration methods.

The work on the self-made MATLAB program is shown despite the bug and the main objectives behind it are described. Finally a data analysis is performed followed by a conclusion for the entire dissertation.

Summarized the main objectives of this dissertation are therefore:

1. To describe the underlying theory behind INS and GPS in order to emphasize the limitations of both systems and understand why integration can be important.
2. To describe different estimation techniques and there use in different INS and GPS integration methods.
3. To develop a software program that can perform the integration between INS and GPS
4. To analyze the performance of position, velocity and attitude during complete GPS data outages where only the INS solution are available and during partial GPS data outages where less than four satellites are available.
5. To analyze the improvements of the time used to determine the fixed ambiguities after GPS data outages with use of different integration methods.

1.2 Dissertation outline

This dissertation contains 9 chapters and 1 appendix and is organized as described below.

Chapter 1: Presents the objectives for this dissertation and give a short description of the outline.

Chapter 2: Describes INS in detail with the emphasize put on the algorithm steps and the advantage/limitations of using INS.

Chapter 3: Gives a short description of GPS in order to understand it limitations.

Chapter 4: Presents different estimation techniques for dynamic and non-linear systems that are part of the theory behind integration of INS and GPS.

Chapter 5: Describes the different integration methods that can be used in integration of INS and GPS. The lever arm effect and the time synchronization problem are briefly mentioned.

Chapter 6: Presents the objectives of the software program and gives an idea of the implementation technique that was used.

Chapter 7: Presents various analyzed output data from SAINT™ in order to determine the performance of different integration methods. The changes in specific user variables are analyzed too.

Chapter 8: Summarize the objectives of this dissertation.

Chapter 9: List the references used in this dissertation.

Appendix A: Show information about the ambiguities not shown in the dissertation.

2 Inertial navigation

This chapter describes the principles of inertial navigation. First the basics about modeling motion in space are described. This leads to Newton's 1st and 2nd law that are essential in understanding inertial navigation. Second an introduction to inertial sensors is given followed by the relevant equations that relate the output from inertial measurements to useful information like position, velocity and attitude. Finally the limitations of Inertial Navigation Systems (INS) are investigated in order to understand why INS sometimes is integrated with other navigation systems and not just operating in stand-alone mode.

2.1 Motion in space

In most aspects of navigation systems, describing the motion of an object is the main purpose. The general motion of an object in space is typically described by three position and three orientation parameters. Assuming a rigid body, the motion of any point in the body can be illustrated by two vectors with 3 components as shown in figure 2.1 (El-Sheimy, 2006).

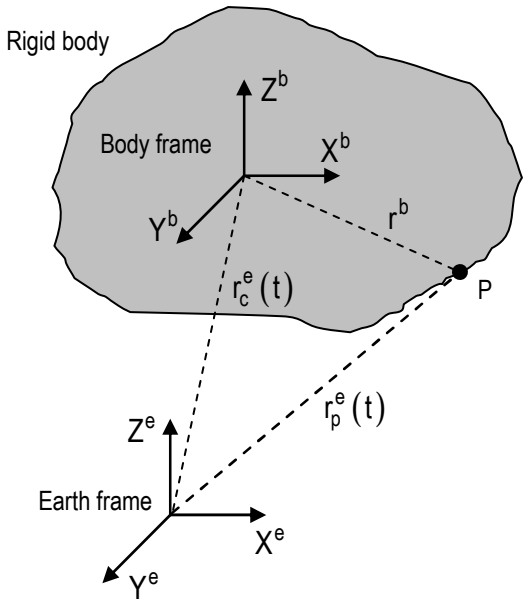

Figure 2.1: Rigid body motion in space described by two vectors

The first vector, $r_c^e(t)$ describe the time variable position vector, of the rigid body's center of mass in the Earth-Centered-Earth-Fixed coordinate frame (ECEF, further shorten to just Earth frame). The second vector, r^b describe the rotation of the rigid body as a vector between the center of mass and the point, P in the body. To describe the motion of P a time variable rotation matrix from body frame to Earth frame, $R_b^e(t)$ is needed. The motion of P can therefore be described as the time variable position vector, $r_p^e(t)$ given as (El-Sheimy, 2006)

$$r_p^e(t) = r_c^r(t) + R_b^e(t) \cdot r^b \qquad \text{(Eq. 2.1)}$$

The position vector and rotation matrix as functions of time are called navigation states variables. Normally the velocity vector as function of time is included in the navigation states variables, but as the velocity is related to the position through differentiation it is only required to determine six parameters to describe the general motion of an object in space. This is discussed further in chapter 2.5 about the equation of motion.

Determining of all the navigation states variables require a system that can measure six independent quantities. A navigation sensor measure one or more of the quantities. A system that combine a number of navigation sensors so all six parameters can be measured is called a navigation system. IINS is such a system, as its output contains all necessary information to georeference a moving object at all times.

Navigation systems can be classified by two main concepts for obtaining the navigations state variables. INS uses the "dead reckoning" (DR) system that determines the current position from knowledge of a previous position and the measurement of the direction of motion and the distance traveled. Another way is by using "position fixing" that determines the current position from knowledge of known reference points. Position fixing is used e.g. by Global Positioning System (GPS) / Global Navigation Satellite System (GNSS). These systems are further discussed in chapter 3.

2.2 Principle of inertial sensors

The principle of inertial navigation is highly related to Newton's 1st and 2nd law that in short term concludes that "changes in motion are caused by outside forces" (1st law) and "acceleration is proportional and in the same direction as the resultant force" (2nd law) (El-Sheimy, 2006). Taking an object in space the 1st law tells that keeping an eye on all outside forces on the object, knowledge of whether the object is moving or not and whether it is continuing its uniform motion or changes its course are known. The 2nd law tells that measuring the resultant forces that affect the object knowledge of the objects acceleration is known. And from the acceleration it is easy to determine the velocity and displacement by integration once and twice respectively. Similarity can be found for angular rotation so e.g. angular velocity is related to angular rotation by integration. (El-Sheimy, 2006)

A detector that measure acceleration therefore plays a crucial role in inertial navigation. Together with a detector that measure angular velocity is it possible to determine the navigation state variables by combining these detectors of each. Such detectors are called accelerometers and gyroscopes (together they are called inertial sensors) and will be discussed below here. Another crucial thing is the importance of relating the measurement of acceleration and angular velocity to some known coordinates. Hence an inertial frame of reference is needed. This reference frame is fixed in space (most often fixed by the stars) and is considered to be non-rotating and non-accelerating relative to far-off galaxies. Any motion of an object or the surrounding medium (e.g. the Earth) can therefore be described in relation to this reference frame. This is discussed in chapter 2.3.3.

2.2.1 Accelerometers

An accelerometer is generally a proof mass that is kept away from a case by a pair of springs. In zero acceleration the proof mass will be in a specific calibrated position called the equilibrium position. Each accelerometer has a sensitive axis indicated by the arrow in figure 2.2. Any acceleration along this axis will cause the proof mass to be displaced along the axis. The movement of the proof mass is

proportional to the force of acceleration (Newton's 2nd law), so measuring the amount of displacement from the equilibrium position will give the acceleration along the axis.

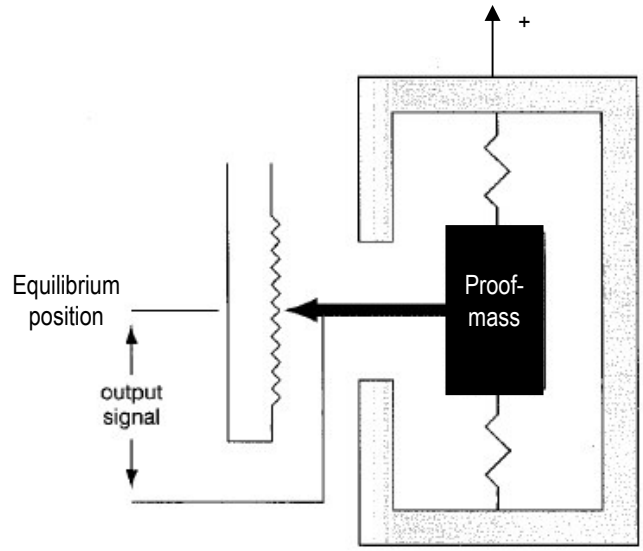

Figure 2.2: Basic model of an accelerometer in zero acceleration (partly from Weston et al., 2000)

An accelerometer measure all types of acceleration irrespective of it comes from gravitational acceleration or from e.g. vehicle acceleration. For an accelerometer in a gravitational field (with acceleration in the negative direction of the sensitive axis) the proof mass will be displayed in positive of the sensitive axis like on figure 2.3. But as this is also true for e.g. vehicle acceleration in the positive direction, the output of gravitation and vehicle acceleration are opposite in sign.

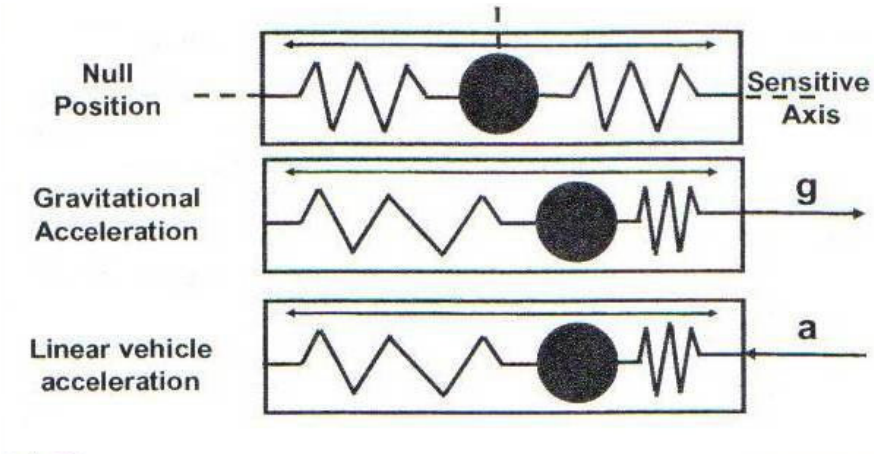

Figure 2.3: The "difference" between gravitational acceleration and vehicle acceleration (El-Sheimy, 2006)

For use in inertial navigation the acceleration with respect to the inertial frame is needed. The output from an accelerometer measure (vehicle) acceleration minus gravitational acceleration, called specific force. As the acceleration with respect to the inertial frame is the same as the vehicle acceleration the formula for calculating this is simply:

$$a = f - g \qquad \text{(Eq. 2.2)}$$

Where a is the acceleration with respect to the inertial frame (vehicle acceleration), f is the acceleration produced by non-gravitational forces (specific force) and g is the acceleration due to gravity.

Different types of accelerometers have been invented since the first accelerometer, originally known as the Atwood machine, was invented by the English physicist George Atwood (1746-1807) in 1783. There are generally to main types known as the “open loop” and “closed loop” accelerometer. The difference is in the way they measure the specific force. Open loop measures the proof mass displacement from the equilibrium position (like in figure 2.2) while closed loop measures the force needed to keep the proof mass in its equilibrium position.

Today accelerometers are used for a wide variety of scientific and engineering systems. Some of the smallest accelerometers are part of the micro electro-mechanical system (MEMS) and can be less than one mm in each dimension and weigh less than one gram. Such small devices are used in e.g. airbags systems and therefore need to be very cheap to manufacture. More expensive accelerometers are used for high performance purposes like in INS. Output from accelerometer is normally expressed in [m/s^2] for specific force and in [m/s] for velocity increment vector due to specific force.

2.2.2 Gyroscopes

A gyroscope (often shorten to just a gyro) is a sensor that measure or maintain angular rotation. It works with respect to the principle of conservation of angular momentum and was first invented in 1852 by the French physicist Leon Foucault (1819-1868). The first gyroscopes were purely mechanical and worked with a rotor (spinning mass) that could spin about one axis. The rotor was mounted in two gimbals (rings) that further were mounted to a base. This gave a total of 3 degrees of freedom to the rotor and made it possible to keep its orientation while the base was rotated in any direction. Due to friction between the moving parts, errors in keeping the orientation will always occur. Figure 2.4 show a picture of a traditional mechanical gyroscope.

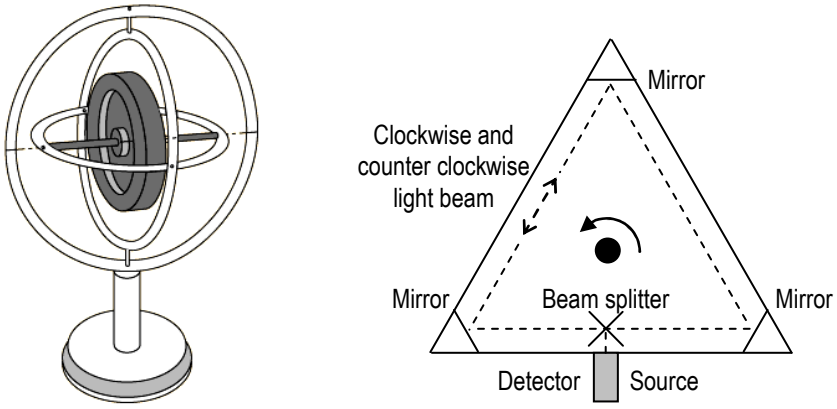

Figure 2.4: Basic model of a mechanical gyroscope and a ring laser gyroscope (partly from Weston et al. 2000)

Optical gyroscopes (ring laser gyroscopes and fiber-optic gyroscopes) without moving parts have been invented to prevent friction errors and to minimize the size and cost of gyroscopes. The precision of the optical gyroscopes is still not at the same high level as the best mechanical gyroscopes but they can already replace a lot of the common applications for gyroscopes. The principle of the fiber-optic gyroscopes is to measure the phase shift between two light beams send at the same time from a common source. They both go through the same closed fiber optic cable but respectively clockwise and counter clockwise. If the fiber-optic gyroscope is giving a rotation the two light beams will reach the source (that now works as s detector) at different times due to increase/decrease of the beams trajectory. It results in a phase shift that can be converted to angular velocity.

Similar the ring laser gyro sends two laser beams against three or four mirrors to measure the differences at arrival time. Smaller gyroscopes are possible through MEMS based technology but the precision is still to far from both the optical and the mechanical gyroscopes in order too be used in high performance INS. Like accelerometers the output from gyroscopes needs to be measured with respect to an inertial frame. The output is normally expressed in [deg/hr or rad/s] for angular velocity or [deg or rad] for angular rotation.

2.2.3 Sensor errors

Measurement from both accelerometers and gyroscopes are subject to errors. The following errors are often subject to much confusion but are necessary to understand in order to evaluate performance of inertial sensors:

Bias is the output that has no correlation with the input. It can be asymmetric for positive and negative inputs and have an instability that is given by random variation if the output is computed over a specified sample interval. The instability of bias is also called bias drift. Bias is normally expressed in [m/s^2 or mg] for accelerometers and [deg/hr or rad/s] for gyroscopes.

Scale factor is the ratio of change in the measured output to the intended input. It will normally be expressed in [ppm] (parts per million) for both accelerometers and gyroscopes. Like for bias scale factor can be asymmetric for positive and negative inputs. **Sensitivity** is related to scale factor and is some times mixed up by manufactories. The difference is that sensitivity relates to a secondary input e.g. change in temperature while scale factor relates to an intended primary input.

Both bias (not bias drift) and scale factor can be determined by calibration. The most accurately calibration methods is through use of e.g. three-axial turn tables, six-position static test and angle rate tests. They generally determine the bias and scale factor by comparing known parameters e.g. the earth gravity or well known angels to measured output.

Repeatability is the closeness of repeated measurements of the same input variable under the same conditions. It is expressed in [m/s^2 or mg] for accelerometers and [deg/hr or rad/s] for gyroscopes.

Resolution is the minimum value of input greater than the noise level that gives and output above a certain level. It is expressed in [m/s^2 or mg] for accelerometers and [deg/hr or rad/s] for gyroscopes.

Stability is the ability to give the same output while measuring a constant input. It is measured over a single run. It is expressed in [m/s^2 or mg] for accelerometers and [deg/hr or rad/s] for gyroscopes.

Noise is the random or stochastic error that occurs in output and can only be removed by stochastic models. It is most often modeled as a 1^{st} order Gauss Markov process. In evaluating accelerometers and gyroscopes the term random walk is often used to describe a stochastic process with zero mean and standard deviation that grows as the square root of time. The most common random walk process is the angle random walk that for gyroscopes describe the error that build up with time due to white noise in angular rate. Angle random walk is normally expressed in [deg/$\sqrt{h}$]. Parameters for the stochastic models can be estimated through long time collection of static data for both accelerometers and gyroscopes.

Accelerometers and gyroscopes are often mounted in groups of 3 sensors that make up an orthogonal triad. Errors in **orthogonality** (also called **axes misalignment**) will result in errors of measurement as two sensors measure part of the same input. Axes misalignment can be calibrated or modeled in the INS error equation. Different calibration model will not be discussed further here, but the reader can see examples of different calibration techniques in e.g. (Shin, 2001 and Shin et al., 2002)

Table 2.1 in chapter 2.3.2 gives an idea of the sensor errors for accelerometers and gyroscopes used in different inertial systems.

2.2.4 Importance of sensor calibration

The importance of sensor calibration can easily be seen when considering an orthogonal triad of accelerometers that are tilted with respect to the normal of the Earth gravitational field. The tilt can be observed by the accelerometers as two accelerometers measure part of the Earth gravitation. If the accelerometers at the same time have a bias error will it be impossible to distinguish between the tilt and the bias. The accelerometer bias will therefore determine the accuracy with which we can determine the tilt of the triad. Bias error in accelerometer and gyroscopes will introduce error in velocity and position according to the following (El-Sheimy, 2006).

Error from accelerometer bias:

$$\delta v = b_a \cdot t$$
$$\delta r = \frac{1}{2} \cdot b_a \cdot t^2$$

Error from gyroscope bias:

$$\delta v = \frac{1}{2} \cdot b_g \cdot g \cdot t^2$$
$$\delta r = \frac{1}{6} \cdot b_g \cdot g \cdot t^3$$

(Eq. 2.3)

Where δv and δr are the velocity and position errors.

2.2.5 Sensor measurements

The raw accelerometer and gyroscope measurement can be expressed in different ways according to the type of sensor output. Most low-cost sensors output specific force, $\tilde{f}^b$ and angular rate, $\tilde{\omega}_{ib}^b$ which can be scaled to obtain velocity increments due to specific force, $\Delta\tilde{v}_f^b$ and angular increments, $\Delta\tilde{\theta}_{ib}^b$. The inputs to the computational process (see chapter 2.5) are the increments but the scaling can be performed as followed if specific force and angular rate is outputted instead (Shin, 2005 p. 29).

Velocity increment from specific force:

$$\Delta\tilde{v}_{f,k}^b = \int_{t_{k-1}}^{t_k} \tilde{f}^b dt$$

Angular increments from angular rate:

$$\Delta\tilde{\theta}_{ib,k}^b = \int_{t_{k-1}}^{t_k} \tilde{\omega}_{ib}^b dt$$

(Eq. 2.4)

Where $\Delta t = t_{k+1} - t_k$ is the time increment between two successive measurements at t_k and t_{k+1}.

2.3 Principle of inertial navigation

Given an accelerometer that measure specific force, it is possible to provide estimates of velocity and position through successive integrations. If the velocity and position are used in navigation it is required that it can be related to a specific reference frame. Furthermore a continuous orientation of the accelerometers is needed with respect to the reference frame. This is done through gyroscopes that provide a measure of the attitude with respect to the same reference frame. A typical inertial navigation system (INS) is therefore made up of three accelerometers and three gyroscopes mounted in an orthogonal triad in order to determine the position and the orientation of the INS.

2.3.1 Gimbaled and strapdown systems

Inertial sensors can be implemented in two different ways to build up an INS. The first (and original) is as a stable platform arrangement where the accelerometers are mounted on a gimbaled platform. The platform is kept aligned to a specific navigation frame by mechanical gyroscopes and every output from the accelerometers can therefore be integrated to provide velocity and position in the specific navigation frame. Stable platform system (or gimbaled system) are relatively big and weighs a lot due to the mechanical arrangement of gyroscopes.

The second is as a strapdown arrangement where both the accelerometers and gyroscopes are mounted directly on e.g. a vehicle. As the accelerometers aren't kept aligned to a specific navigation platform the acceleration measurement needs to be transformed into the navigation frame. The rotation rates measured by the gyroscopes are therefore used to update the transformation parameters from the frame they are mounted to (often call body-frame) and to a specific navigation frame.

This dissertation will only describe the use of strapdown arrangement as this is the most common system for general navigation application due to weight, cost and flexibility. The accuracy of the stable platform arrangement is still better than the strapdown arrangement but due to there gimbal platform

they are less immune to shock and vibration forces. They are therefore mainly used for high precision system for e.g. military submarine.

2.3.2 Classification of inertial systems

Inertial systems can be classified into three different types that is cause to some confusion. The simplest type is the inertial sensor assembly (ISA) which output raw data from the inertial sensors like acceleration and angular velocity. If the output from the ISA is compensated for errors e.g. bias and scale factor it is called an inertial measurement unit (IMU). Finally if the output from the IMU is processed through navigation algorithms that determine position, velocity and attitude the strapdown arrangement is called an inertial navigation system (INS). An INS will also be able to give the raw but compensated data from the IMU as output. The difference between are also shown in figure 2.5.

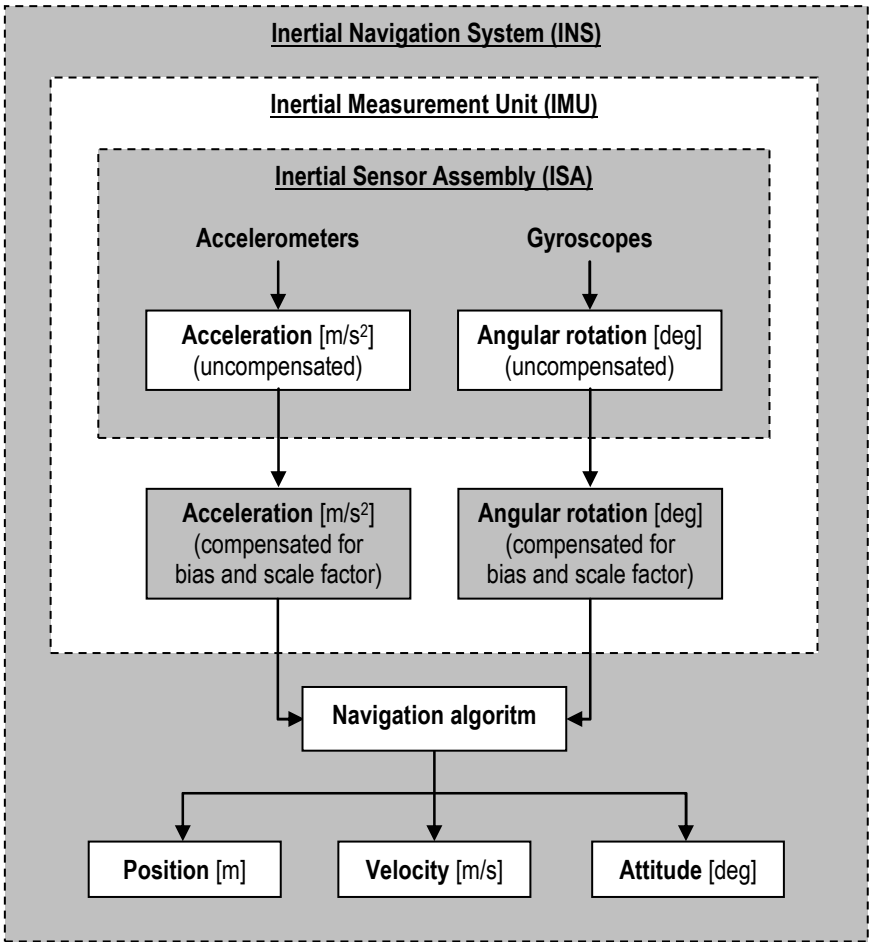

Figure 2.5: Difference between ISA, IMU and INS

In addition to the three different types is it common to classify the inertial systems according to there accuracy. Table 2.1 compares some general specifications for different grades of inertial systems and gives an idea of the approximately prices of the different systems. The grayscale cells refer to specifications for four specific IMUs with the abbreviations: # 1 refers to a Honeywell LRF-111, # 2 refers to a Litton LTN90-100, # 3 refers to a Honeywell HG1700 AG11 and # 4 refers to a low-cost MEMS Crista IMU.

Performance \ Grade		**Strategic**	**Navigation**	**Tactical**	**Automotive**	**Consumer**
Stand alone position errors		< 30 (m/hr)	1 – 4 (km/hr)	20 – 40 (km/hr)	2 (km/min)	3 (km/min)
Gyroscope	Bias [deg/hr]	0.0001	0.005 – 0.010	0.1 – 10	> 100	360
		-	0.003 #1 / 0.01 #2	1 #3	1040 #4	-
	Scale factor [ppm]	-	5 – 50	200 – 500	N/A	-
		-	1 #1 / 5 #2	150 #3	10000 #4	-
	Noise (ARW) [deg/hr/√Hz]	-	0.002 – 0.005	0.2 – 0.5	N/A	-
		-	-	0.125 #3	227 #4	-
Accelerometer	Bias [µg]	1	50 – 500	500 – 1000	> 1200	2400
		-	250 #1 / 500 #2	1000 #3	2500 #4	-
	Scale factor [ppm]	-	10 – 20	400 – 1000	N/A	-
		-	50 #1 / 50 #2	300 #3	10000 #4	-
	Noise [µg /hr/√Hz]	-	5 – 10	200 – 400	N/A	-
		-	-	216 #3	370 #4	-
Approximately price		> 200000 US $	50000 – 200000 US $	10000 – 50000 US $	< 10000 US $	< 100 US $
Applications		Ballistics missiles and submarines	Navigation and high precision georeferencing	INS/GPS and short time system (weapons)	Short time systems	Airbags

Table 2.1: Specifications for different grades of IMU (Shin, 2001, El-Sheimy, 2006, Petovello, 2003 and Godha, 2006)

2.3.3 Reference frames

A couple of reference frames has already been mentioned. The different reference frames used in this dissertation is described below.

Inertial frame (i -frame) has its origin at the centre of the Earth and axes which are non-rotating with respect to fixed stars. Its axes points towards the following:

- Z^i-axis parallel to the spin axis of the Earth
- X^i-axis pointing towards the mean vernal equinox
- Y^i-axis orthogonal to the X and Z axes to complete a right-handed frame

The inertial frame of reference is only referred to as the inertial frame in this dissertation.

Earth-centered-earth-fixed frame (e-frame) is also having its origin at the centre of the Earth but its axes are rotating together with the earth. Its axes points towards the following:

- Z^e-axis parallel to the spin axis of the Earth
- X^e-axis pointing towards the mean meridian of Greenwich
- Y^e-axis orthogonal to the X and Z axes to complete a right-handed frame

The earth-centered-earth-fixed frame is for simplifying purpose referred to as the earth frame in this dissertation.

Body frame (b-frame) has its origin at the centre of the IMU and axes that are assumed to be aligned with the vehicle frame. Its axes points towards the following:

- X^b-axis pointing towards the right of the vehicle
- Y^b-axis pointing towards the front of the vehicle
- Z^b-axis orthogonal to the X and Y axes to complete a right-handed frame

Rotation about the axes is used to describe pitch, roll and heading of the vehicle.

Navigation frame (n-frame) is also having its origin at the centre of the IMU but its axes are rotating together with the Earth. Its axes points towards the following:

- X^n-axis pointing towards the ellipsoid east (geodetic east)
- Y^n-axis pointing towards the ellipsoid north (geodetic north)
- Z^n-axis pointing upward along the ellipsoid normal

This specific navigation frame is also known as the east-north-up (ENU) system. Other way of orienting the axes is as the north-east-down (NED) system. The navigation frame is sometimes referred to as the

local level frame (l-frame) and further is a **Horizontal frame** (h-frame) mentioned once and is simply a navigation frame where the X and Y-axis is pointing in arbitrary positions.

Wander azimuth frame (w-frame) is also a navigation frame with origin at the centre of the IMU but mainly used at high latitudes (around the poles) in stead of the navigation frame mentioned above. As the Y^n-axis always points towards geodetic north an east-west movement close to the poles will result in large rotation rates about the Z^n-axis. In order to avoid this the Y-axis in the wander frame maintains its original alignment according to an initial point P. Any east-west movement will therefore only result in a rotation about the Z^w-axis while there will be an azimuth angle between geodetic north and the Y^w-axis. (El-Sheimy, 2006 and Titterton et al. 2004) Its axes therefore points towards the following:

- Z^w-axis pointing upward along the ellipsoid normal
- Y^w-axis rotated in the level plane by the wander angle, α from north towards west
- X^w-axis orthogonal to the Y and Z axes to complete a right-handed frame

Figure 2.6 show the different frames and the rotation names about the body frame axes.

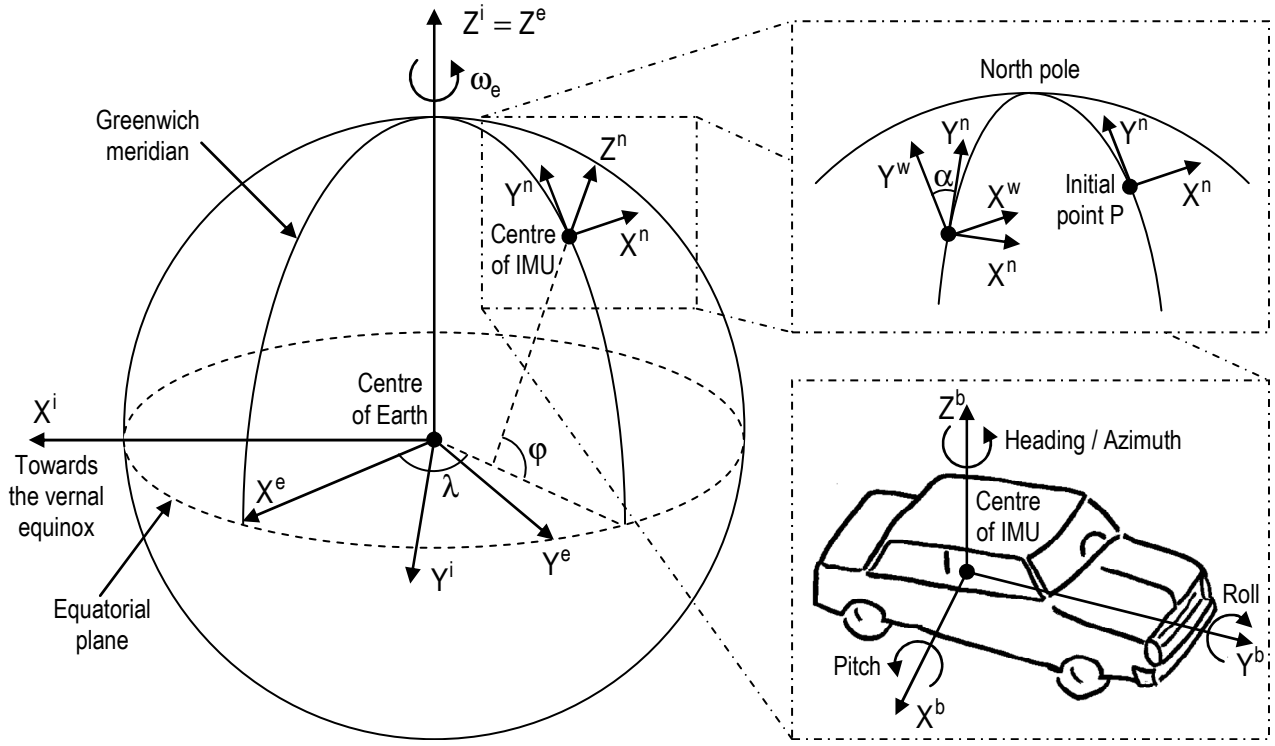

Figure 2.6: The different frames (inertial, Earth, navigation, body and wander azimuth)

2.4 Alignment of strapdown systems

One of the most important things about strapdown systems is the need to establish a relationship between the body frame and the navigation frame. This is needed because the body frame can take any arbitrary orientation. The relationship is usually established through a stationary alignment process before any kinematic measurement is done. In some situation is it necessary to do the alignment in kinematic mode and the system then needs external data e.g. velocity information from GPS.

The above mentioned relationship is normally expressed through a rotation matrix R_b^n. From the gyroscope measurement, R_b^n is updated and used to transform the accelerometer measurements to the navigation frame. Two times integration of the transformed acceleration will result in a position difference of the IMU with respect to the navigation frame. As the initial position is known through e.g. GPS a new position can be calculated. At the same time both velocity and attitude can be updated for the new position. Chapter 2.5 describes this process called the mechanization equation.

The principle of the stationary initial alignment consists of two steps, accelerometer leveling and gyroscope compassing. Accelerometer leveling refers to obtaining the roll and pitch (see figure 2.7) using the accelerometer outputs (with knowledge of the normal gravity vector) and gyroscope compassing refers to obtaining the heading information using the gyroscope outputs (with knowledge of the Earth rotation rate). As the gyroscopes must be able to observe the Earth rotation of only $7.292115 \cdot 10^{-5}$ rad/s or 15.041067 deg/hr only (high end) tactical grade, navigation grade or strategic grade IMUs can perform the gyroscope compassing alignment. Low end tactical grade, automotive grade and consumer grade IMUs need external heading data as there bias and noise levels are smaller than the Earth rotation rate (se table 2.1). Alignment can be classified as either coarse or fine alignment depending on the amount of attitude error it has to deal with.

The following chapter describes different alignment methods done in static mode with both coarse and fine alignment. Alignment in kinematic (in-motion) mode is shortly mentioned.

2.4.1 Coarse alignment

Coarse alignment in static mode is typically done through accelerometer leveling and gyroscope compassing or alternatively through an analytical methods. If an orthogonal accelerometer triad is mis-leveled in the navigation frame the pitch and roll in static mode (while only acting force is the Earth gravity) (El-Sheimy, 2006) can be illustrated according to figure 2.7.

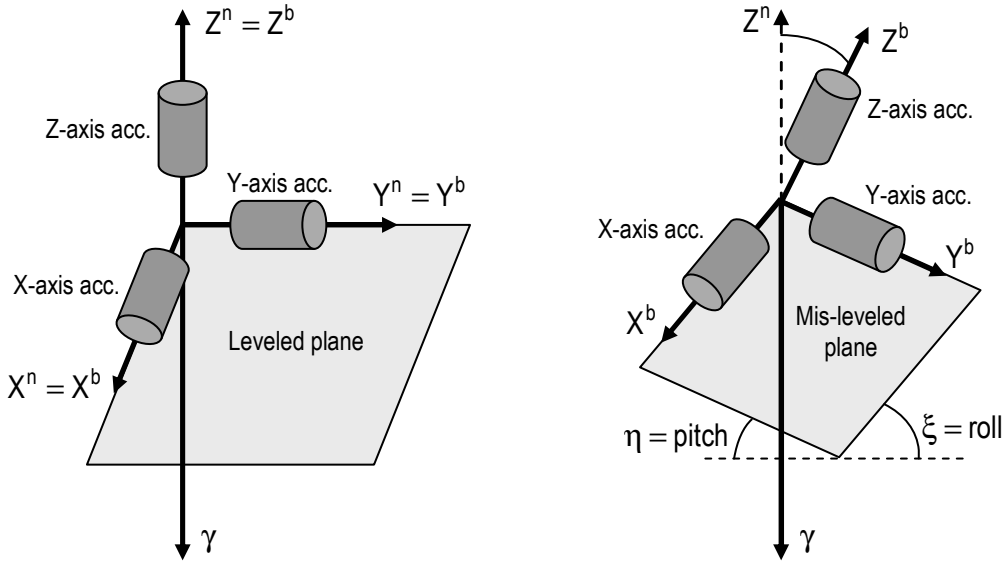

Figure 2.7: Stationary leveled and mis-leveled accelerometer triad

As shown in figure 2.7 a mis-leveling of the X-axis accelerometer result in a roll angle, ξ while a mis-leveling of the Y-axis accelerometer result in a pitch angle, η. As the normal gravity vector, γ is known the roll and pitch can be estimated as functions of the average raw velocity increments, $\overline{\Delta v^b_{x,y}}$ during the entire alignment process (Petovello, 2003 and Godha, 2006)

$$\xi = -\sin^{-1}\left(\frac{\overline{\Delta v^b_x}}{\gamma \cdot \overline{\Delta t}}\right) \qquad \eta = \sin^{-1}\left(\frac{\overline{\Delta v^b_y}}{\gamma \cdot \overline{\Delta t}}\right) \qquad \text{(Eq. 2.5)}$$

Where $\overline{\Delta t}$ is the average time increment between two successive measurements and γ is the normal gravity in $\gamma^n = (0 \quad 0 \quad \gamma)^T$. γ is given as a function of the geodetic latitude φ and the ellipsoidal

height h (Shin, 2001, El-Sheimy, 2006 and Godha, 2006). The reader should be aware that many other gravity functions can be applied instead. See e.g. (Wei et al. 1990).

$$\gamma = a_1 \cdot (1 + a_2 \cdot \sin^2 \varphi + a_3 \cdot \sin^4 \varphi) + (a_4 + a_5 \cdot \sin^2 \varphi) \cdot h + a_6 \cdot h^2 \qquad \text{(Eq. 2.6)}$$

Where $a_1 - a_6$ are constants given as

a_1	= 9.7803267715	a_4	= -0.0000030876910891
a_2	= 0.0052790414	a_5	= 0.0000000043977311
a_3	= 0.0000232718	a_6	= 0.0000000000007211

When roll and pitch are estimated the average raw angular increments, $\Delta\overline{\theta_{ib}^{b}}$ can be rotated into the horizontal frame and the heading can be estimated as (Petovello, 2003 and Godha, 2006).

$$\Delta\overline{\theta_{ib}^{h}} = R_1(-\eta) \cdot R_2(-\xi) \cdot \Delta\overline{\theta_{ib}^{b}} \qquad \text{(Eq. 2.7)}$$

$$\psi = -\tan^{-1}\left(\frac{\left(\Delta\overline{\theta_{ib}^{h}}\right)_X}{\left(\Delta\overline{\theta_{ib}^{h}}\right)_Y}\right) \qquad \text{(Eq. 2.8)}$$

The rotation matrix between body frame and navigation frame, can then be found as (Godha, 2006)

$$R_b^n = R_3(\psi) \cdot R_1(-\eta) \cdot R_2(-\xi) \qquad \text{(Eq. 2.9)}$$

Where R_1, R_2 and R_3 are rotation matrices about the X, Y and Z-axis as given in e.g. (Jekeli, 2000).

For low-cost IMUs there bias and noise exceeds the Earth rotation rate so equation 2.7 and 2.8 is not possible. In order to estimate the heading an external heading source (e.g. a magnetic compass or a magnetometer) is needed. This is not further discussed here but the reader can see more in (Godha, 2006).

In stead of using the above mentioned methods an analytical method for the coarse alignment can be used. The method uses a defined vector, ν that is orthogonal to both the specific force vector, f and the angular rate vector, ω_{ib} as (Britting, 1971).

$$\nu = f \times \omega_{ib} \qquad \text{(Eq. 2.10)}$$

The derivation of the rotation matrix, R_b^n between body frame and navigation frame is derived in (Shin, 2001) but only the one step solution is only mentioned here. It uses the average raw specific force measurement, $\overline{f^b}$ and the average raw angular rate measurement, $\overline{\omega_{ib}^b}$ during the entire alignment process, together with the normal gravity vector, γ (from Eq. 2.6), the Earth rotation rate, ω_e and the geodetic latitude φ as follows.

$$R_b^n = \begin{pmatrix} \frac{-\tan\varphi}{\gamma} & \frac{1}{\omega_e \cdot \cos\varphi} & 0 \\ 0 & 0 & \frac{-1}{\gamma \cdot \omega_e \cdot \cos\varphi} \\ \frac{-1}{\gamma} & 0 & 0 \end{pmatrix} \cdot \begin{pmatrix} \left(\overline{f^b}\right)^T \\ \left(\overline{\omega_{ib}^b}\right)^T \\ \left(\overline{f^b} \times \overline{\omega_{ib}^b}\right)^T \end{pmatrix} \qquad \text{(Eq. 2.11)}$$

For both method apply that the rotation matrix between body frame and navigation are calculated for average data over 3-10 min (see chapter 2.4.3). Hence both methods yield the average rotation matrix over the alignment time. This can cause errors between the true and calculated attitude as the IMU even under static condition are affected by small attitude changes from e.g. wind gusts. This is the reason for performing the fine alignment after the coarse alignment and will be described further in chapter 2.4.2.

Coarse alignment in kinematic mode is sometimes necessary as 3-10 min. of static mode isn't always possible. External forces will therefore act on the accelerometers so other alignment techniques must be used. A GPS derived velocity is normally available during kinematic mode and can be used if the

velocity vector is approximately parallel to the forward axis (X-axis). This is most often true for land vehicle applications while aircrafts and ships can have lateral and vertical velocity due to wind or maneuver. In such cases other alignment method must be used (Shin, 2005). For most land applications the roll, ξ, pitch, η and heading, ψ can therefore be initialized or estimated as (Godha, 2006 and Shin, 2005).

$$\xi \approx 0° \qquad \eta = \tan^{-1}\left(\frac{v_{GPS}^{U}}{\sqrt{\left(v_{GPS}^{E}\right)^2 + \left(v_{GPS}^{N}\right)^2}}\right) \qquad \psi = \tan^{-1}\left(\frac{v_{GPS}^{E}}{v_{GPS}^{N}}\right) \qquad \text{(Eq. 2.12)}$$

Where $v_{GPS}^{E/N/U}$ are the GPS-derived velocities in east, north and up direction respectively. The accuracy of the heading is derived in (Godha, 2006) but it should be mentioned here that greater vehicle velocity results in better heading accuracy. Hence heading estimated by GPS derived velocity is only used while the vehicle speed is more than 5 m/s (Godha, 2006).

It should be mentioned that for IMUs where the heading is completely unknown an Extended Kalman Filter (EKF) with a large heading uncertainty (LHU) must be used in order to perform the coarse alignment. This is not discussed further here but the reader can see more in (Shin, 2005).

2.4.2 Fine alignment

Since the coarse alignment only give an estimate of the average of the rotation matrix a fine alignment is most often done after the coarse alignment in order to get a more accurate estimate. This is usually done through an Extended Kalman Filter (EKF) with small heading uncertainty (SHU). The main purpose is to estimate the error states of the system based on updates from the EKF. Known quantities in the filter are usually observations from e.g. zero velocity update (ZUPT) or coordinate update (CUPT) (Petovello, 2003). This will be discussed further in chapter 4 about the Kalman filter.

2.4.3 Alignment time

In order to achieve a specific azimuth accuracy the stationary alignment has to be done over a given time period. The specific azimuth accuracy, δA is inverse proportional with the alignment time, T_a and depends on the geodetic latitude, φ and the gyroscope angle random walk, ARW. Higher latitude will result in longer alignment time in order to achieve the same azimuth accuracy (El-Sheimy, 2006)

$$\delta A = \frac{ARW}{\omega_e \cdot \cos(\varphi) \cdot \sqrt{T_a}} \qquad \Rightarrow \qquad T_a = \left(\frac{ARW}{\omega_e \cdot \cos(\varphi) \cdot \delta A} \right)^2 \qquad \text{(Eq. 2.13)}$$

2.5 Equation of motion

A mathematical way of describing the motion of a vehicle is through the equation of motion. It is a set of first order differential equation that describes the changes of a system with time. As mentioned in chapter 2.1 the position vector, r velocity vector, v and rotation matrix, R as functions of time are called navigation state variables. A three dimensional vector including all the three mentioned state variables are called a state vector and are given as (El-Sheimy, 2006)

$$\dot{x}^a = \begin{pmatrix} \dot{r}^a & \dot{v}^a & \dot{R}_b^a \end{pmatrix}^T \qquad \text{(Eq. 2.14)}$$

Where a dot represents a time derivative and “a” represents the frame the state vector is formulated in. The rotation matrix is always from the body frame as the accelerometer measurement, f^b and gyroscopes measurements, ω_{ib}^b are given in the body frame (El-Sheimy, 2006). It should be noted that the rotation matrix can be given as a three dimensional vector as the matrix can be parameterized by three independent angles (Euler angles).

The state vector can be formulated in different frames according to its use. In order to derive the equation of motion in the navigation frame the time derivative of the position vector $\dot{r}^n$, velocity vector, $\dot{v}^n$ and rotation matrix, $\dot{R}_b^n$ need to be analyzed.

The position vector as described in the navigation frame is expressed in terms of curvilinear coordinates (geodetic latitude, φ, geodetic longitude, λ and ellipsoidal height, h) as (Shin, 2001).

$$r^n = \begin{pmatrix} \varphi & \lambda & h \end{pmatrix}^T \qquad \text{(Eq. 2.15)}$$

The velocity as described in the (ENU) navigation frame is expressed by three components, $v_{E,N,U}$ along the three axes (east, north and up) and can be related to the curvilinear coordinates as (Shin, 2001)

$$v^n = \begin{pmatrix} v_E \\ v_N \\ v_U \end{pmatrix} = \begin{pmatrix} 0 & M+h & 0 \\ (N+h)\cdot\cos\varphi & 0 & 0 \\ 0 & 0 & -1 \end{pmatrix} \cdot \begin{pmatrix} \dot{\varphi} \\ \dot{\lambda} \\ \dot{h} \end{pmatrix} \qquad \text{(Eq. 2.16)}$$

Where the radius of curvature in meridian, M and prime vertical, N are given as function of the semi-major axis, a and linear eccentricity, e of the reference ellipsoid (Jekeli, 2000)

$$M = \frac{a\cdot\left(1-e^2\right)}{\left(1-e^2\cdot\sin^2\varphi\right)^{3/2}} \qquad N = \frac{a}{\left(1-e^2\cdot\sin^2\varphi\right)^{1/2}} \qquad \text{(Eq. 2.17)}$$

The time derivative of the position can therefore be expressed as (Shin, 2001 and El-Sheimy, 2006)

$$\dot{r}^n = \begin{pmatrix} \dot{\varphi} \\ \dot{\lambda} \\ \dot{h} \end{pmatrix} = \begin{pmatrix} 0 & \frac{1}{M+h} & 0 \\ \frac{1}{(N+h)\cdot\cos\varphi} & 0 & 0 \\ 0 & 0 & -1 \end{pmatrix} \cdot \begin{pmatrix} v_E \\ v_N \\ v_U \end{pmatrix} = D^{-1}v^n \qquad \text{(Eq. 2.18)}$$

The time derivative of the velocity as described in the navigation frame can be derived from the specific force measurement considering the Earth rotation rate, ω_{ie}^n, the change of orientation of the navigation

frame with respect to the Earth, ω_{en}^{n} and the Earth gravity field, γ^{n}. The specific force measurements from the accelerometers can be transformed to the navigation frame as (El-Sheimy, 2006).

$$f^{n} = R_{b}^{n} \cdot f^{b} \qquad \text{(Eq. 2.19)}$$

The Earth rotation rate, ω_{ie}^{n} as described in the navigation frame is functions of the latitude and given as an angular velocity vector as (El-Sheimy, 2006).

$$\omega_{ie}^{n} = R_{e}^{n} \cdot \omega_{ie}^{e} = \begin{pmatrix} -\sin\lambda & \cos\lambda & 0 \\ -\sin\varphi \cdot \cos\lambda & -\sin\varphi \cdot \sin\lambda & \cos\varphi \\ \cos\varphi \cdot \cos\lambda & \cos\varphi \cdot \sin\lambda & \sin\varphi \end{pmatrix} \cdot \begin{pmatrix} 0 \\ 0 \\ \omega_{e} \end{pmatrix} = \begin{pmatrix} 0 \\ \omega_{e} \cdot \cos\varphi \\ \omega_{e} \cdot \sin\varphi \end{pmatrix} \qquad \text{(Eq. 2.20)}$$

The change of orientation of the navigation frame with respect to the Earth, ω_{en}^{n} is given as an angular velocity vector as (El-Sheimy, 2006).

$$\omega_{en}^{n} = \begin{pmatrix} -\dot{\varphi} \\ \dot{\lambda} \cdot \cos\varphi \\ \lambda \cdot \sin\varphi \end{pmatrix} = \begin{pmatrix} -\dfrac{v_{N}}{M+h} \\ \dfrac{v_{E}}{N+h} \\ \dfrac{v_{E} \cdot \tan\varphi}{N+h} \end{pmatrix} \qquad \text{(Eq. 2.21)}$$

The Earth gravity field is given according to the normal gravity model from equation 2.6 as

$$\gamma^{n} = \begin{pmatrix} 0 \\ 0 \\ -\gamma \end{pmatrix} \qquad \text{(Eq. 2.22)}$$

Taking into consideration all the above mentioned factors the time derivative of the velocity can therefore be expressed as (El-Sheimy, 2006).

$$\dot{v}^n = R_b^n \cdot f^b - \left(2 \cdot \Omega_{ie}^n + \Omega_{en}^n\right) \times v^n + \gamma^n \qquad \text{(Eq. 2.23)}$$

Where Ω_{ie}^n and Ω_{en}^n are the skew symmetric matrices of the vectors in Eq. 2.20 and 2.21.

Finally the time derivative of the rotation matrix can be expressed as the following differential equation (El-Sheimy, 2006).

$$\dot{R}_b^n = R_b^n \cdot \Omega_{nb}^b = R_b^n \cdot \left(\Omega_{ib}^b - \Omega_{in}^b\right) \qquad \text{(Eq. 2.24)}$$

The state vector in the navigation frame can therefore be written as (El-Sheimy, 2006).

$$\dot{x}^n = \begin{pmatrix} \dot{r}^n \\ \dot{v}^n \\ \dot{R}_b^n \end{pmatrix} = \begin{pmatrix} D^{-1} \cdot v^n \\ R_b^n \cdot \boxed{f^b} - (2 \cdot \Omega_{ie}^n + \Omega_{en}^n) \times v^n + g^n \\ R_b^n \cdot (\boxed{\Omega_{ib}^b} - \Omega_{in}^b) \end{pmatrix} \qquad \text{(Eq. 2.25)}$$

Where the matrix D^{-1} is given as

$$D^{-1} = \begin{pmatrix} 0 & \frac{1}{M+h} & 0 \\ \frac{1}{(N+h) \cdot \cos\varphi} & 0 & 0 \\ 0 & 0 & -1 \end{pmatrix} \qquad \text{(Eq. 2.26)}$$

The variables in a square $\boxed{f^b}$ and $\boxed{\omega_{ib}^b}$ are the measurements from the accelerometers and gyroscopes.

In a similar way the state vector can be formulated in the inertial and Earth frame (see El-Sheimy, 2006). The solution to the equation of motion in the navigation frame is described in chapter 2.6.

2.6 Mechanization equations

The solution to the equation of motion is called the mechanization equations and consists of four steps. Chapter 2.6.1 – 2.6.3 are only describing the mechanization equations in navigation frame. For a description of the mechanization equations in other frames the reader can see more in (Godha, 2006, El-Sheimy, 2006 and Jekeli, 2000).

2.6.1 Known error compensation of raw data

Any measurements contain deterministic errors that can be corrected if the errors are known through calibrations. The errors typically include bias, scale factor and axis non-orthogonalities as described in chapter 2.2.3.

The raw gyroscope measurement expressed as angular increments, $\Delta\tilde{\theta}_{ib}^{b}$ can be compensated for gyroscope bias, d and gyroscope scale factor, $S_{x,y,z}^{g}$ as (Godha, 2006).

$$\Delta\theta_{ib}^{b} = \begin{pmatrix} 1/(1+S_x^g) & 0 & 0 \\ 0 & 1/(1+S_y^g) & 0 \\ 0 & 0 & 1/(1+S_z^g) \end{pmatrix} \cdot \left(\Delta\tilde{\theta}_{ib}^{b} - d \cdot \Delta t \right) \qquad \text{(Eq. 2.27)}$$

Where $\Delta t = t_{k+1} - t_k$ is the time increment between two successive measurements at t_k and t_{k+1},

The raw accelerometer measurement expressed as velocity increments due to the specific force, $\Delta\tilde{v}_{f}^{b}$ can be compensated for accelerometer bias, b and accelerometer scale factor, $S_{x,y,z}^{a}$ as (Godha, 2006).

$$\Delta v_{f}^{b} = \begin{pmatrix} 1/(1+S_x^a) & 0 & 0 \\ 0 & 1/(1+S_y^a) & 0 \\ 0 & 0 & 1/(1+S_z^a) \end{pmatrix} \cdot \left(\Delta\tilde{v}_{f}^{b} - b \cdot \Delta t \right) \qquad \text{(Eq. 2.28)}$$

As shown in chapter 5 the deterministic errors can also be estimated during the navigation process.

2.6.2 Attitude update

Three different method is commonly used for determine the updated rotation matrix R_b^n. Euler angle, direction cosines and quaternion. Because of the robustness of the quaternion against singularities and their computational efficiency (Shin, 2001 and El-Sheimy, 2006) this dissertation only uses the quaternion method. The two other methods can be seen in many navigation books e.g. (Jekeli, 2001).

The quaternion method is based on an idea that a transformation from one frame to another can be affected by a single rotation about a vector. A basic in this method is a four dimensional vector called the quaternion expressed as (Shin, 2001).

$$q = \begin{pmatrix} q_1 & q_2 & q_3 & q_4 \end{pmatrix}^T \quad \text{(Eq. 2.29)}$$

The elements of the quaternion should satisfy a normality condition given as (Shin, 2001).

$$q_1^2 + q_2^2 + q_3^2 + q_4^2 = 1 \quad \text{(Eq. 2.30)}$$

And if the normality condition isn't fulfilled the quaternion can be normalized as (Shin, 2001).

$$\hat{q} = \frac{q}{\sqrt{q^T \cdot q}} \quad \text{(Eq. 2.31)}$$

The transformation between the quaternion, q and the rotation matrix R_b^n is given as (Shin, 2001)

$$q = \begin{pmatrix} q_1 \\ q_2 \\ q_3 \\ q_4 \end{pmatrix} = \begin{pmatrix} 0.5 \cdot (R_{32} - R_{23}) \cdot \sqrt{1 + R_{11} + R_{22} + R_{33}} \\ 0.5 \cdot (R_{13} - R_{31}) \cdot \sqrt{1 + R_{11} + R_{22} + R_{33}} \\ 0.5 \cdot (R_{21} - R_{12}) \cdot \sqrt{1 + R_{11} + R_{22} + R_{33}} \\ 0.5 \cdot \sqrt{1 + R_{11} + R_{22} + R_{33}} \end{pmatrix} \quad \text{(Eq. 2.32)}$$

and

$$R_b^n = \begin{pmatrix} \left(q_1^2 - q_2^2 - q_3^2 + q_4^2\right) & 2\cdot\left(q_1\cdot q_2 - q_3\cdot q_4\right) & 2\cdot\left(q_1\cdot q_3 + q_2\cdot q_4\right) \\ 2\cdot\left(q_1\cdot q_2 + q_3\cdot q_4\right) & \left(q_2^2 - q_1^2 - q_3^2 + q_4^2\right) & 2\cdot\left(q_2\cdot q_3 - q_1\cdot q_4\right) \\ 2\cdot\left(q_1\cdot q_3 - q_2\cdot q_4\right) & 2\cdot\left(q_2\cdot q_3 + q_1\cdot q_4\right) & \left(q_3^2 - q_1^2 - q_2^2 + q_4^2\right) \end{pmatrix} \quad \text{(Eq. 2.33)}$$

Where R_{ij} is the $(i,j)^{th}$ elements of R_b^n.

The time derivative of the quaternion is described by a first-order differential equation as (Shin, 2001)

$$\dot{q} = \frac{1}{2}\cdot\Omega(\omega)\cdot q = \frac{1}{2}\cdot\begin{pmatrix} 0 & \omega_z & -\omega_y & \omega_x \\ -\omega_z & 0 & \omega_x & \omega_y \\ \omega_y & -\omega_x & 0 & \omega_z \\ -\omega_x & -\omega_y & -\omega_z & 0 \end{pmatrix}\cdot q \quad \text{(Eq. 2.34)}$$

Where $\omega_{nb}^b = \begin{pmatrix} \omega_x & \omega_y & \omega_z \end{pmatrix}^T$ is the angular velocity of the body rotation.

If the rotation matrix is updated using the angular increments, $\Delta\omega_{nb}^b$ then Euler's method give the following solution to the first order differential equation in Eq. 2.34 (Shin, 2001 and El-Sheimy, 2006).

$$q_{t+1} = q_t + \frac{1}{2}\cdot\Omega(\omega_t)\cdot q\cdot\Delta t \;\Leftrightarrow$$

$$\begin{pmatrix} q_1 \\ q_2 \\ q_3 \\ q_4 \end{pmatrix}_{t+1} = \begin{pmatrix} q_1 \\ q_2 \\ q_3 \\ q_4 \end{pmatrix}_t + \frac{1}{2}\cdot\begin{pmatrix} c & s\cdot\Delta\theta_z & -s\cdot\Delta\theta_y & s\cdot\Delta\theta_x \\ -s\cdot\Delta\theta_z & c & s\cdot\Delta\theta_x & s\cdot\Delta\theta_y \\ s\cdot\Delta\theta_y & -s\cdot\Delta\theta_x & c & s\cdot\Delta\theta_z \\ -s\cdot\Delta\theta_x & -s\cdot\Delta\theta_y & -s\cdot\Delta\theta_z & c \end{pmatrix}\cdot\begin{pmatrix} q_1 \\ q_2 \\ q_3 \\ q_4 \end{pmatrix}_t \quad \text{(Eq. 2.35)}$$

Where $\Delta\theta_{nb}^b = (\Delta\theta_x \quad \Delta\theta_y \quad \Delta\theta_z)^T = \Delta\theta_{ib}^b - \Delta\theta_{in}^b = \Delta\theta_{ib}^b - R_n^b\cdot(\omega_{ie}^n + \omega_{en}^n)\cdot\Delta t$. R_n^b, ω_{ie}^n and ω_{en}^n is from the previous updated rotation matrix and angular velocity vectors. The coefficients c and s are computed by $c = 2\cdot\left(\cos\left(\Delta\theta/2\right) - 1\right)$ and $s = 2/\Delta\theta\cdot\sin\left(\Delta\theta/2\right)$, where $\Delta\theta = \sqrt{\Delta\theta_x^2 + \Delta\theta_y^2 + \Delta\theta_z^2}$. When q_{t+1} are obtained, Eq. 2.33 can be used to update the rotation matrix (El-Sheimy, 2006).

2.6.3 Transformation of specific force and velocity/position integration

In order to transform the body frame velocity increment due to specific force, Δv_f^b into the navigation frame, the rotation matrix, R_b^n either before or after the update is used as (Godha, 2006).

$$\Delta v_f^n = \left(R_b^n\right)_{\text{Before update}} \cdot \begin{pmatrix} 1 & -0.5\cdot\Delta\theta_z & 0.5\cdot\Delta\theta_y \\ 0.5\cdot\Delta\theta_z & 1 & -0.5\cdot\Delta\theta_x \\ -0.5\cdot\Delta\theta_y & 0.5\cdot\Delta\theta_x & 1 \end{pmatrix} \cdot \Delta v_f^b \qquad \text{(Eq. 2.36)}$$

$$\Delta v_f^n = \left(R_b^n\right)_{\text{After update}} \cdot \begin{pmatrix} 1 & 0.5\cdot\Delta\theta_z & -0.5\cdot\Delta\theta_y \\ -0.5\cdot\Delta\theta_z & 1 & 0.5\cdot\Delta\theta_x \\ 0.5\cdot\Delta\theta_y & -0.5\cdot\Delta\theta_x & 1 \end{pmatrix} \cdot \Delta v_f^b \qquad \text{(Eq. 2.37)}$$

Where $\Delta\theta_{x,y,z}$ is given in Eq. 2.35.

After transformation the velocity increment needs to be corrected for Coriolis acceleration and gravity similar to the time derivative of the velocity from Eq. 2.23 as (Shin, 2001).

$$\Delta v^n = \Delta v_f^n - (2\omega_{ie}^n + \omega_{en}^n) \times v^n \cdot \Delta t + \gamma^n \cdot \Delta t \qquad \text{(Eq. 2.38)}$$

The updated velocity in the navigation frame at t+1 can be found by simple integration as (Shin, 2001).

$$v_{t+1}^n = v_t^n + \Delta v_{t+1}^n \qquad \text{(Eq. 2.39)}$$

And finally the new updated position can be found by integration using the second order Runge-Kutta method as. The second order Runge-Kutta is expected to be a good second order approximation of the analytic solution. Other numerical integration techniques e.g. Euler's method (first order) and four stage Runge-Kutta method (fourth order) can also be used in order to perform the integration. They are not discussed here but the reader can see more in (El-Sheimy, 2006 and Jekeli, 2000).

The updated position is given as (Shin, 2001)

$$r_{t+1}^{n} = r_{t}^{n} + \frac{1}{2} \cdot \begin{pmatrix} 0 & \frac{1}{(N+h)\cdot\cos\varphi} & 0 \\ \frac{1}{M+h} & 0 & 0 \\ 0 & 0 & -1 \end{pmatrix} \cdot \left(v_{t}^{n} + v_{t+1}^{n} \right) \cdot \Delta t \qquad \text{(Eq. 2.40)}$$

A summarize of all mechanization equations described can be illustrated as in figure 2.8.

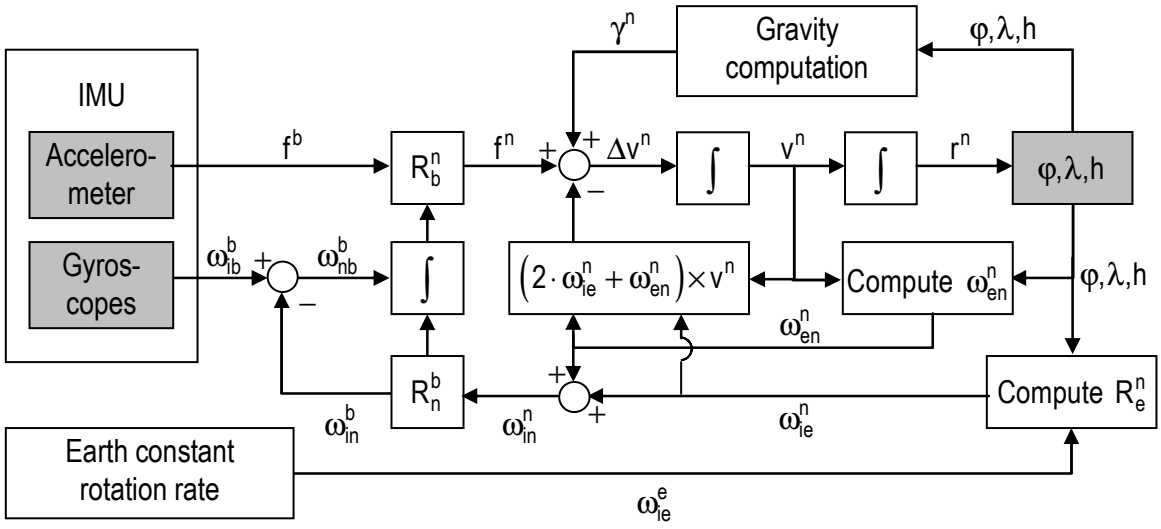

Figure 2.8: The INS navigation frame mechanization

The mechanization equations real input from accelerometers and gyroscopes are grey-scaled to the left while the curvilinear coordinates that are the real output are grey scaled to the right. The integration-signs are referring to the integration happening in Eq. 2.35, 2.39 and 2.40.

Similar figures for the mechanization equations in other frames can be seen in (El-Sheimy, 2006).

2.7 INS error state model

The equation of motion and mechanization equations discussed in the previous chapters gives no information about the errors of the system. It blindly processes the data from the IMU in order to update the state vector. The raw data from the IMU contain errors that will increase with time due to the time integration performed during the mechanization equations. Hence error models are required for estimation of the different errors.

As the state vector, x^n includes a position vector, a velocity vector and a rotation matrix, an error state vector, δx^n includes position errors, velocity errors and attitude errors as (El-Sheimy, 2006)

$$\delta x^n = \begin{pmatrix} \delta r^n & \delta v^n & \delta R_b^n \end{pmatrix}^T = \begin{pmatrix} \delta\varphi & \delta\lambda & \delta h & \delta v^E & \delta v^N & \delta v^U & \delta\eta & \delta\xi & \delta\psi \end{pmatrix}^T \quad \text{(Eq. 2.41)}$$

Where $\delta r^n = \begin{pmatrix} \delta\varphi & \delta\lambda & \delta h \end{pmatrix}$ are the position errors described in curvilinear coordinates, $\delta v^n = \begin{pmatrix} \delta v^E & \delta v^N & \delta v^U \end{pmatrix}$ are the Earth referenced velocity errors given in the navigation frame and $\delta R_b^n = \begin{pmatrix} \delta\eta & \delta\xi & \delta\psi \end{pmatrix}$ are the attitude errors due to errors in the rotation matrix R_b^n.

The accelerometer and gyroscope measurements was compensated for known deterministic errors in chapter 2.6.1 but since the measurements still contain stochastic errors these are modeled to in the error state vector. (El-Sheimy, 2006) The error state vector therefore becomes

$$\delta x^n = \begin{pmatrix} \delta r^n & \delta v^n & \delta R_b^n & \delta\omega & \delta f^b \end{pmatrix}^T \Leftrightarrow \quad \text{(Eq. 2.42)}$$
$$\delta x^n = \begin{pmatrix} \delta\varphi & \delta\lambda & \delta h & \delta v^E & \delta v^N & \delta v^U & \delta\eta & \delta\xi & \delta\psi & \delta\omega_x & \delta\omega_y & \delta\omega_z & \delta f_x & \delta f_y & \delta f_z \end{pmatrix}^T$$

Where $\delta\omega = \begin{pmatrix} \delta\omega_x & \delta\omega_y & \delta\omega_z \end{pmatrix}$ is the gyroscope bias error and $\delta f^b = \begin{pmatrix} \delta f_x & \delta f_y & \delta f_z \end{pmatrix}$ is the accelerometer bias error. Since all the errors are variable in time due to the dynamics of the system they are usually described by differential equations. As the state vector is non-linear the most common way to derive a set of linear differential equations are done by linearization.

2.7.1 Position errors

The time derivative of the position was defined in Eq. 2.18. As the position errors is the difference between the unknown true coordinates r^n and the computed coordinates $\hat{r}^n$, the differential equation for the position error can be described using a Taylor series expansion to a 1st order approximation as (El-Sheimy, 2006).

$$\delta \dot{r}^n = \dot{\hat{r}}^n - \dot{r}^n = \frac{\partial}{\partial r^n}\left(\dot{r}^n\right)\delta r^n = \frac{\partial}{\partial r^n}\left(\begin{pmatrix} 0 & \frac{1}{M+h} & 0 \\ \frac{1}{(N+h)\cdot\cos\varphi} & 0 & 0 \\ 0 & 0 & -1 \end{pmatrix}\begin{pmatrix} v_E \\ v_N \\ v_U \end{pmatrix}\right)\delta r^n \qquad \text{(Eq. 2.43)}$$

After differentiation this will lead to (El-Sheimy, 2006).

$$\delta \dot{r}^n = D^{-1}\delta v^n + D^{-1}D_r\delta r^n \qquad \text{(Eq. 2.44)}$$

Where D^{-1} is given in Eq. 2.26 and D_r is given as (El-Sheimy, 2006)

$$D_r = \begin{pmatrix} -v_E\tan\varphi & 0 & \frac{v_E}{N+h} \\ 0 & 0 & \frac{v_N}{M+h} \\ 0 & 0 & 0 \end{pmatrix} \qquad \text{(Eq. 2.45)}$$

Fully written Eq. 2.44 will be as (El-Sheimy, 2006).

$$\delta \dot{r}^n = \begin{pmatrix} 0 & \frac{1}{M+h} & 0 \\ \frac{1}{(N+h)\cdot\cos\varphi} & 0 & 0 \\ 0 & 0 & -1 \end{pmatrix}\begin{pmatrix} \delta v_E \\ \delta v_N \\ \delta v_U \end{pmatrix} + \begin{pmatrix} 0 & 0 & \frac{-v_N}{(M+h)^2} \\ \frac{v_E\cdot\tan\varphi}{(N+h)\cdot\cos\varphi} & 0 & \frac{-v_E}{(N+h)^2\cdot\cos\varphi} \\ 0 & 0 & 0 \end{pmatrix}\begin{pmatrix} \delta\varphi \\ \delta\lambda \\ \delta h \end{pmatrix} \qquad \text{(Eq. 2.46)}$$

As the term to the right with the velocity components, $\left(v_E, v_N\right)$ divided by the radius of curvature in meridian, M or prime vertical, N are very small it can be neglected (El-Sheimy, 2006).

2.7.2 Velocity errors

The time derivative of the velocity was defined in Eq. 2.23. As similar with the position errors, the velocity errors is the difference between the unknown true velocities, v^n and the computed velocities, $\hat{v}^n$. The differential equation for the velocity error can be described using a Taylor series expansion to a 1st order approximation as (El-Sheimy, 2006).

$$\delta\dot{v}^n = \dot{\hat{v}}^n - \dot{v}^n = \frac{\partial}{\partial v^n}\left(\dot{v}^n\right)\delta v^n = \frac{\partial}{\partial v^n}\left(R_b^n \cdot f^b - \left(2\cdot\Omega_{ie}^n + \Omega_{en}^n\right)\times v^n + \gamma^n\right)\delta v^n \qquad \text{(Eq. 2.47)}$$

After differentiation this will lead to (El-Sheimy, 2006).

$$\delta\dot{v}^n = \delta R_b^n f^b - \left(2\cdot\Omega_{ie}^n + \Omega_{en}^n\right)\delta v^n - \left(2\cdot\delta\Omega_{ie}^n + \delta\Omega_{en}^n\right)v^n + \delta\gamma^n + R_b^n\delta f^b \qquad \text{(Eq. 2.48)}$$

or

$$\delta\dot{v}^n = -F^n\varepsilon^n + R_b^n b - \left(2\cdot\Omega_{ie}^n + \Omega_{en}^n\right)\delta v^n - V^n\left(2\cdot\delta\Omega_{ie}^n + \delta\Omega_{en}^n\right) + \delta\gamma^n \qquad \text{(Eq. 2.49)}$$

Where F^n is the skew symmetric matrix of the specific force vector, f^n, $\varepsilon^n = \begin{pmatrix}\varepsilon_E^n & \varepsilon_N^n & \varepsilon_U^n\end{pmatrix}$ are the misalignment error states for the transformation between body frame and navigation frame, $b = \begin{pmatrix}b_1 & b_2 & b_3\end{pmatrix}$ is the accelerometer bias errors from δf^b, V^n is the skew symmetric matrix of the velocity vector, v^n and $\delta\gamma^n$ is the gravity error.

The full derivation of Eq. 2.49 will not be given here but the reader can see it in (El-Sheimy, 2006) and (Shin, 2001). However the solution can fully write be given as (El-Sheimy, 2006).

$$\delta\dot{v}^n = \begin{pmatrix} 0 & f_E & -f_U \\ -f_U & 0 & f_E \\ f_N & -f_E & 0 \end{pmatrix}\begin{pmatrix}\delta\eta \\ \delta\xi \\ \delta\psi\end{pmatrix} + R_b^n\begin{pmatrix}\delta f_x \\ \delta f_y \\ \delta f_z\end{pmatrix} + \ldots$$

$$\dot{\delta r}^n = \begin{pmatrix} (2\omega_e \sin\varphi)v_U + (2\omega_e \cos\varphi)v_N + \dfrac{v_N v_E}{(N+h)\cos^2\varphi} & 0 & 0 \\ (-2\omega_e \cos\varphi)v_E - \dfrac{(v_E)^2}{(N+h)\cos^2\varphi} & 0 & 0 \\ (-2\omega_e \sin\varphi)v_E & 0 & \dfrac{2\gamma}{R} \end{pmatrix} \begin{pmatrix} \delta\varphi \\ \delta\lambda \\ \delta h \end{pmatrix} + \ldots$$

$$\begin{pmatrix} \dfrac{-v_U}{N+h} + \dfrac{v_N}{N+h}\tan\varphi & 2\omega_e \sin\varphi + \dfrac{v_E \tan\varphi}{N+h} & -2\omega_e \cos\varphi - \dfrac{v_E}{N+h} \\ -2\omega_e \sin\varphi - \dfrac{2v_E \tan\varphi}{N+h} & -\dfrac{v_U}{M+h} & -\dfrac{v_N}{M+h} \\ 2\omega_e \cos\varphi + \dfrac{2v_E}{N+h} & \dfrac{2v_N}{M+h} & 0 \end{pmatrix} \begin{pmatrix} \delta v_E \\ \delta v_N \\ \delta v_U \end{pmatrix} \quad \text{(Eq. 2.50)}$$

The two last terms with the velocity components, (v_E, v_N, v_U) divided by the radius of curvature in meridian, M or prime vertical, N are very small and can eventual be neglected (El-Sheimy, 2006).

2.7.3 Attitude errors

The differential equation for the rotation matrix can also be defined using a Taylor series expansion to a 1st order approximation as (El-Sheimy, 2006).

$$\dot{\varepsilon}^n = -\Omega_{in}^n \varepsilon^n - \delta\omega_{in}^n + R_b^n d \quad \text{(Eq. 2.51)}$$

Where $d = (d_1 \quad d_2 \quad d_3)$ is the gyroscope bias error from $\delta\omega$. Again the full derivation of Eq. 2.51 will not be given here as the reader can see it in (El-Sheimy, 2006) and (Shin, 2001). But the solution can fully written be given as (El-Sheimy, 2006).

$$\dot{\varepsilon}^n = \begin{pmatrix} 0 & \dfrac{1}{N+h} & 0 \\ \dfrac{-1}{M+h} & 0 & 0 \\ \dfrac{-\tan\varphi}{N+h} & 0 & 0 \end{pmatrix} \begin{pmatrix} \delta v_E \\ \delta v_N \\ \delta v_U \end{pmatrix} + R_b^n \begin{pmatrix} \delta\omega_x \\ \delta\omega_y \\ \delta\omega_z \end{pmatrix} + \ldots$$

$$\dot{\delta r} = \begin{pmatrix} 0 & 0 & -\frac{v_N}{(M+h)^2} \\ \omega_e \sin\varphi & 0 & \frac{v_E}{(N+h)^2} \\ -\omega_e \cos\varphi - \frac{v^E}{(N+h)\cos^2\varphi} & 0 & \frac{v_E \tan\varphi}{(N+h)^2} \end{pmatrix} \begin{pmatrix} \delta\varphi \\ \delta\lambda \\ \delta h \end{pmatrix} + \ldots$$

$$\begin{pmatrix} 0 & \omega_e \sin\varphi + \frac{v_E \tan\varphi}{N+h} & -\omega_e \cos\varphi - \frac{v_E}{N+h} \\ -\omega_e \sin\varphi - \frac{v_E \tan\varphi}{N+h} & o & -\frac{v_N}{M+h} \\ \omega_e \cos\varphi + \frac{v_E}{N+h} & \frac{v_N}{M+h} & 0 \end{pmatrix} \begin{pmatrix} \delta\eta \\ \delta\xi \\ \delta\psi \end{pmatrix} \quad \text{(Eq. 2.52)}$$

Similarly to the velocity error the two last terms with the velocity components, (v_E, v_N, v_U) divided by the radius of curvature in meridian, M or prime vertical, N are very small and can be neglected (El-Sheimy, 2006).

2.7.4 Gyroscope bias error

The residual stochastic part of the gyroscope bias (also called gyro drift and therefore the reason for the name d) can be modeled as a first order Gauss-Markov process with a differential equation as (El-Sheimy, 2006).

$$\dot{d} = -\alpha d + w_d = \begin{pmatrix} -\alpha_x & 0 & 0 \\ 0 & -\alpha_y & 0 \\ 0 & 0 & -\alpha_z \end{pmatrix} \begin{pmatrix} d_1 \\ d_2 \\ d_3 \end{pmatrix} + w_d \quad \text{(Eq. 2.53)}$$

Where α is the reciprocal of the correlation time, τ and w_d is the Gauss-Markov process noise. The Gauss-Markov correlation time and Gauss-Markov temporal standard deviation (used in calculating w_d) are obtained from the autocorrelation function of raw static data. Many other noise models can be used in stead of a Gauss-Markov process but it is the most common used in navigation systems (Godha, 2006).

2.7.5 Accelerometer bias error

The residual stochastic part of the accelerometer bias can also be modeled as a first order Gauss-Markov process with a differential equation as (El-Sheimy, 2006).

$$\dot{b} = -\beta b + w_b = \begin{pmatrix} -\beta_x & 0 & 0 \\ 0 & -\beta_y & 0 \\ 0 & 0 & -\beta_z \end{pmatrix} \begin{pmatrix} b_1 \\ b_2 \\ b_3 \end{pmatrix} + w_b \qquad \text{(Eq. 2.54)}$$

Where β is the reciprocal of the correlation time, τ and w_b is the Gauss-Markov process noise similar to the one from Eq. 2.53.

2.7.6 Error state equation

Combining Eq. 2.46, 2.49, 2.52, 2.53 and 2.54 give a set of linear differential equations for the error states in the navigation frame as (El-Sheimy, 2006).

$$\dot{x}^n(t) = \begin{pmatrix} \delta\dot{r}^n \\ \delta\dot{v}^n \\ \dot{\varepsilon}^n \\ \dot{d} \\ \dot{b} \end{pmatrix} = \begin{pmatrix} D^{-1}\delta v^n \\ -F^n\varepsilon^n + R_b^n b - \left(2\cdot\Omega_{ie}^n + \Omega_{en}^n\right)\delta v^n - V^n\left(2\cdot\delta\Omega_{ie}^n + \delta\Omega_{en}^n\right) + \delta\gamma^n \\ -\Omega_{in}^n\varepsilon^n - \delta\omega_{in}^n + R_b^n d \\ -\alpha d + w_d \\ -\beta b + w_b \end{pmatrix} \qquad \text{(Eq, 2.55)}$$

2.7.7 Process model

With the error state equation given in Eq. 2.55 it can be applied in a model for describing the process of a dynamic system. One of the most common process models for INS is given as (El-Sheimy, 2006)

$$\dot{x}(t) = F(t)x(t) + G(t)w(t) \qquad \text{(Eq. 2.56)}$$

Where $x(t)$ is the error state, $F(t)$ is a system dynamic matrix, $G(t)$ is a noise coefficient matrix (shaping matrix) and $w(t)$ is the process driving noise. See more in chapter 5.

2.8 Advantage and limitations of INS

Seen in an overall perspective is INS a perfect navigation system, as it provides continuous navigation information without being affected by the surrounding environment. Orthogonal mounted accelerometers and gyroscopes measure specific force and angular rate that can be combined with the mechanization equation and error state equation in order to get position, velocity and attitude increments in a certain navigation frame. When the increments are integrated over time, they describe any motion of the INS as a function of time (Godha, 2006).

However the INS computation process is more complicated as it sounds because any errors in the accelerometer or gyroscope measurements will lead to errors in the determined position, velocity and attitude. Gyroscope errors will result in errors in the transformation matrix between body and navigation frame, while accelerometer errors will result in errors in the integrated velocity and position. The integration will result in errors proportional to the integration time, t and its square, t^2 for velocity and position respectively. For inertial sensors with large errors this will lead to errors increasing without limits in a very short time. The main problem about using INS to navigation systems is therefore the unlimited errors that will occur over time if no precautions are taken. The system therefore seems to drift with time (El-Sheimy, 2006).

In order to minimize these errors, external measurements at regular time intervals must be utilized. Different types of update measurements can be used in order to update the position, the velocity or the attitude. GPS is one of the main position update methods and the only one discussed in this dissertation (see chapter 3). Other methods could be velocity update from a wheel speed sensor or attitude update from a compass.

Integration between the INS measurement and the one from the external systems are normally done by use of different filtering techniques. Kalman filtering is a very common method in order to limit the noise from the two systems. This will be discussed in chapter 4 and 5.

3 GPS

This chapter describes the principles of the Global Positioning System (GPS) with emphasis to the advantages and limitations. First the basics about system and the signal structure are reviewed followed by a short introduction to differential GPS and the different errors that must be expected.

3.1 GPS signal and system structure

The NAVSTAR GPS (NAVigation System with Timing And Ranging – Global Positioning System) is a all weather, worldwide, satellite-based navigation system, developed by the United States Department of Defense (DoD) during the late 1960s, and approved in 1973 (Misra et al., 2001). In 1978 the first prototype satellite was launched and the system was fully operational in July 1995 (Lachapelle, 2005).

It was original designed for metre-level positioning accuracies but due to several developments since the beginning, centimetre-level positioning is now common. Its main concept is the ability to determine range from a known signal transmitted from a satellite to a user, by measuring the transmit time. The transmit time is measured as precise time marking on the signal is performed by very precise synchronized clock onboard the satellites (Misra et al., 2001).

The system consists of three segments shown in figure 3.1.

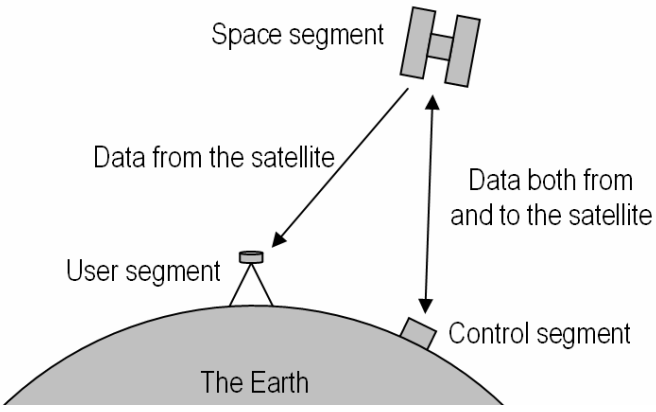

Figure 3.1: Segments of the GPS system

3.1.1 Space segment

The space segment consists of 24 satellites (minimum 21 active) plus a number of active spares in almost circular orbits with a radius of approximately 20.200 km above the Earth. The satellites are arranged in six planes with an inclination of 55˚ relative to the equatorial plane and have a circulation time of 11 hours and 58 minutes (Lachapelle, 2005). Each satellite contains a couple of high precision clocks (cesium and rubidium) that manage the time onboard. The GPS system uses its own time system (GPS-time) that is a continuous timescale characterized by the number of weeks since the 5th of January 1980 at. 00.00 Universal Coordinated Time (UTC) and the number of seconds since the beginning of the present week (midnight between Saturday and Sunday). As UTC-time sometimes adds an extra second (leap second) due to the Earth rotation, and GPS-time doesn't the difference between the two time-systems are 14 seconds as of July 2006 (Misra et al. 2001 and Lachapelle, 2005).

3.1.2 Control segment

The control segment consists of a number of ground elements (three ground antennas, six monitor stations and one master control station) that operates the entire GPS system. The monitor stations track the satellites and send back data from the satellites to the master control station in Colorado Springs, U.S. The master control station analysis the data and send back updated and corrected information to the satellites, through the ground antennas (Misra et al., 2001).

3.1.3 User segment

The user segment is the largest and most dynamic segment as it consist of several hundreds (maybe even thousand) different antennas and receiver-processor models. All capable of measure and decoding the signal from the satellites, in order to give useful position information to the user. The sale of private GPS receivers has increased dramatically during the last decade and more and more GPS applications become a bigger part of our daily live. Take e.g. GPS receivers in cell phones, hand-held navigation systems, car navigation systems, surveying instruments etc. (Godha, 2006 and Misra et al., 2001).

3.1.4 Signal structure

Each satellites continuously transmit a signal on two different carrier frequencies (L1 = 1575.42 MHz and L2 = 1227.60 MHz). These signals are modulated by two Pseudo-Random Noise (PRN) codes and a navigation message telling information about the satellite ephemeris, clock bias and health status. The first PRN code is the Coarse-Acquisition code (C/A-code) only modulated on L1, with a frequency of 1.023 MHz and repeated each millisecond. The second is the Precise code (P-code) that is modulated on both L1 and L2 with a frequency of 10.23 MHz. It has a length of 266 days but is reset every week. The P-code is encrypted by a Y-code in order to limit its use to military applications. This is referred to as Anti-Spoofing (AS) (Lachapelle, 2005). From the signals three different types of measurements can be obtained namely, pseudorange code measurements, carrier phase measurements and Doppler measurements (Petovello, 2003).

3.1.5 Pseudorange code measurement

The first measurement is derived from the PRN codes where a copy of the entire code is generated in the receiver and then compared to the measured code. Whenever the two codes correlates the best the transmit time of the signal can be determined, and from that the pseudorange. The pseudorange is the distance between satellite and receiver including the clock bias between the satellite and receiver clock (if the clock bias is removed from the distance it would only be a range instead). An observation equation for the pseudorange by code measurements can be expressed as (Godha, 2006 and Lachapelle, 2005).

$$p = \rho + c \cdot dt - c \cdot dT + d_{orb} - d_{ion} + d_{trop} + d_{noise} \qquad \text{(Eq. 3.1)}$$

Where p is the measured pseudorange from code measurements, ρ is the true range between satellite and receiver, c is the speed of light in vacuum, dt is the satellite clock error, dT is the receiver clock error, d_{orb} is the satellite orbital error, d_{ion} is the ionospheric error, d_{trop} is the tropospheric error and d_{noise} is the error due to noise (e.g. multipath). The errors sources will be discussed in chapter 3.5. Further information about pseudorange code measurements is given in almost any basic GPS book see e.g. (Misra et al. 2001 and Dueholm et al. 2002).

3.1.6 Carrier phase measurement

The second set of measurements is derived from the phase of the incoming carrier frequencies. The method is similar to the first mentioned, as a copy of the signal is generated by the receiver and compared to the measured. The ambiguity (an unknown number of whole wavelengths between the satellite and the receiver) need to be known and several methods have been developed for this purpose (e.g. the LAMBDA method shown in (Lachapelle, 2005)). After each period with lack of data (known as a cycle slip) a new ambiguity has to be determined. An observation equation for the range by carrier phase measurements can be expressed as (Dueholm et al., 2002, Godha, 2006).

$$\phi = \rho - \lambda N + c \cdot dt - c \cdot dT + d_{orb} - d_{ion} + d_{trop} + d_{noise} \qquad \text{(Eq. 3.2)}$$

Where ϕ is the measured range from phase measurements, λ is the carrier phase wavelength, N is the ambiguity and the rest of the variables is the same as in Eq. 3.1. The errors sources will be discussed in chapter 3.5. Further information about carrier phase measurements is given in almost any basic GPS book see e.g. (Misra et al. 2001 and Dueholm et al. 2002).

3.1.7 Doppler measurement

The third and last set of possible measurements is derived from the rate of change of the carrier phase measurements and known as the Doppler shift. If the rate of change is scaled by the carrier phase wavelength (typically L1) an observation equation for the range rate by Doppler measurements can be expressed as (Godha, 2006 and Lachapelle, 2005).

$$\dot{\phi} = \dot{\rho} + c \cdot \dot{dt} - c \cdot \dot{dT} + \dot{d}_{orb} - \dot{d}_{ion} + \dot{d}_{trop} + \dot{d}_{noise} \qquad \text{(Eq. 3.3)}$$

Where $\dot{\phi}$ is the measured range rate from Doppler measurements, $\dot{\rho}$ is the true range rate between satellite and receiver, c is the speed of light in vacuum, $\dot{dt}$ is the satellite clock error drift, $\dot{dT}$ is the receiver clock error drift, $\dot{d}_{orb}$ is the satellite orbital error drift, $\dot{d}_{ion}$ is the ionospheric error drift, $\dot{d}_{trop}$ is the tropospheric error drift and $\dot{d}_{noise}$ is the drift error due to noise (e.g. multipath). It should be noted that that the ambiguity term is gone after time derivation calculus.

3.2 Absolute GPS

When the code pseudorange between the satellite and the user are known, the user position can be determined by knowledge of the satellites position. This is called absolute GPS. From the navigation message (see chapter 3.1.4) a large number of ephemeris parameters are known for each tracked satellite. By use of these parameters the satellite position can be determined to a given time. The procedure can be seen in many GPS books e.g. (Tsui, 2005). If the data processing is performed in post-mission mode the satellite coordinates can be determined from post-processed precise ephemeris. Depending on the precision of the ephemeris are they available from a couple of hours an up to 2 week after the measurement. The International GNSS Services (IGS) (formerly the International GPS Services) make the post-processed ephemeris available on their website (see http://igscb.jpl.nasa.gov).

A simple relationship between the coordinates for the user and a given satellite (all expressed in the Earth frame) together with the pseudorange can be given as (Dueholm et al., 2002).

$$\text{range} = \sqrt{(X_{user} - X_{sat})^2 + (Z_{user} - Z_{sat})^2 + (Z_{user} - Z_{sat})^2} + c \cdot dT \qquad \text{(Eq. 3.4)}$$

Where “range” is the measured pseudorange from either code or carrier phase measurements, $(X/Y/Z_{user})$ are the unknown user coordinates, $(X/Y/Z_{sat})$ are the known satellite coordinates calculated from the ephemeris parameters, c is the speed of light in vacuum and dT is the unknown receiver clock error. All other error terms given in Eq. 3.1 and 3.2 are, as described later (see chapter 3.3), small compared to the receiver clock error and therefore not mentioned in Eq. 3.4. They can instead be minimized by modulation or other techniques as shown later.

As Eq. 3.4 contains four unknown, is it necessary to have measurements between four satellites and the user, in order to determine all unknown parameters. If more than four measurements to different satellites are known it will result in more equations than needed and the least square method can be used in order to perform an element smoothing of the unknown parameters (Dueholm et al. 2002).

3.3 Differential GPS

In stead of using absolute GPS another and more precise technique can be used. It is called differential GPS and the idea is to measure simultaneous with a minimum of two receivers. One of the receivers (the master) is placed in a well known point, while the other (the rover) measure relative to it.

3.3.1 DGPS

If the pseudorange measurement is used in differential GPS the technique is shorten to just DGPS. It was original developed to eliminate Selective Availability (SA), an error on the satellite clock and in the ephemeris parameter. SA is controlled by the DoD, in order to degrade the precision of GPS for civil users. It was removed on the 2nd of May 2000 and instantaneously the accuracy of using pseudorange code measurement was increased by a factor ten (Dueholm et al., 2002). When SA is no longer active the technique is mainly used to minimize the atmospheric errors in the signal (see chapter 3.4). If two receivers are measuring close to each other (the distance between the receivers is called baseline) the atmospheric conditions above them are almost the same. As the master point is known, the measured coordinates can be compared to the computed ones. The difference is therefore an estimate of the actual error caused by the atmosphere and the other error terms in Eq. 3.1. Hence the error can be used as a correction for the pseudorange measured by the rover to the same satellite. The corrected pseudorange can then be used to calculate the position of the rover by using Eq. 3.4 (Lachapelle, 2005).

3.3.2 Relative positioning

If the carrier phase measurement is used instead, the technique is called relative positioning. It deviate from DGPS in the way that is makes linear combinations of the observation equation from Eq. 3.2 in order to reduce the different error term. A linear combination is then the difference between two observation equations. The most simple is to make a difference between two receiver observations to the same satellite. As the difference is made to the same satellite, the satellite clock error, dt and the satellite orbital error, d_{orb} is the same and can be removed. With a short baseline the atmospheric conditions is assumed the same and the ionospheric and tropospheric error, d_{ion} and d_{trop} can be removed. This difference is called a single-difference and can be written as (Lachapelle, 2005).

$$\begin{aligned}
&\phi_{R1} = \rho_{R1} - \lambda N_{R1} + c \cdot dt - c \cdot dT_{R1} + d_{orb} - d_{ion} + d_{trop} + d_{noise} \\
&\phi_{R2} = \rho_{R2} - \lambda N_{R2} + c \cdot dt - c \cdot dT_{R2} + d_{orb} - d_{ion} + d_{trop} + d_{noise} \\
&\Updownarrow \\
&\phi_{R12} = \phi_{R1} - \phi_{R2} = \rho_{R1} - \rho_{R2} - \lambda\left(N_{R1} - N_{R2}\right) + c \cdot \left(dT_{R1} - dT_{R2}\right) + d_{noise}
\end{aligned} \qquad \text{(Eq. 3.5)}$$

Where the subscript "R1" and "R2" refer to two different receivers and all other variables is described in the previous equations. If a new difference is made for two single differences for different satellites it is called a double-difference. As the receiver clock is the same for two different but simultaneous measurements it can be remove and the double-difference can be written as (Lachapelle, 2005).

$$\begin{aligned}
&\phi_{R12}^{S1} = \rho_{R1}^{S1} - \rho_{R1}^{S1} - \lambda\left(N_{R1}^{S1} - N_{R1}^{S1}\right) + c \cdot \left(dT_{R1} - dT_{R2}\right) + d_{noise} \\
&\phi_{R12}^{S2} = \rho_{R1}^{S2} - \rho_{R2}^{S2} - \lambda\left(N_{R1}^{S2} - N_{R1}^{S2}\right) + c \cdot \left(dT_{R1} - dT_{R2}\right) + d_{noise} \\
&\Updownarrow \\
&\phi_{R12}^{S12} = \phi_{R12}^{S1} - \phi_{R12}^{S2} = \rho_{R1}^{S1} - \rho_{R1}^{S1} - \rho_{R1}^{S2} + \rho_{R2}^{S2} - \lambda\left(N_{R1}^{S1} - N_{R1}^{S1} - N_{R1}^{S2} + N_{R1}^{S2}\right) + d_{noise}
\end{aligned} \qquad \text{(Eq. 3.6)}$$

Where the subscript "S1" and "S2" refer to two different satellites and all other variables is described in the previous equations. Finally if a new difference is made for two double-differences for two different time epoch, the ambiguities would be the same and can be removed as long as no cycle slip occurs. This is called a triple-difference and can be written as (Lachapelle, 2005).

$$\begin{aligned}
&\phi_{R12}^{S12}(t_1) = \rho_{R1}^{S1}(t_1) - \rho_{R1}^{S1}(t_1) - \rho_{R1}^{S2}(t_1) + \rho_{R2}^{S2}(t_1) - \lambda\left(N_{R1}^{S1} - N_{R1}^{S1} - N_{R1}^{S2} + N_{R1}^{S2}\right) + d_{noise} \\
&\phi_{R12}^{S12}(t_2) = \rho_{R1}^{S1}(t_2) - \rho_{R1}^{S1}(t_2) - \rho_{R1}^{S2}(t_2) + \rho_{R2}^{S2}(t_2) - \lambda\left(N_{R1}^{S1} - N_{R1}^{S1} - N_{R1}^{S2} + N_{R1}^{S2}\right) + d_{noise} \\
&\Updownarrow \\
&\phi_{R12}^{S12}(t_1,t_2) = \phi_{R12}^{S12}(t_2) - \phi_{R12}^{S12}(t_1) \\
&\Updownarrow \\
&\phi_{R12}^{S12}(t_1,t_2) = \rho_{R1}^{S1}(t_2) - \rho_{R1}^{S1}(t_2) - \rho_{R1}^{S2}(t_2) + \rho_{R2}^{S2}(t_2) - \rho_{R1}^{S1}(t_1) + \rho_{R1}^{S1}(t_1) + \rho_{R1}^{S2}(t_1) - \rho_{R2}^{S2}(t_1)
\end{aligned} \qquad \text{(Eq. 3.7)}$$

Normally the ambiguity is found through specific methods (see chapter 3.1.6) and only the double-difference is used. The triple-difference can be used for coarse error check (Dueholm et al., 2002)

3.4 GPS errors

A number of different errors are mentioned in the previous chapters and they can be classified into two different groups. The common errors are the one that are common to all receivers operated in a limited geographic area and include satellite clock error, orbital error, ionospheric error and tropospheric error. On the other hand the on-common errors are the one that are on-common to receivers operated in the same geographical area and include receiver clock error, multipath and noise (Godha, 2006).

3.4.1 Satellite clock error

The satellite clock error is the offset of the satellite clock with respect to the GPS-time. It is getting smaller as the satellite clocks are getting better and the corrections for the error can be determined better and better by the control segment (see chapter 3.1.2). The error is typically around a few meters and changes only slowly over time. It can be fully removed by differential GPS (Misra et al., 2001).

3.4.2 Orbital error

The orbital error (also known as satellite ephemeris error) is the prediction error of the satellite position derived from the ephemeris compared to the true satellite positions. They are also slowly changing over time and gets smaller as the predicting by the control segment gets better. A typical orbital error is a few meters and can be almost fully removed through differential GPS. Large orbital errors will only occur if the baseline is very large, due to fact that the line of sight (geometrical line between the receiver and the satellite) is separated more from each other when the baseline is long. But as given in (Misra et al., 2001), an estimate of the uncompensated orbital error after performing of differential GPS is less than 5 cm.

3.4.3 Ionospheric error

The ionospheric error is the error caused by a delay of the signal as it travels through the ionosphere. The ionosphere is the layer from about 50 to 1000 km above the earth (Godha, 2006) and consist of ionized air (free electrons and ions) caused by the suns radiation. When the signal travels through the ionized air, the signal speed decrease from the vacuum speed of light and therefore results in phase advance and code delay. This can be expressed through the Total Electron Content (TEC) over the

signals entire path through the ionosphere as described in e.g. (Misra et al., 2001). The ionospheric error is typically around 2 to 20 m depending on the elevation angle but most of it can be removed through differential GPS (Dueholm et al., 2002 and Misra et al., 2002). After performing of differential GPS the ionospheric error is around 5 to 20 cm for baseline length of up to 100 km, but can be up 1 m during high ionospheric activity (Godha, 2006).

3.4.4 Tropospheric error

The tropospheric error is caused by the troposphere layer from the Earth surface and up to around 50 km above. Like the ionosphere it will cause a delay of the signal, but this delay is instead due to the moisture, pressure and temperature along the signals path in the troposphere. Normally the delay is divided into a dry and wet component. The dry component results in around 90 % of the total delay in the troposphere and is due to the dry gases. The wet component is instead a result of the moisture and is much more difficult to predict as it can vary a lot due to e.g. clouds and other weather phenomenon (Godha, 2006). The tropospheric error is uncompensated around a couple of meters but can be reduced significantly while performing differential GPS and/or meteorological modeling. The compensated error is therefore around 0.1 to 1 m after modeling and around 0.2 m after differential GPS (Misra et al., 2001). Due to longer signal path for satellites at lower elevation angels, an obliquity factor is added to the measurements (Godha, 2006).

3.4.5 Receiver clock error

The receiver clock error is the offset of the receiver clock with respect to the GPS-time. It is a constant error for the same receiver at simultaneous measurements, but is else varying with time. It is normally calculated in the least square method of a minimum of four equations of Eq. 3.4 but can also be removed from the double differences in Eq. 3.6. The receiver error can vary from a couple of meters and up to many thousand meters depending on the quality of the receiver (Godha, 2006).

3.4.6 Multipath

Multipath is the phenomenon that a signal – instead of going directly from the satellite to the receiver antenna (line of sight) – reaches the antenna after a couple of reflections performed by local reflectors

such as glass and metal. The signal path therefore gets longer and this can result in huge errors that sometimes dominate the entire error budget (Godha, 2006). Since it is a very local phenomenon it can not be removed by differential GPS. Instead a couple of different techniques have been developed in order to minimize the amount of highly reflective things close to the antenna. High elevations masks are also one of the main solutions to multipath. The error is way higher for code measurements (0 to 5 m (Dueholm et al., 2002)) compared to phase measurements (1 to 3 cm (Godha, 2006)) and it is therefore one of the biggest advantage of using phase measurements instead of code measurements.

3.4.7 Noise

Noise mainly includes receiver noise on both code and phase measurements. It is introduced by e.g. antennas and cables in the receivers and is normally estimated by an initial zero-baseline test, as it can not be reduced through differential GPS. In the test two receivers are connected to a single antenna through a signal splitter (Godha, 2006). Then performing double differencing removes all significant errors except for the receiver specific errors (noise) and multipath. The receiver noise is generally about 0.25 to 0.5 m for code measurements and only a couple of mm for phase measurements (Misra et al., 2001).

3.4.8 Satellite constellation

The accuracy of the position measurement also depends on the satellite constellation. Satellites being split apart from each other on the sky will give a more accurate position than satellites being close to each other. This is expressed through different Dilution Of Precision (DOP) values. For three dimensional positions the most common to use is the position DOP (PDOP). It is the reciprocal value of the volume spanned by the four satellites (remember that four satellites were needed to determine a position) and the receiver (Stenseng, 2002). If PDOP is less than 4 there is very good measure conditions, and up to 6 is acceptable. As future PDOP values can be predicted through knowledge of the satellite constellation in the ephemeris, the best period for measuring can be determined from home (Dueholm et al., 2002).

3.4.8 Error summary

Finally all the errors discussed in the previous chapter can be summarized in order to get an idea of the total errors for GPS measurements. A summarize is performed in table 3.1.

Error source	Uncompensated code measurement	After differential GPS
Satellite clock error	0-3 m	0 m
Orbital error	0-3 m	~ 0 m
Ionospheric error	2-20 m	0.05-0.20 m
Tropospheric error	0.5-5 m	0.1-1 m
Receiver clock error	0-10 m	0 m
Multipath	0-5 m	No effect (0-5 m)
Noise (other errors)	0.25-0.50 m	No effect (0.25-0.50 m)
Total error summary	~ 10-15 m	0-3 m

Table 3.1: Error summary (Dueholm et al., 2002, Misra et al., 2001 and Godha, 2006)

3.5 Advantages and limitations of GPS

Under good conditions will GPS be able to provide continuous and accurate positioning to the user at all time. But unfortunately good conditions will not always occur as the signal from the satellites can be blocked be e.g. mountains and high buildings. Further as the electromagnetic signal travels from the satellites to the Earth it can be influenced by magnetic fields, areas with high amount of free electrons and moisture air that cause the signal to travel slower than expected (speed of light in vacuum). At the Earth the signal can be extended by reflections from e.g. glass and the clocks onboard the satellites and in the receivers can be unsynchronized and therefore cause more errors on the signal. Some of these errors can be reduced or even removed by use of e.g. differential GPS but not all.

Hence any sophisticated urban navigation system can not depend on GPS as a stand-alone system. In stead one can integrate two (or more) different navigation systems. This dissertation uses integration of GPS with INS. The idea is that as INS solutions tend to drift with time, it will be updated as often as possible with measurements from the GPS. Further there error dynamics are totally different and uncorrelated what makes them perfect for integration (Jekeli, 2000).

4 Estimation techniques

Estimation is basically the method of obtaining unknown parameters from a set of observations. Many different estimation techniques can be used dependent on the amount of observations available and the system that want to be estimated. One of the simplest estimation techniques is the least square technique used when only measurements of the system are available. However if knowledge of the systems dynamic over time are available a better estimate of the parameters can be obtained (Godha, 2006). As most navigation systems behave as non-linear systems is it common to perform a linearization of the system (Julier et al. 2004). This chapter describes estimation techniques commonly used in integration of INS and GPS. A direct use of the techniques can be seen in chapter 5.

4.1 Estimation of dynamic systems

The dynamics of an INS system could be described as the process model given in Eq. 2.56. All subscripts indicate a certain time epoch.

$$\dot{x}_t = F_t x_t + G_t w_t \qquad \text{(Eq. 4.1)}$$

In order to compute optimal estimates of the state vector, x_t while using knowledge of the behaviors of the systems dynamic a Kalman filter is used. It is recursive algorithm that uses a series of prediction and measurement update steps with a minimum of variance (Godha, 2006).

The Kalman filter assumes that the process can be modeled as (Petovello, 2003).

$$x_{t+1} = \Phi_{t,t+1}\, x_t + w_t \qquad \text{(Eq. 4.2)}$$

Where $\Phi_{t,t+1}$ is the transition matrix of the system taking it from time epoch t to t+1 and the other variables are described at Eq. 2.56.

The transition matrix can under the assumption that the time interval between the two time epoch t and t+1 are small (high data rate) be given as an exponential function as (Gelb, 1974).

$$\Phi_{t,t+1} = e^{F_t \Delta t} = I + F_t \Delta t + \frac{(F_t \Delta t)^2}{2!} + \frac{(F_t \Delta t)^3}{3!} + \ldots \quad \text{(Eq. 4.3)}$$

Where I is the identity matrix and Δt is the time interval between the two time epoch t and t+1. Often will the higher order terms be neglected (El-Sheimy, 2006).

A measurement model is needed in the Kalman filter in order to relate the observation to the unknown parameters. The measurement model for the time epoch t can be written as (Petovello, 2003).

$$z_t = H_t x_t + \eta_t \quad \text{(Eq. 4.4)}$$

Where z_t is the observation matrix, H_t is a design matrix and η_t is the measurement noise with a covariance matrix, R_t.

When we assume that the process driving noise, w_t and the measurement noise, η_t are zero mean white noise sequences with zero correlation, an updated estimate of the state vector and its covariance can be found as (Petovello, 2003).

$$\hat{x}_t^+ = \hat{x}_t^- + K_t \nu_t \quad \text{(Eq. 4.5)}$$

$$P_t^+ = (I - K_t H_t) P_t^- \quad \text{(Eq. 4.6)}$$

Where "-" and "+" denotes before and after measurements update respectively, K_t is the Kalman gain, ν_t is the innovation sequence and P_t is the covariance.

The Kalman gain, K_t is given as (Petovello, 2003).

$$K_t = P_t^- H_t^T \left(H_t P_t^- H_t^T + R_t \right)^{-1} \quad \text{(Eq. 4.7)}$$

And the innovation sequence, ν_t is the difference between the actual observation, z_t and the predicted observation, $\hat{z}_t$ given as (Godha, 2006).

$$\nu_t = z_t - \hat{z}_t = z_t - H_t \hat{x}_t^- \quad \text{(Eq. 4.8)}$$

Hence the innovation sequence is the amount of new information being introduced into the system. If no new information is introduced to the system, the actual and the predicted observation is equal and thus follow that the updated state vector, $\hat{x}_t^+$ equals the predicted ones, $\hat{x}_t^-$. On the other hand if there is a difference between the actual and predicted observation then some new and unpredictable information is introduced to the system. As measurements contain measurement noise (see Eq. 4.4) it is not given that the system should fully accept the new measurement. The Kalman gain matrix is therefore a weighting factor that indicates how much of the new information that should be accepted in order to produce a minimum of error variance. If the measurement noise covariance, R_t is small then the Kalman gain will be large as the measurement is very reliable, but on the other hand if the measurement noise covariance is small then the Kalman gain will be small as the measurement contain noise.

The predicted state vector and its covariance forward in time can be found as (Petovello, 2003).

$$\hat{x}_{t+1}^- = \Phi_{t,t+1} \hat{x}_t^+ \quad \text{(Eq. 4.9)}$$

$$P_{t+1}^- = \Phi_{t,t+1} P_t^+ \Phi_{t,t+1}^T + Q_t \quad \text{(Eq. 4.10)}$$

Where $\Phi_{t,t+1}$ is the transition matrix given as in Eq. 4.3 and Q_t is the process noise matrix given as (Godha, 2006).

$$Q_t = \int_t^{t+1} \Phi_{C,t,t+1} \, G(t) \; Q_C(t) \; G^T(t) \; \Phi_{C,t,t+1}^T \, dt \quad \text{(Eq. 4.11)}$$

Where $\Phi_{C,t,t+1}$ is the continuous-time transition matrix between the two time epoch t and t+1, Q_C is the continuous-time spectral density matrix of w_t and $G(t)$ is defined in Eq. 2.56.

Combining Eq. 4.5, 4.6, 4.7, 4.9 and 4.10 results in a step by step Kalman filter algorithm as figure 4.1.

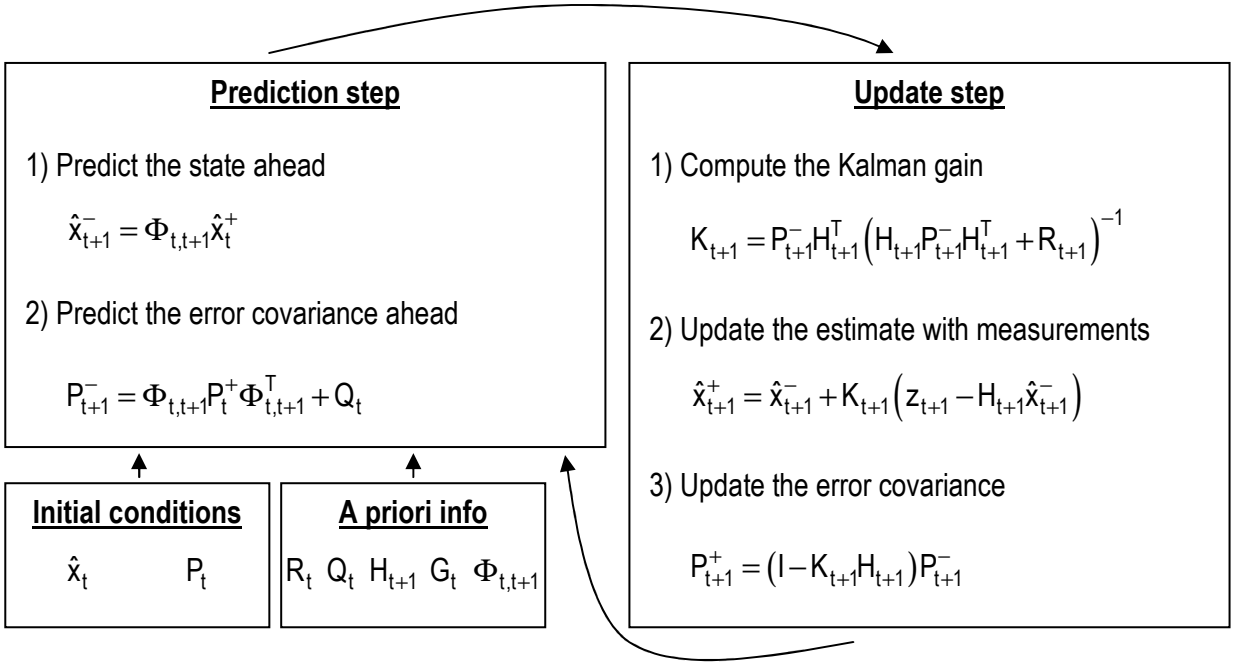

Figure 4.1: Step by step Kalman filter algorithm

The above section describes a Kalman filter used when the process model in Eq. 4.1 and the measurement model in Eq. 4.4 are assumed to be linear. However in many situations non-linear process models or non-linear measurements model occur. Hence a linearization technique is therefore needed in order to linearize the non-linear models and then use the Kalman filter algorithm in figure 4.1 (Godha, 2006).

4.2 Estimation of non-linear systems

A non-linear process model and measurement model can be given as (Petovello, 2003).

$$\dot{x}_t = f(x_t, t) + G_t w_t \qquad \text{(Eq. 4.12)}$$

$$z_t = h(x_t, t) + \eta_t \quad \text{(Eq. 4.13)}$$

Where f and h are non-linear functions representing the behavior of the process model and the relation relating between the state and the observation respectively.

In order to linearize Eq. 4.12 and 4.13 a nominal state vector, x_t^* is selected as (Godha, 2006).

$$x_t = x_t^* + \delta x_t \quad \text{(Eq. 4.14)}$$

Where δx_t is the perturbation from the nominal state vector value.

If it can be assumed that the perturbation from the nominal state vector are small, a first order Taylor series expansion of Eq. 4.12 and 4.13 can be performed about the nominal state vector as (Godha, 2006).

$$\delta x_t = \Phi_{t,t+1}\delta x_t + w_t \quad \text{(Eq. 4.15)}$$

$$\delta z_t = H_t \delta x_t + \eta_t \quad \text{(Eq. 4.16)}$$

In stead of process and measurement models expressed by the state vector (see Eq. 4.2 and 4.4), Eq. 4.15 and 4.16 forms new linear models expressed by the error state vectors, δx_t and the difference between the actual and predicted measurements δz_t (Godha, 2006).

If the linearization is done about the nominal state vector as described above the Kalman filter is called a Linearized Kalman Filter (LKF). However if the linearization is done about the last computed solution, x_{t-1} the Kalman filter is called an Extended Kalman Filter (EKF) (Petovello, 2003).

After the linearization the Kalman filter algorithm from figure 4.1 can be used in order to obtain the errors state estimate, δx_t and Eq. 4.14 can be used to obtain the state vector, x_t (Godha, 2006).

4.2 Reliability testing

As the update measurement used in the previous sections can contain errors a test for detecting such errors (blunders) is needed in order to maintain the optimal state. The ability to identify and reject errors is called reliability and it is performed via testing of the innovation sequence (difference between the actual and predicted observation, see Eq. 4.8). If the measurement comes from e.g. GPS the errors could due to e.g. multipath or poor satellite geometry (see chapter 3). Such errors are not detected by the measurement model since they are distinct from the measurement noise in Eq. 4.4 (Godha, 2006 and Petovello, 2003).

By testing the innovation sequence one will find that any measurement outlier will cause the innovation sequence to depart from the otherwise zero mean and normally distribution given as (Godha, 2006).

$$\nu_t \sim N\left(0, \sigma_{\nu,t}\right) \qquad \text{(Eq. 4.17)}$$

Where $\sigma_{\nu,t}$ is the variance of the innovation sequence at time t given as (Godha, 2006).

$$\sigma_{\nu,t} = H_t P_t^{-} H_t^T + R_t \qquad \text{(Eq. 4.18)}$$

Where all variables are described in the previous sections. In stead the innovation sequence will be biased and follow a normally distribution given as (Godha, 2006).

$$\nu_t \sim N\left(M_t \nabla_t, \sigma_{\nu,t}\right) \qquad \text{(Eq. 4.19)}$$

Where M_t is a design matrix that maps the outlier, ∇_t into the observations at time t.

In order to detect the outlier a global Chi-Square test is performed for two hypotheses (bias free and biased) with the number of freedoms equal to the assumed number of outliers (Petovello, 2003). An isolation of the outlier can then be done by a local Chi-Square test.

The reader can see more about reliability testing in (Petovello, 2003).

5 Integration of INS and GPS

Integration of INS and GPS data can be done by several methods. This chapter discusses the most common methods followed by a description of the conditions of the lever arm effect and the time synchronization problems.

5.1 Integration methods

The basic of all methods used in integration of INS and GPS data is that the IMU provide the reference trajectory while the GPS serves as the updating system. This is mainly due to the fact that the INS measurement frequency is many times higher than the one from GPS (normally around 100–400 Hz for INS and 1–10 Hz for GPS) (Jekeli, 2000). The state vector parameters will therefore be determined with high frequency but only updated (corrected) with low. The main difference between them then lies in the data flow. Some methods share the same data e.g. the raw INS and GPS data in a common filter while other use the data individual of each other in separate filters. Further some methods provide feedback information to improve its performance while others don't (Godha, 2006).

As the loose and tight integration strategy are the most commonly used methods (Petovello, 2003) they will be used in the later data analysis and will be discussed the most. Two other methods will be mentioned briefly.

5.1.1 Loose integration

The loose integration method contains two different Kalman filters that operates individual of each other. One for the GPS measurements (called the GPS Kalman filter) and one for the INS measurements (called the INS Kalman filter). The two filters are discussed further in chapter 5.2.1 and 5.2.2. The basic step in the loose integration method can be described through the following steps (Jekeli, 2000).

1) Processing of the raw GPS measurements through a GPS Kalman filter in order to determine the position and velocity from GPS, $\left(r^n_{GPS}, v^n_{GPS}\right)$.

2) Processing of the raw INS measurements, $\left(\Delta\theta^b_{ib}, \Delta v^b\right)$ through the mechanization equations in order to determine the position and velocity from INS, $\left(r^n_{INS}, v^n_{INS}\right)$.

3) Use of the position and velocity from 1) as input to an INS Kalman filter. The filter takes the difference between the position and velocity from 1) and 2), $\left(\Delta r^n, \Delta v^n\right)$ in order to determine the error estimates of the position and velocity, $\left(\delta r^n, \delta v^n\right)$ plus the misalignment error, $\left(\varepsilon^n\right)$.

4) Use the error estimates from 3) to update the position and velocity from 2) in order to get a full state vector, $\left(r^n, v^n, R^n_b\right)$.

The loose integration method is shown in figure 5.1.

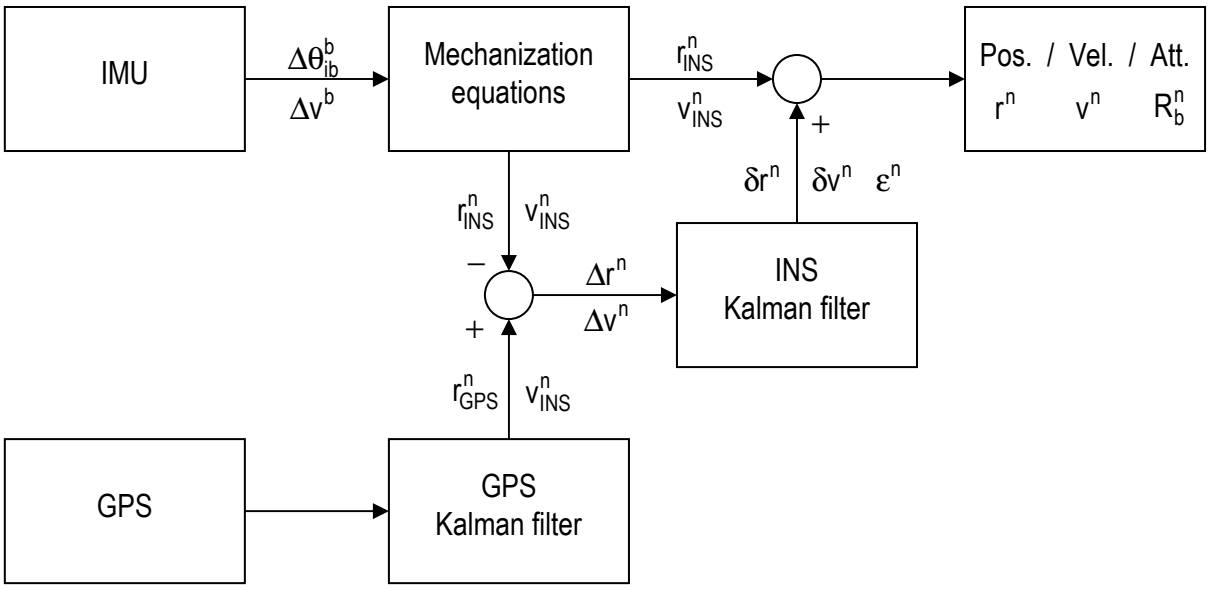

Figure 5.1: Loose integration

The advantage of the loose integration method is mainly its simplicity in implementation and its robustness, as if one of the sensors (INS or GPS) fail, a solution is still given by the other sensor

(Godha, 2005). Other advantage of the loose integration can be seen in the processing time of the algorithm due to generally smaller state vectors (Petovello, 2003). This is not discussed further here as all processing is done in post-mission and the processing time is then only of minor importance.
The disadvantage is mainly that it is impossible to provide measurement update from the GPS filter during poor GPS cover (less than four satellites). This is not the case for the tight integration method and therefore one of the reasons why tight integration method often do better than loose integration especially in urban areas (Godha, 2006). Due to the two different Kalman filters the loose integration strategy in some literature is referred to as the decentralized integration method (Jekeli, 2000).

5.1.2 Tight integration

The tight integration method contains only a single Kalman filter (called the INS/GPS Kalman filter). The filter is discussed further in chapter 5.2.3. The basic step in the tight integration method can be described through the following steps (Godha, 2006)

1) Processing of the raw INS measurements, $\left(\Delta\theta_{ib}^{b}, \Delta v^{b}\right)$ through the mechanization equations in order to determine the position and velocity from INS, $\left(r_{INS}^{n}, v_{INS}^{n}\right)$.

2) Use the raw GPS ephemeris information and the position and velocity from 1) to predict pseudoranges and Doppler measurement, $\left(\phi_{INS}, \dot{\phi}_{INS}\right)$.

3) Use of the predicted pseudorange and Doppler measurements from 2) as input to an INS/GPS Kalman filter. The filter takes the difference between the pseudorange and Doppler measurements from 2) and the raw GPS pseudorange and Doppler measurements, $\left(\phi_{GPS}, \dot{\phi}_{GPS}\right)$ in order to determine the error estimates of the position and velocity, $\left(\delta r^{n}, \delta v^{n}\right)$ plus misalignment error, $\left(\varepsilon^{n}\right)$.

4) Use the error estimates from 3) to update the position and velocity from 1) in order to get a full state vector, $\left(r^{n}, v^{n}, R_{b}^{n}\right)$.

The main advantage of the tight integration is that even during poor satellite coverage (less than four satellites) updating of the INS can still be performed. This is due to the use of predicted and raw pseudorange and Doppler measurements (Godha, 2005). The tight integration is therefore mainly used in urban areas where it is common that the GPS solution falls out now and then.

The disadvantages are mainly that the state vector increases in size, due to single Kalman filter with both INS and GPS measurements, and this leads to larger processing times (Petovello, 2003). Due to the main (and only) Kalman filter the tight integration strategy in some literature is referred to as the centralized integration method (Jekeli, 2000).

The tight integration method is shown in figure 5.2.

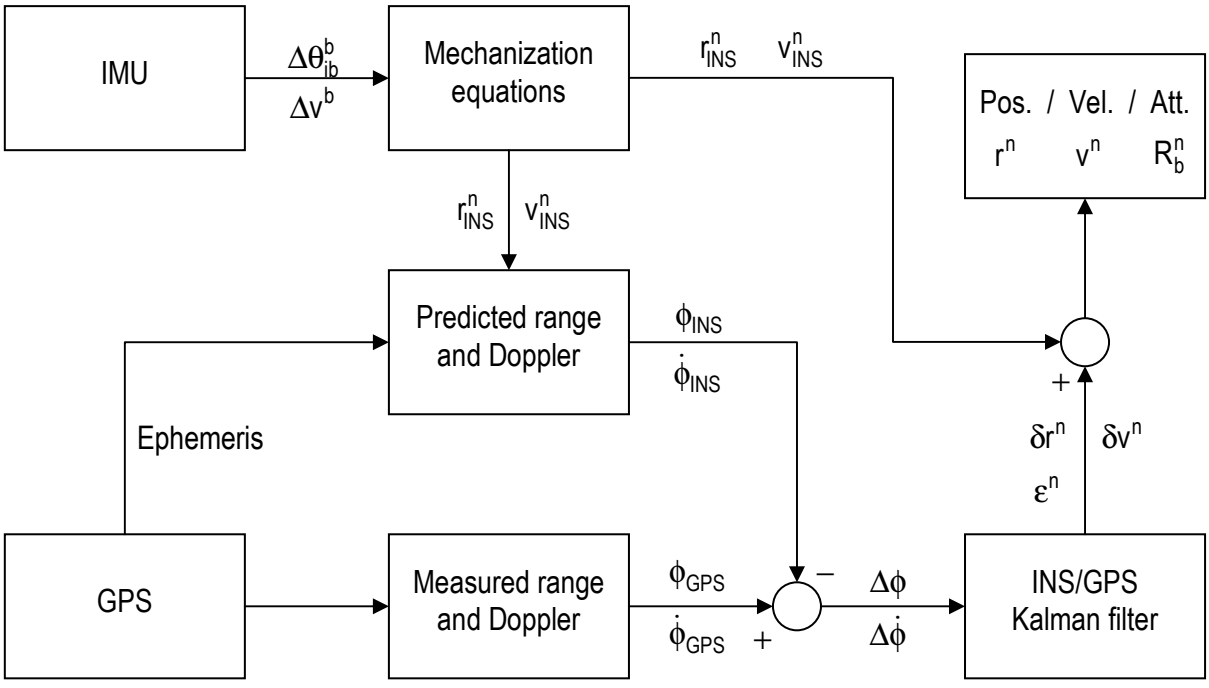

Figure 5.2: Tight integration

5.1.3 Other integration methods

Of other integration methods are the “uncoupled” and the “deep/ultra-tight” integration the most common. The first is a simple method that uses the GPS solution if available and otherwise uses the

INS solution. When the GPS solution is available it resets the INS position and velocity to the current one from the GPS. The system gives no feedback of errors estimate back to the mechanization equation so the position and velocity error will keep increasing during periods with no GPS solutions (Jekeli, 2000). This method is normally not very accurate and is therefore not used in high-accuracy navigation systems (Petovello, 2003).

The second methods combine the INS and GPS in an extremely tight way (therefore the name ultra-tight) with update from GPS to INS solutions and aiding the reverse way. It requires access to the GPS receiver firmware and is therefore mainly used by the manufacturers of the GPS (Petovello, 2003).

5.1.4 Implementation strategies

There are mainly two different ways to implement the loose and tight integration. One is called “closed loop” or “feedback” and the other is called “open loop” or “feed forward”. In the “closed loop” all the error estimates plus misalignment error from either the INS Kalman filter (loose integration) or the INS/GPS Kalman filter (tight integration) is used to correct the mechanization parameters. The mechanization equation therefore propagates small errors (Godha, 2006). From the two mentioned Kalman filters estimates of the bias for both accelerometers and gyroscopes is possible output. These bias estimates are therefore feed back to raw sensor output and used in the known error compensation (see chapter 2.6.1).

In the “open loop” no error estimates, misalignment errors or sensor bias are send back to the mechanization equation or the raw sensor output. The errors will therefore grow more rapidly and some of the neglected second order terms in the mechanization equations could be of significant impact (Godha, 2006). “Open loop” implementation is therefore only possible for high end inertial sensors as there sensor errors are small.

In stead the “closed loop” implementation is used where sensor errors are large e.g. in low cost MEMS-based IMUs. The “closed loop” implementation is shown in figure 5.3. Only the relevant part of the loose and tight integration is shown as the rest is shown in figure 5.1 and 5.2.

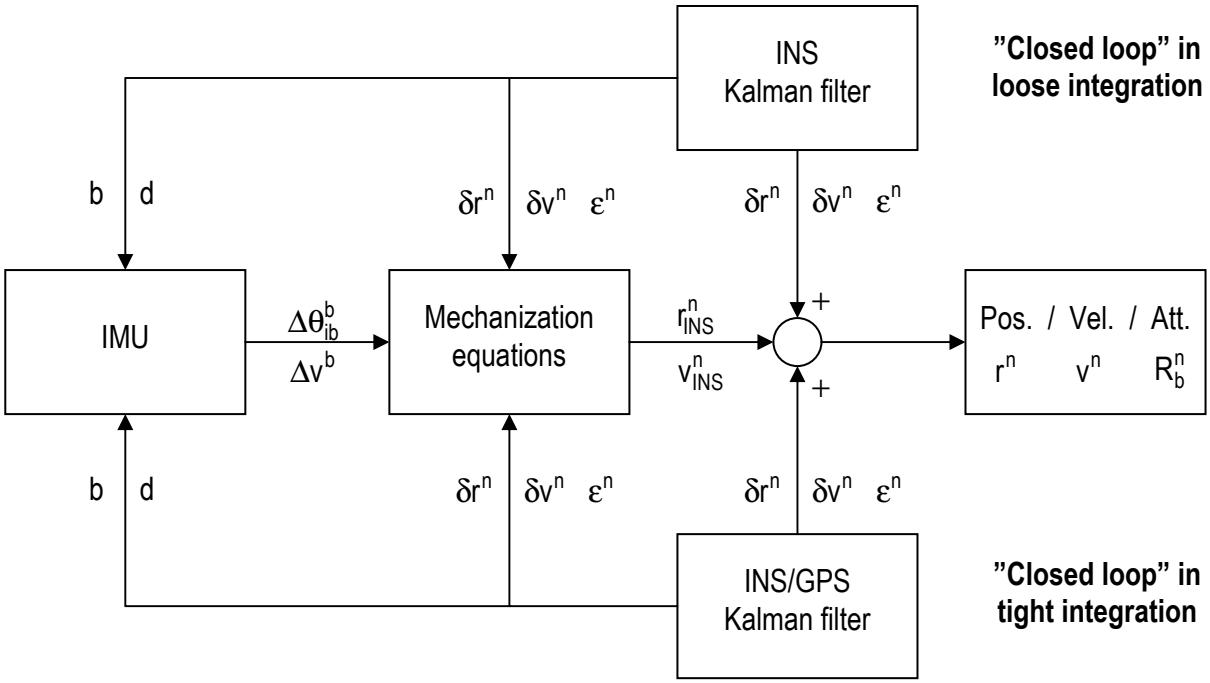

Figure 5.3: Closed loop implementation for loose and tight integration

5.1.5 INS and GPS Kalman filters

As mentioned in the previous chapter a number of different Kalman filter are used in the loose and tight integration methods. They will not be described further in this dissertation but the reader can see more in e.g. (Godha, 2006 and Petovello, 2003).

5.2 Lever arm effect

Since both the IMU and GPS cannot be installed at the same place the position and velocity of the IMU is different from the one of the GPS. This is called the lever arm effect (Shin, 2001). In order to correct this, knowledge of the vector from the centre of the IMU and to the GPS antenna must be known. Usually this is done through a total station survey in a temporary mapping frame (m-frame) and the vector is given as (El-Sheimy, 2006).

$$\ell^m = \begin{pmatrix} X^m_{IMU} - X^m_{GPS} \\ Y^m_{IMU} - Y^m_{GPS} \\ Z^m_{IMU} - Z^m_{GPS} \end{pmatrix} \quad \text{(Eq. 5.X)}$$

Where ℓ^m is the lever arm vector in the mapping frame and $(X,Y,Z)^m_{IMU/GPS}$ are the coordinate of the IMU and the GPS respectively given in the mapping frame. Either the rotation matrix between the body frame, and mapping frame, R^b_m or the rotation matrix between the navigation frame and the mapping frame, R^n_m must be known in order to calculate the corrected position of the IMU as (Shin, 2001).

$$r^n_{IMU} = r^n_{GPS} - \begin{pmatrix} \frac{1}{M+h} & 0 & 0 \\ 0 & \frac{1}{(N+h)\cos\varphi} & 0 \\ 0 & 0 & -1 \end{pmatrix} R^n_m \, \ell^m \quad \text{(Eq. 5.X)}$$

Where r^n_{IMU} and r^n_{IMU} are the curvilinear coordinates of the IMU and GPS respectively expressed in the navigation frame. The corrected velocity can be calculated as (Shin, 2001).

$$v^n_{IMU} = v^n_{GPS} + \left(\Omega^n_{ie} + \Omega^n_{en}\right) R^n_b \ell^b - R^n_b \Omega^b_{ib} \ell^b$$

Where r^n_{IMU} and r^n_{IMU} are the velocity of the IMU and GPS respectively as described in the (ENU) navigation frame, $\left(\Omega^n_{ie}, \Omega^n_{en}\right)$ are the skew symmetric matrices of the vectors in Eq. 2.20 and 2.21 and Ω^b_{ib} is the skew symmetric matrix of the gyroscope measurements.

5.3 Measurement time and synchronization

As the IMU and GPS measurements usually are made at different time the IMU position and velocity need to be interpolated or extrapolated in order to coincide with the GPS measurements. If instead the last IMU measurements before the GPS measurement was used an error will occur that for high

dynamic vehicles (e.g. aircrafts) could be a couple of meters for a 100 Hz IMU (El-Sheimy, 2006). Even for low dynamic vehicle (e.g. cars) the interpolation/extrapolation is still done.

A linear interpolation method between the IMU measurements before and after the GPS measurement is usually enough and can be performed as (Shin, 2001)

$$r^n_{t_{GPS}} = \frac{t_k - t_{GPS}}{t_k - t_{k-1}} r^n_{t_{k-1}} + \frac{t_{GPS} - t_{k-1}}{t_k - t_{k-1}} r^n_{t_k} \quad \text{(Eq. 5.X)}$$

$$v^n_{t_{GPS}} = \frac{t_k - t_{GPS}}{t_k - t_{k-1}} v^n_{t_{k-1}} + \frac{t_{GPS} - t_{k-1}}{t_k - t_{k-1}} v^n_{t_k} \quad \text{(Eq. 5.X)}$$

Where the time subscript refer to the time epoch in figure 5.4.

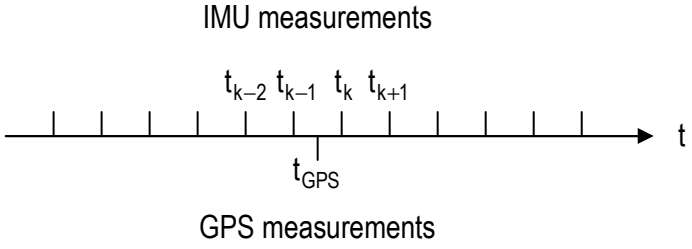

Figure 5.4: IMU and GPS measurements

If high dynamic vehicles are used other integration techniques must be used. Usually the La-grange interpolation is used. More about the La-grange interpolation can be seen in e.g. (Shin, 2001). Further it can be mentioned that if the IMU isn't time tagged with GPS-time, synchronization need to be done. This is done by use of the 1 pulse per second signal send from the GPS to the computer that collects the IMU measurement (El-Sheimy, 2006).

6 MATLAB program

In order to analyze the performance of the INS and GPS integration theory as described in the previous four chapters, a program was created in MATLAB.

6.1 Program objective and expectations

The main objective of the program was to integrate INS and GPS data in a post-mission mode. The input to the program was data from two GPS receivers working in differential mode and from an IMU placed in a rigid body with the rover. The data from the GPS receivers were observation data (that contained the raw code, phase and Doppler measurements) and navigation data (that contained the ephemeris parameters). Only the navigation data from the master receiver was used. The input format was limited to the following format:

Observation data (GPS)	Binary files and RINEX obs. files
Navigation data (GPS)	Binary files and RINEX nav. files
IMU data	Binary files and text files

Table 6.1: Input formats

The binary and text files where easy to load into the program as all data where stored in rows (for each measurement epoch) with equal number of columns (for all the measured variables). In loading the RINEX files other methods had to be used as some of the information where written in a header where the program had to perform a search in the header labels. Further all the observation where written in groups with different amount of rows depending on how many satellites where available. The process made it a little more difficult to read RINEX files compared to more raw measurement files from the receiver in either binary or text files format.

Many expectations were put in the program, but some had to be limited. The loose integration was given most attention and therefore the method that was tried implemented first. The tight integration could then be implemented at a later stage. For the loose integration the INS and GPS derived positions where calculated independent of each other and the program could therefore be split in two different parts.

The first part calculates the GPS derived position by using the differential method. The implementation strategy for this part could be expressed by the following steps.

1. Calculate the coordinates for the satellites by using the ephemeris data from the navigation file.
2. Calculate the (true) ranges between the satellites and the master station by using the coordinates from 1. and the known coordinates from the master station (initial condition).
3. Calculate the range between the satellites and the master station by using the pseudorange and carrier phase measurements from the observation file. This is done by carrier smoothing where the very accurate range differences derived from carrier phase complements the pseudorange measurements.
4. Calculate corrections for the difference between the ranges from 2. and 3.
5. Calculate the ranges between the satellites and the GPS receiver by using the pseudorange and carrier phase measurements from the observation file (same procedure as for 3.).
6. Add the corrections from 4. to the ranges from 5.
7. Calculate the position of the GPS receiver by using the corrected ranges from 6. This is done through the least square method.

The next part calculates the INS derived position by using the mechanization equation described in chapter 2.6. Before the mechanization can be used an alignment over a user specified interval has to be done in order to determine the rotation matrix between the body frame and the navigation frame. A search for the first kinematic measurement is found by analyzing the difference between two successive GPS derived positions. A stop criterion can be a difference of e.g. 5 cm/s. From the first kinematic

measurement the start time of alignment can be calculated and the alignment can be performed as described in chapter 2.4. The user specified alignment interval can eventually be calculated according to the wanted azimuth accuracy and the angle random walk of the gyroscopes.

When the rotation matrix is calculated in the alignment procedure, the mechanization equation can be used to estimate a new INS-derived position and velocity. The difference between these and the one derived from GPS is then used in a Kalman filter (according to chapter 5.1.1) in order to get error estimates of the position and velocity together with misalignment error. These are then used to update the INS-derived position and velocity (these are the final guidance estimates) and calculate a new rotation matrix that can be used with a new set of measurements in the same way.

6.2 Program bugs

When the programming started a number of problems occurred. The first was that the corrections to the calculated and true ranges for some satellites were too high (up to a couple of hundred kilometers!!). There was surely a bug in the differential part of the program but even during intense debugging the bug wasn't found. In order to limit the expectations and still perform the integration of INS and GPS data, Trimble Geomatics Office (TGO) was used to the differential part of the program. When the observation and navigation data were processed in TGO, the position could be exported to a file and then loaded into the program.

A second problem occurred when the mechanization equation was implemented. Apparently another bug occurred here and it resulted in wrong INS derived positions. The program code was again checked for errors but not even after intense debugging the bug was found. The bug resulted in wrong INS derived position when it was compared to the GPS derived positions. Of cause errors between them could occur (especially the INS stand alone position was expected to drift away from the GPS derived), but when the same trajectory was plotted over a short period (100 seconds) the INS simply couldn't

keep up with the GPS derived. This can be seen in figure 6.1 where the two lines indicate the GPS and INS derived trajectory for the same time interval.

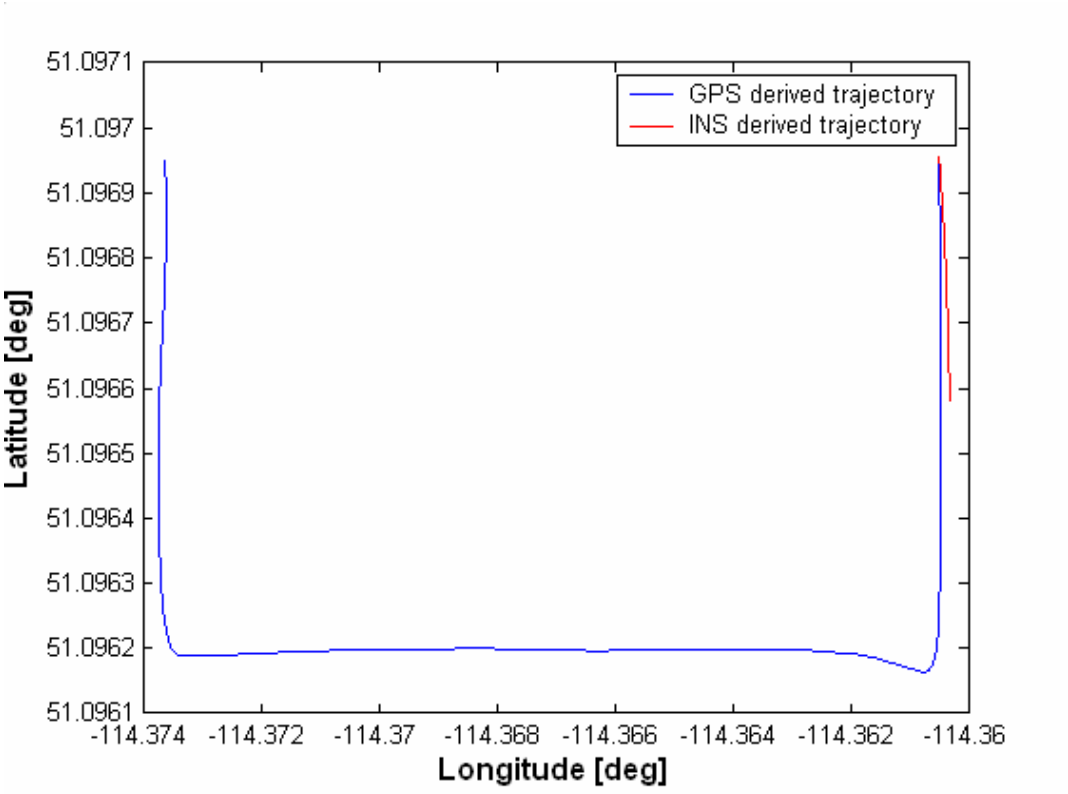

Figure 6.1: Trajectory from own program with bug (the GPS and INS derived trajectory should have been same length!)

If it wasn't known, the INS derived trajectory errors in figure 6.1 would look like drift errors. But as the two trajectories were expected to be the same length (they are plotted over the same time interval), something was wrong. Further it looks like the INS derived position just kept following a line without changing orientation. But on figure 6.2 the beginning of the two trajectories are plotted and it can be seen that the INS derived position actually changes orientation in the beginning. A check for the IMU data has also been performed as the GPS derived trajectory is from the GPS only measurements. An error in the INS data would therefore make it impossible to compare the two results. Unfortunately no error was found in the INS data (the raw gyroscopes measurement showed the same swing tendency as on the GPS derived trajectory). The error was therefore somewhere in the mechanization equations but became unfound.

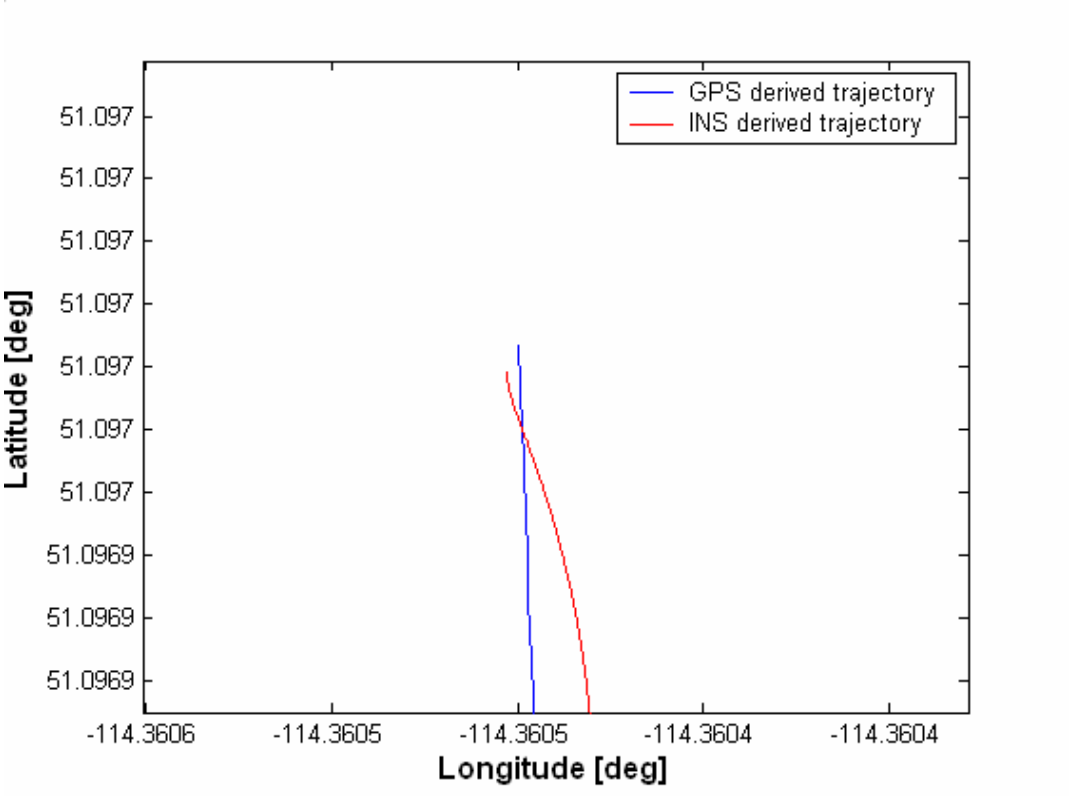

Figure 6.2: Zoom in on the start of the two trajectories from figure 6.1

Due to the unfound bugs of the program another method had to be used in order to analyze integrated INS and GPS data. During my month in Calgary I used a complete INS and GPS integration program from the University of Calgary to some different processing. To my luck I was still having the processed data and could therefore use them in the data analysis in chapter 7. Further processing than the one already done was impossible as the program was encoded and needed a special program key to run.

6.2.1 Program run from CD

The reader can see the code of all the program files and data files on the enclosed CD following this dissertation. The program that results in figure 6.1 and 6.2 can be seen by running the MATLAB m-file "GINIS.m". Make sure that all the other files contained on the CD are in the same directory as "GINIS.m" when running it.

It is the program files named "Alignment.m" and "MechanizationEquation.m" that have a bug.

7 Data analysis

This chapter presents a data analysis performed on output from processed INS and GPS data. The main objectives is to assess the integrated systems performance hereby determine the position and velocity accuracy during data outages and under different conditions. Details of the data and the analysis method used are presented first followed by determination of the position, velocity and attitude accuracy. Finally the time in which the ambiguities are fixed after a data outages are presented followed by a small analysis of the accelerometer and gyroscopes bias calculated during the processing.

As the MATLAB program had some hidden and unfound bugs (see chapter 6) the data analysis had to be done with use of another program. In stead the C++ class based SAINT™ (Satellite And Inertial Navigation Technology) software was used.

7.1 SAINT™

SAINT™ was developed in 2003 by the Position, Location and Navigation (PLAN) group in the Department of Geomatics Engineering at the University of Calgary at the University of Calgary. It is a software that is capable of integrating data from INS and GPS in order to obtain precise estimates of position, velocity and attitude in both real-time and post-mission mode. All data analysis was done in post-mission mode.

The software starts with reading an option file in which the user can select different processing strategies and specify different parameters and variables including simulated GPS data outage (gaps). Once the option file was successfully read all data processing happened automatically. After processing a wide variety of output files was available. It is the data from the different output files that are analyzed in the following sections.

7.2 Test data

The test data was collected by Saurabh Godha in February 2005 as part of another GPS/INS project. They test area was situated west of Calgary near Spring Bank airport and was selected because it provided good satellite visibility and had some reference pillars with well known coordinates. This made it possible to determine a good reference trajectory before GPS data outages were simulated in SAINT™. The dataset began with a static alignment period of about 12 minutes and were followed by 30 minutes of kinematic data. The kinematic data were split up by five short periods of 1-2 minutes with zero velocity update. The zero velocity update was not used in this data analysis. Figure 7.1 show the reference trajectory in an east-north coordinate system with marks where the static alignment and ZUPT were done including the position of the master station. In order to make it easier to compare two coordinates all positions are transformed into a local north-east-up (N,E,U) frame with origin at the place where the static alignment were done. As the terrain around Spring Bank is relatively flat only the east and north trajectory are shown in figure 7.1 and 7.2.

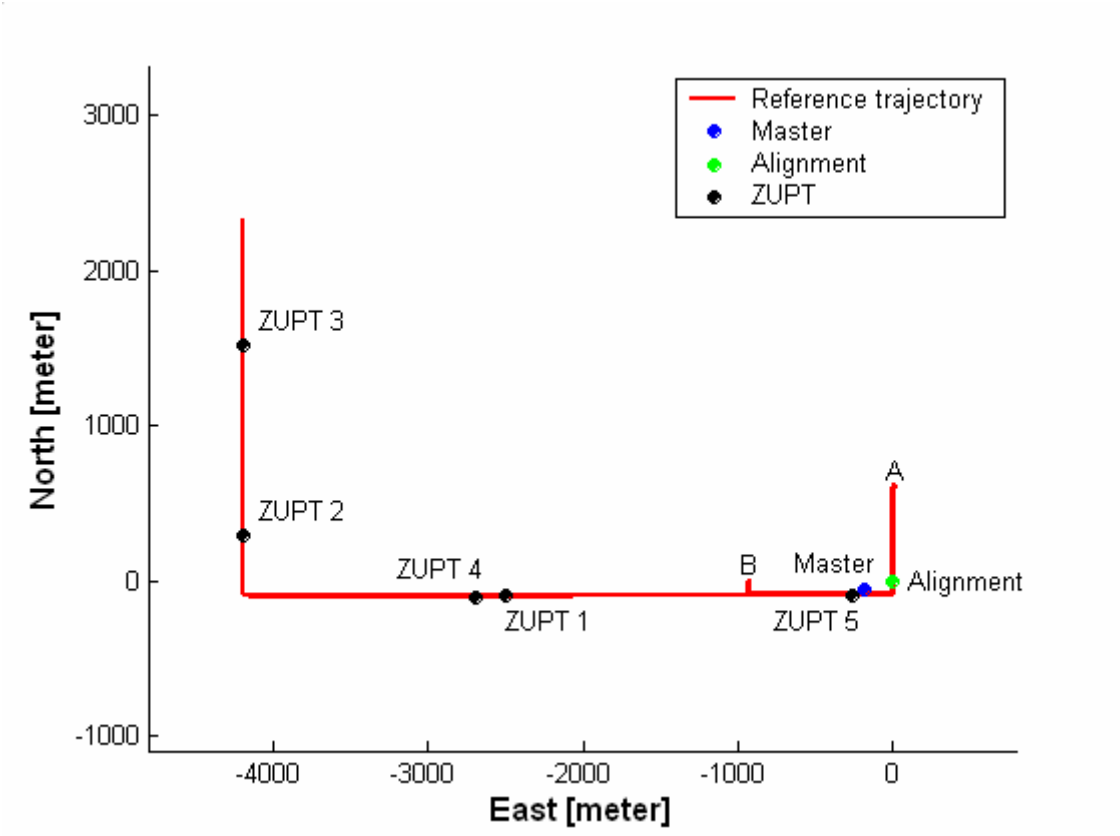

Figure 7.1: Reference trajectory

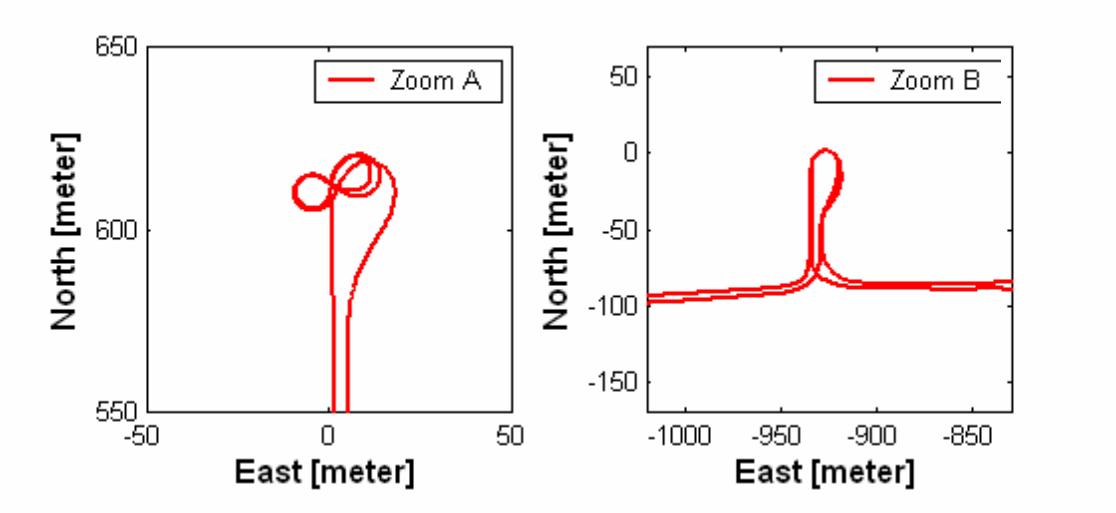

Figure 7.2: Zooms at the reference trajectory

As it can be seen the test data were measured in a trajectory with both turns and straight forward driving. This was done in order to imitate different dynamic performance. Due to the chosen area most of the roads were going east-west or north-south, so during two turnaround situations marked A and B a couple of circular movements were done. These areas are shown in two zoomed windows.

7.2.1 Measurement instruments

The IMU and GPS that was used in collection of the test data were the tactical grade Honeywell HG 1700 AG11 and the NovAtel OEM4 dual-frequency receiver with a NovAtel 600 antenna. The IMU data was time tagged with the GPS-time from the GPS and the synchronization was expected to be better than 1 ms (Petovello, 2003). Both the master and rover were using the above mentioned receivers and antennas. The IMU and GPS for the rover were rigidly fixed to a wooden board that was mounted to the roof of a test van from University of Calgary. The lever arm between the GPS antenna and IMU was measured with a total station (Godha, 2006). Technical specifications of the IMU are seen in table 7.1.

Specifications for HG 1700	**Accelerometers**	**Gyroscopes**
Bias (1σ)	1.000 μg	1 deg/hr
Scale factor (1σ)	300 ppm	150 ppm
Random walk (max)	0.00216 m/s/√hr	0.125 deg/√hr

Table 7.1: Specifications for Honeywell HG 1700 tactical grade IMU (Petovell0, 2003 and Godha, 2006)

7.3 Analysis method

In order to perform the data analysis two different trajectories were needed. The first computed the reference trajectory with constant full coverage of GPS, while the second computed a trajectory with simulated GPS data outages (only INS measurements during the GPS outage). The difference between the two trajectories during and after the GPS outages was then used in the analysis of how well the integrated INS/GPS solution was computed.

7.3.1 Processing parameters

Before processing of the data a lot of parameters and variables were determined in the option file. Most of the parameters were kept fixed during all data processing and only two parameters were chosen to be changeable in order to analyze there impact on the performance. As the data weren't collected with this dissertation in purpose, the changeable parameters could have been chosen better if further processing were possible (this were not the case due to the encoding of the program and the need for a special program key). Table 7.2 shows important parameters and variables determined in the option file.

Constant parameters	
Parameter	*Fixed values*
Coarse alignment time [s]	90
Fine alignment time [s]	600
Elevation mask [deg]	10
Use Code measurements	Yes
Code standard deviation [m]	0.50
Use L1 Doppler measurements	Yes
L1 Doppler standard deviation [m/s]	0.03
L1 carrier phase standard deviation [m]	0.03
L2 carrier phase standard deviation [m]	0.025
Changeable parameters	
Parameter	*Values*
Phase measurements	L1 / WL
INS/GPS integration strategy	Tight / Loose

Table 7.2: Constant and changeable parameters during the data processing in SAINT™ (Petovello, 2003 and Godha, 2006)

As seen in table 7.1 only the choice of phase measurements, L1 or Wide Lane (a linear combination of L1 and L2) and the GPS/INS integration strategy was changeable during processing. Comparison between the changeable values is analyzed in chapter 7.4.

7.3.2 Reference trajectory

The reference trajectory was performed by using both GPS and INS measurements in order to get the highest quality. Of the two changeable parameters from table 7.4, L1 and tight integration was used. It was expected that L1 had lesser noise than WL, and that tight integration was better than loose because even during poor satellite coverage (less than four satellites) updating of the INS could still be performed (Petovello, 2003).

As it can be seen in figure 7.3 the GPS satellite visibility was good during the test. The average number of satellites being tracked were a little more than 7 and a minimum of 6 satellites were all the time available. Unless other is mentioned all figures and plots are from the start of the alignment and to the end of the kinematic measurements.

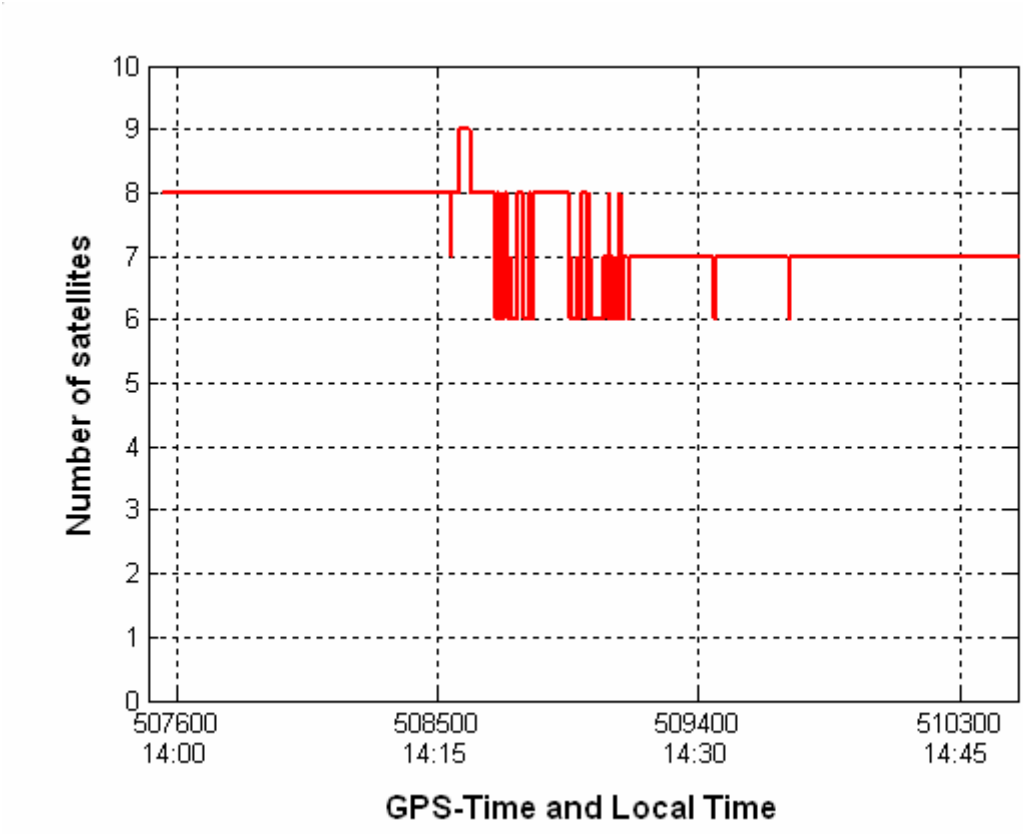

Figure 7.3: Satellite availability

Fixed ambiguities were found for all the satellites except for one (satellite 21) during the static alignment and kept during all dynamic mode. This can be seen in appendix A. The problem with satellite 21 was that it became visible during the dynamic mode and had problem solving its ambiguity to a fixed value on-the-fly. But as it were the only one of the satellites with ambiguity problems, the position accuracy was still expected to be high.

Further the distance from the vehicle to the master was only between 0 and 4.7 km as seen on figure 7.1 and the accuracy of the differential GPS solution was therefore expected to be good as the orbital, tropospheric and ionospheric errors could be corrected very precise (see also chapter 3.4).

All of the above mentioned have been relate to the GPS measurement, but in order to evaluate the influence of the INS measurement, the magnitude of the corrections applied to the INS derived position, velocity and attitude from GPS update are shown in table 7.3. It gives a good indication of how smooth the reference trajectory is, as large corrections after each update will result in a saw tooth like behavior of the trajectory.

Position correction		**Velocity correction**		**Attitude correction**	
East	5,1 mm	*East*	1.8 mm/s	*Pitch*	0.14 mrad
North	4.7 mm	*North*	1.5 mm/s	*Roll*	0.30 mrad
Up	3.3 mm	*Up*	0.8 mm/s	*Azimuth*	0.41 mrad
3D	7.6 mm	*3D*	2.4 mm/s	-	

Table 7.3: RMS corrections of INS position, velocity and attitude during GPS update for reference trajectory

As the three-dimensional (3D) RMS (root mean square) correction is at centimeter level for the position, it is expected that the reference trajectory is accurate to a couple of centimeters in 3D position at all time. The 3D velocity is at the same time accurate to about 3 mm/s and therefore will the reference trajectory be good enough to compare with during the next sections. Further as the precision is at centimeter level all fixed ambiguities that where found are assumed to be correct as they are significant small compared to a wavelength of both the L1 and WL (Petovello, 2003).

7.3.3 Simulated GPS data outage

In order to analyze the performance of integrated INS and GPS data, five different GPS data outage (gaps) were simulated. The gaps were selected to encompass different dynamic situations of a vehicle and the duration were up to 40 seconds for each gap. The locations of the gaps are shown in figure 7.4.

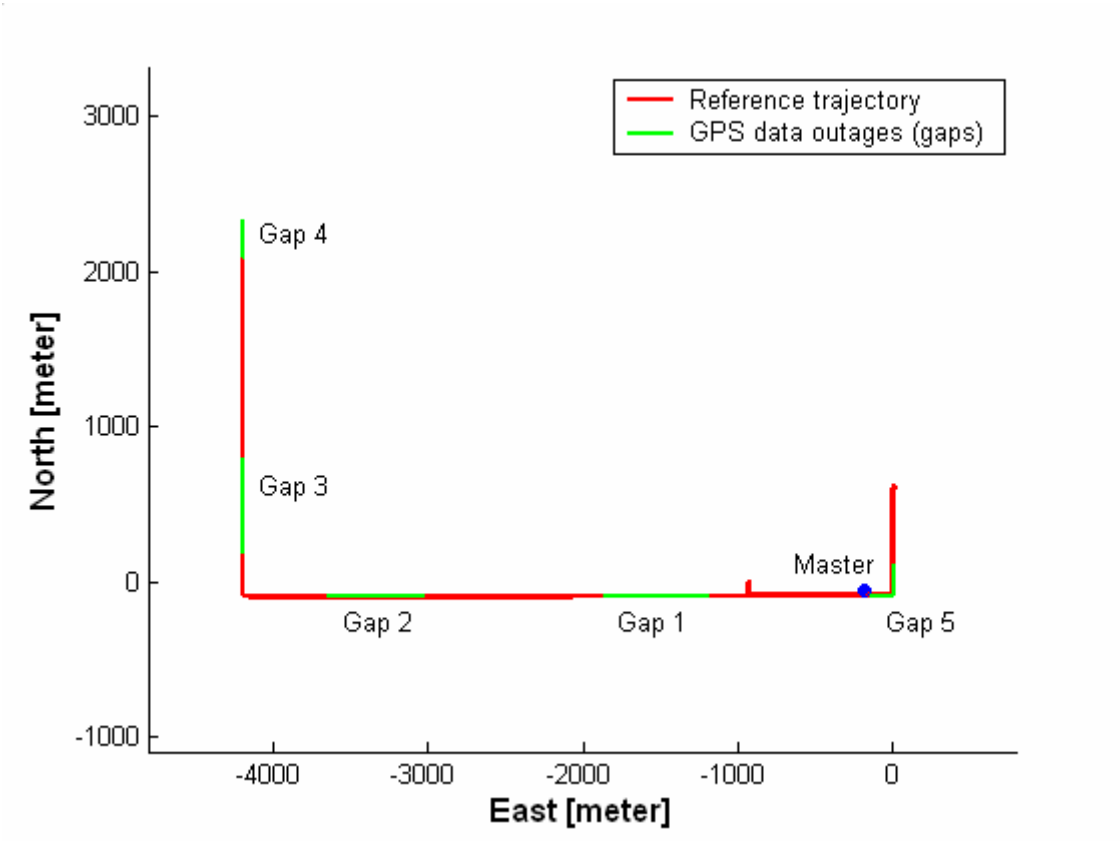

Figure 7.4: Satellite availability

The gaps shown in figure 7.4 are the full 40 seconds gaps. It can be seen that the location of the gaps also where chosen in order to get different baseline length from the master station as this could affect some of the common errors (see chapter 3.4).

Instead of only simulation gaps without any GPS coverage, two different levels of data gaps were used. The complete gap was the used in order to simulate e.g. tunnel situations where no form of GPS signal was available (only the INS solution was used), while the partial gap was used in order to simulate urban area situations. Here the elevation mask was raised to 50˚ in order to minimize the amount of

satellites so less than four were available. A stand alone GPS solution was therefore impossible. When so, the GPS measurements were useless unless the tight integration solution was used (remember from chapter 5.1.2 that it had a INS/GPS Kalman filter that could use any raw GPS measurements regardless of how few there were). The number of visible satellites during the partial gaps was therefore important during partial gaps.

7.4 Position accuracy

The position accuracy of the integrated INS and GPS solution, where calculated as the RMS error between the position of the reference trajectory and the position found during the outage. The RMS error was calculated across all five gaps in order to minimize the effect of large errors for a single gap and get a better estimate for the average accuracy. As the reference trajectory was assumed to be of centimeter precision (see chapter 7.2.2), the position error of the integrated solution was expected to be the main reason for the RMS error. Hence the RMS error was a good estimate of the performance of the integrated solution to centimeter level. Five different RMS errors were computed in the analysis. The east, north and up position error were single axis errors while the horizontal and 3D error were two and three axis errors respectively. All RMS errors are shown as function of time since outage was started.

7.4.1 Comparison between complete and partial data outage

The RMS error for complete and partial gaps using L1 carrier phase measurements and the tight integration can be seen in figure 7.5 and 7.6 (next page). As shown in figure 7.5 will the position accuracy degrade with the square of the time from the beginning of the complete outage. This was expected as the position error was the double integrated of the acceleration bias (see chapter 2.2.4). The RMS 3D error is about 1 m after the entire 40 seconds gap. As no GPS signals are available during complete gaps the error is only due to the use of the INS solution. From table 3.1 it was shown that the accuracy of the differential GPS code solution was a couple of meters. Hence use of the INS solution will result in almost the same level of accuracy after 40 seconds of complete gaps than for the differential GPS code solution. A clear effect can be seen between using complete and partial gaps. For partial gaps and during tight integration the error is a function of the quality of the remaining visible satellites. For all the gaps either two or three satellites were visible during the partial gaps.

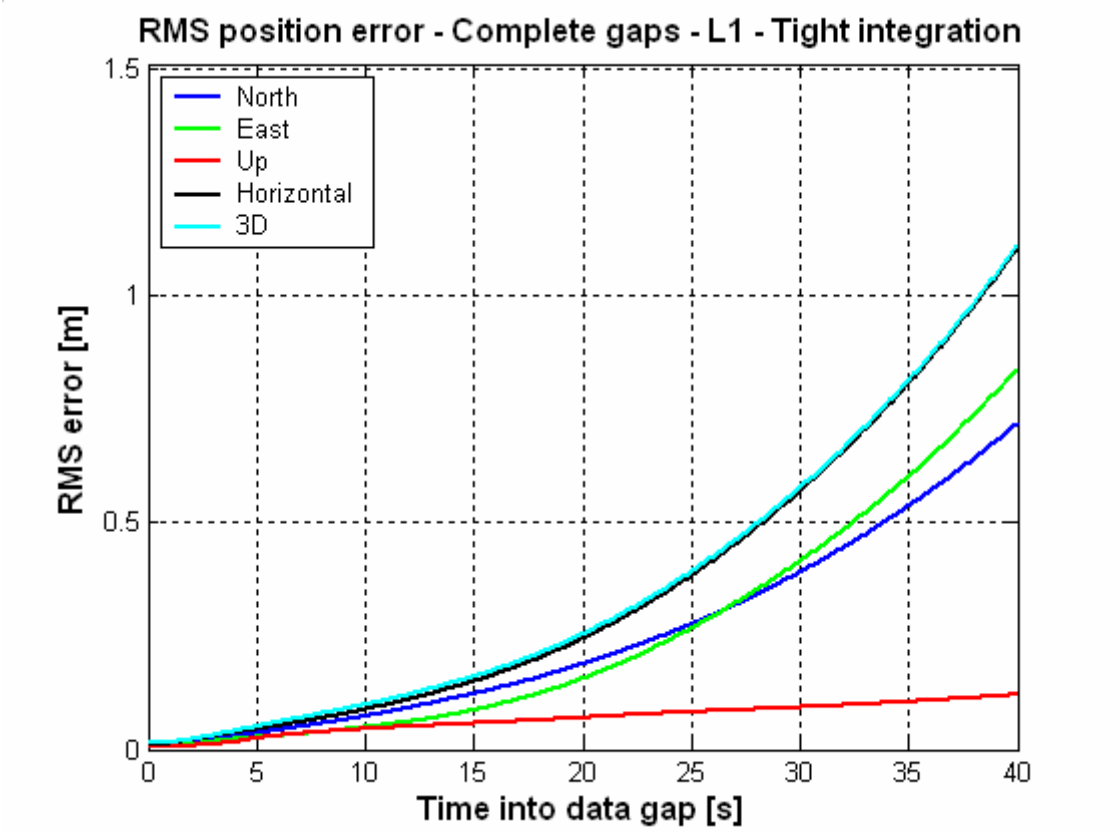

Figure 7.5: RMS position error during complete gaps and using L1 carrier phase measurement and tight integration

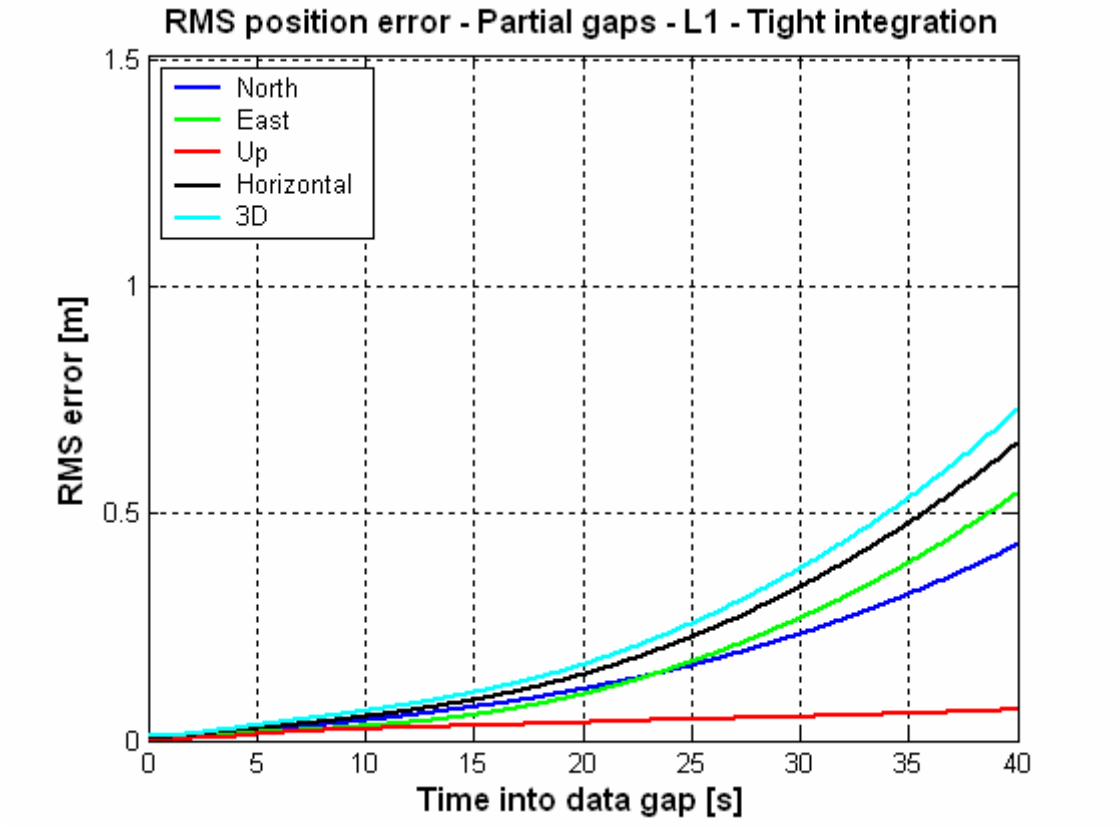

Figure 7.6: RMS position error during partial gaps and using L1 carrier phase measurement and tight integration

7.4.2 Comparison between loose and tight integration

In stead of comparing complete and partial gaps for L1 and tight integration the integration method is changed. Figure 7.7 show the RMS error for complete gaps using L1 carrier phase measurements and the loose integration method. It can be seen that there is there is no significant difference when figure 7.7 is compared to figure 7.5. This was expected too as there is little difference between the loose and tight integration when there is no GPS signal. The difference is instead seen for partial gaps where the tight integration is better than the loose due to the information from the remaining satellites. Even that two or three satellites is available during the gaps it is enough to get a better position accuracy. After 40 seconds of partial gaps the RMS position error is 0.75 m and 1 m for tight and loose integration respectively. During vehicle movements in e.g. urban areas where the line of sight to a number of satellites sometimes disappear (so less than four satellites are available) the tight integration therefore show better performance compared to the loose.

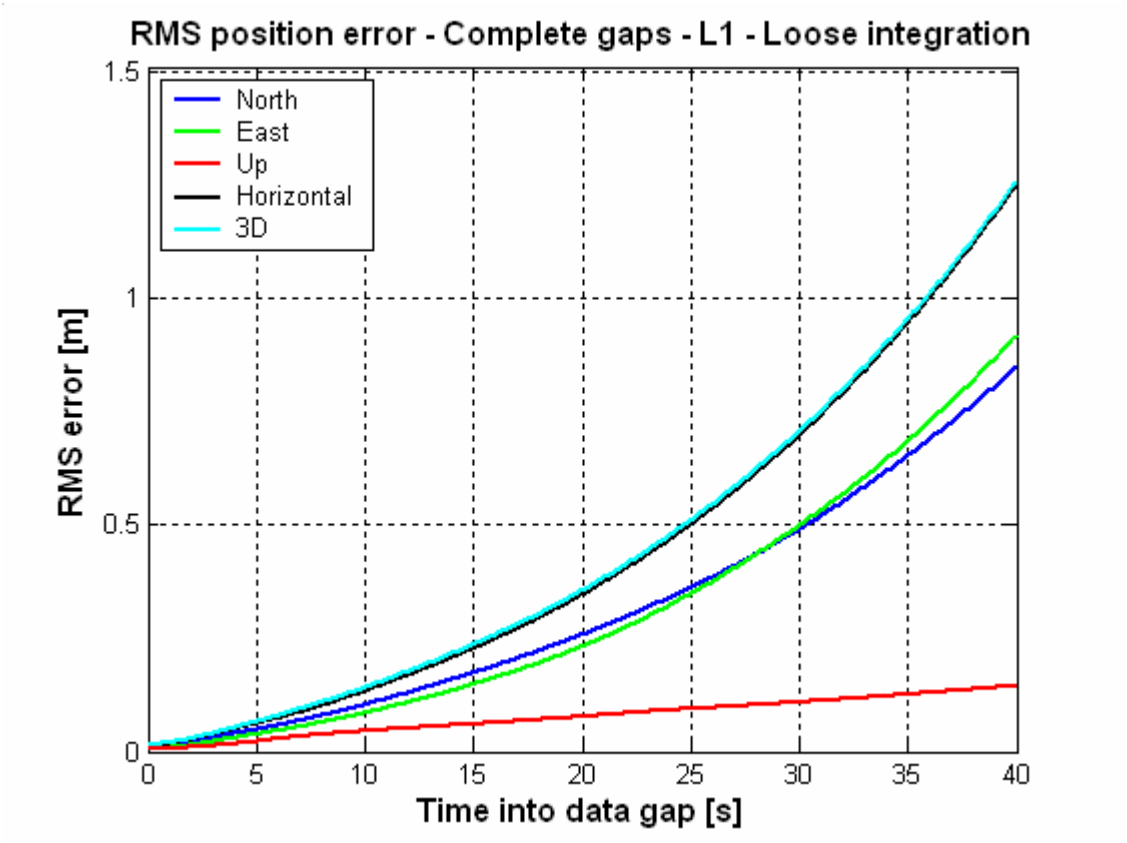

Figure 7.7: RMS position error during complete gaps and using L1 carrier phase measurement and loose integration

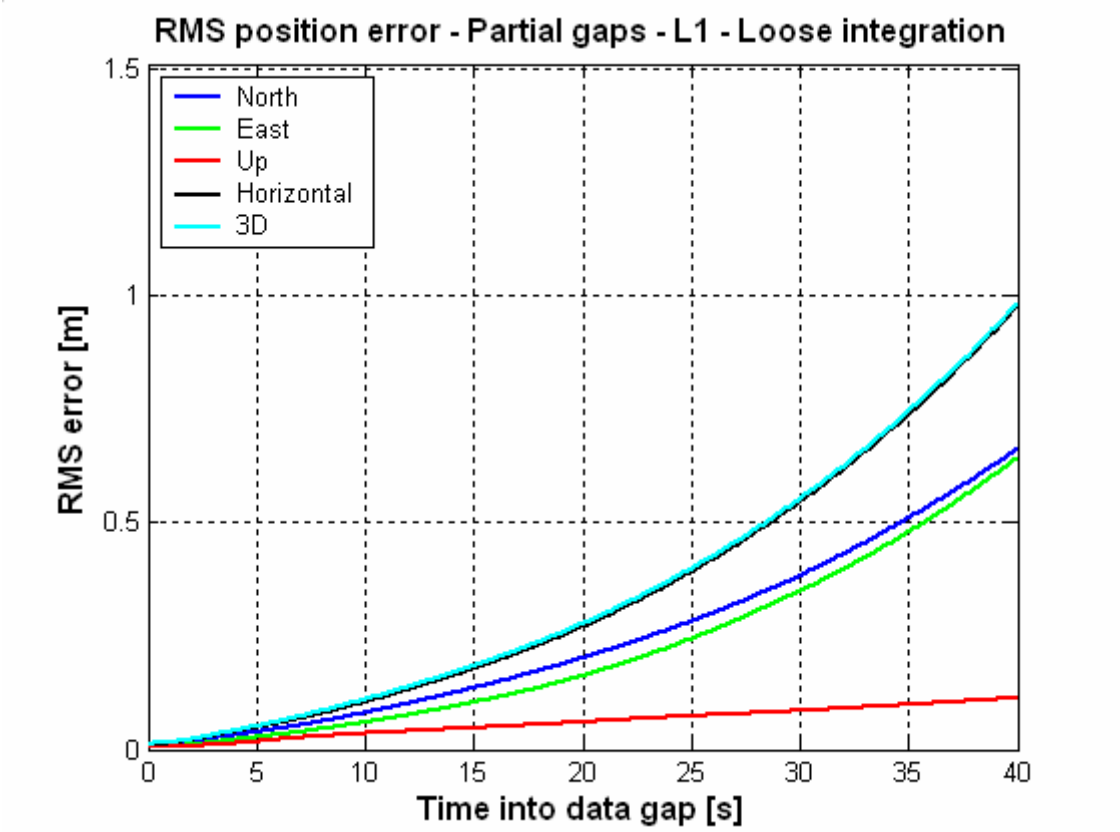

Figure 7.8: RMS position error during partial gaps and using L1 carrier phase measurement and loose integration

7.4.3 Comparison between L1 and WL phase measurements

Finally in the comparison of the position accuracy, using either the L1 carrier phase measurements or the Wide Lane (WL) (linear combination of L1 and L2 carrier phase measurements) are also analyzed. Figure 7.9 and 7.10 (next page) show the RMS position error during complete and partial gaps and using WL. They can be compared to figure 7.5 and 7.6. Due to longer wavelength of WL (0.89 m compared to 0.19 m for L1 (Petovello, 2003)) it was expected that the measurement noise would increase and that the accuracy of using WL was worse than using L1. This is especially true for partial gaps where the accuracy of the few GPS signals that were available played a crucial role. Using L1 instead of WL therefore show better performance for partial gaps.

Overall will the RMS position error be about 25 cm for gaps less than 20 seconds in most of the previous comparisons. For larger gaps there is a more clear difference. It has been shown that the tight integration show better performance than loose, and that use of L1 show better performance than WL. It is especially shown for partial gaps as the influence of just a few available GPS signals is clear.

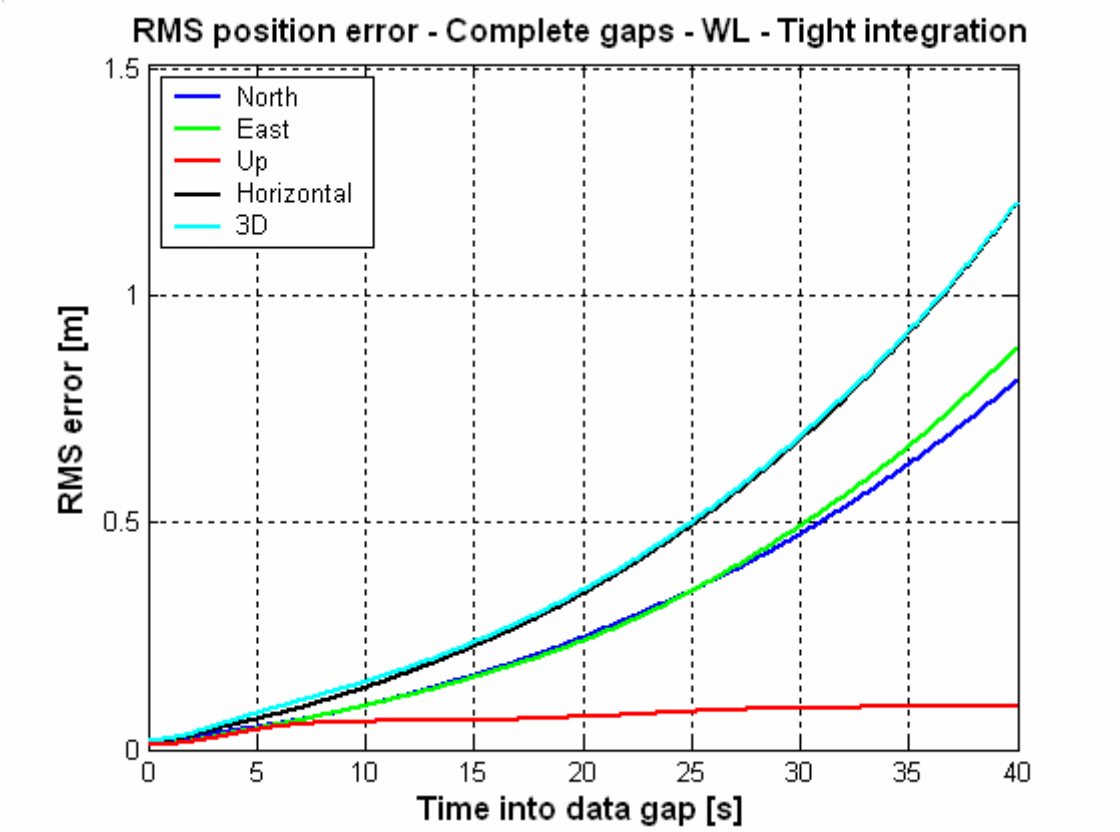

Figure 7.9: RMS position error during partial gaps and using WL carrier phase measurement and tight integration

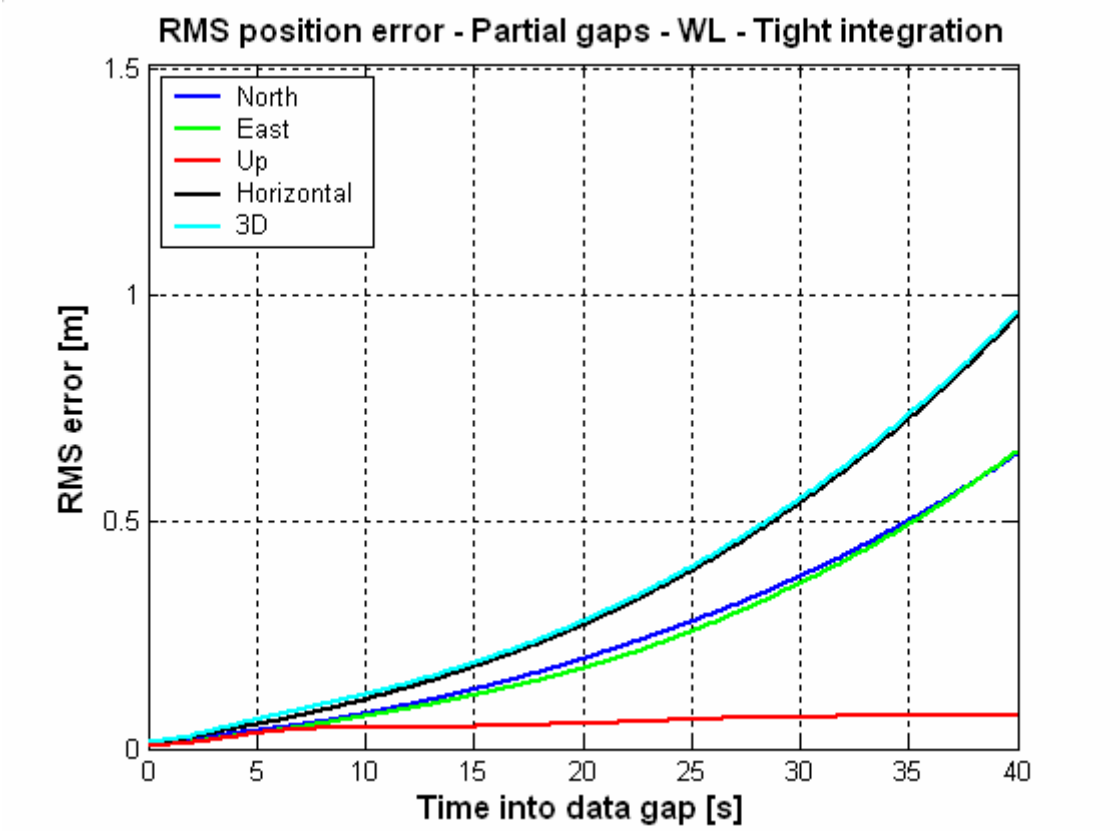

Figure 7.10: RMS position error during partial gaps and using WL carrier phase measurement and loose integration

7.5 Velocity accuracy

The same kind of comparisons that were done in the previous sections for the position accuracy can be done for the velocity accuracy. As seen in figure 7.11 and 7.12 (next page) will the velocity RMS error grow more linearly compared to the position RMS error. This is due to the fact that the error from the mechanization of the specific force only is integrated once compared to the position that is integrated twice. The RMS velocity error during complete gaps with use of L1 carrier phase measurements and tight integration are about 7 cm/s after 40 seconds and about 3.5 cm/s for partial gaps for the same duration. The north and east error looks a little bit strange in figure 7.11 as they cross each other about 13 seconds into the gaps. The reason has been impossible to find, but a guess could be strange behavior in one or more of the gaps due to special vehicle movements.

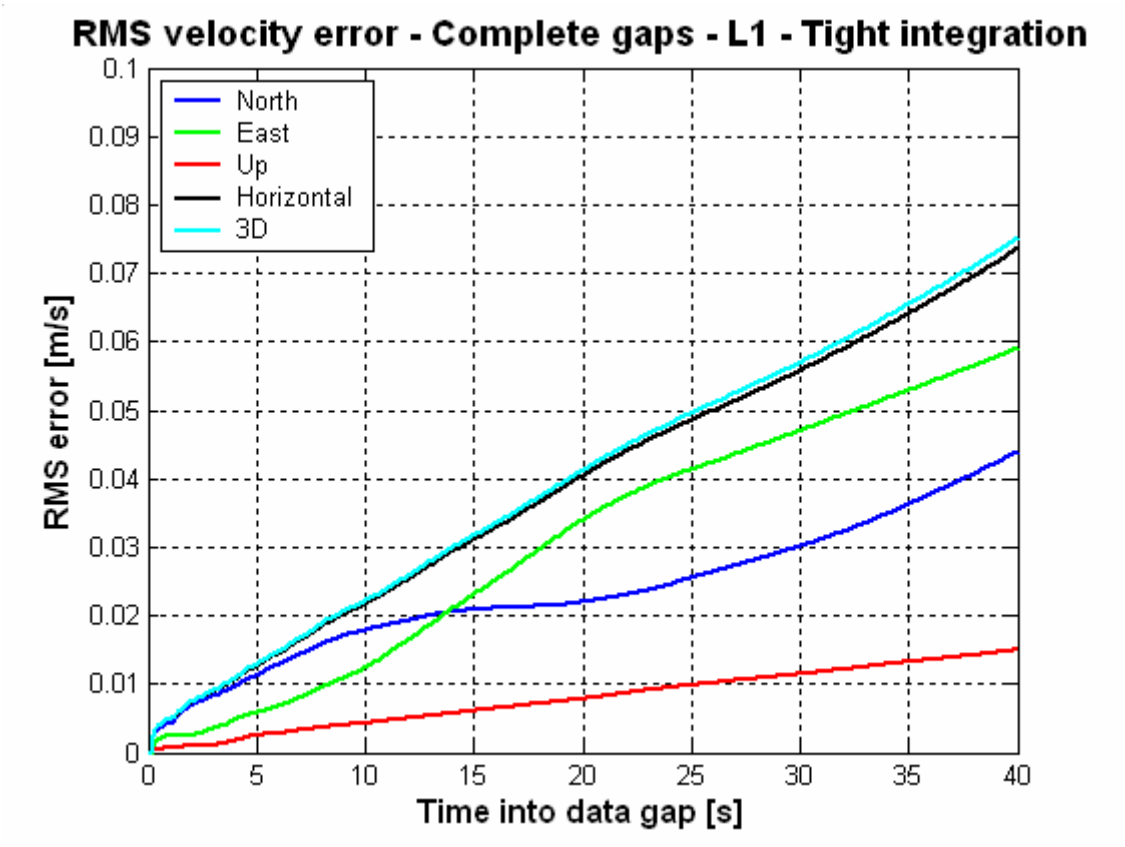

Figure 7.11: RMS velocity error during complete gaps and using L1 carrier phase measurement and tight integration

Figures of the velocity accuracy can be made for other combinations of phase measurements and integration strategy, but as they acted in a similar ways they are not further mentioned here.

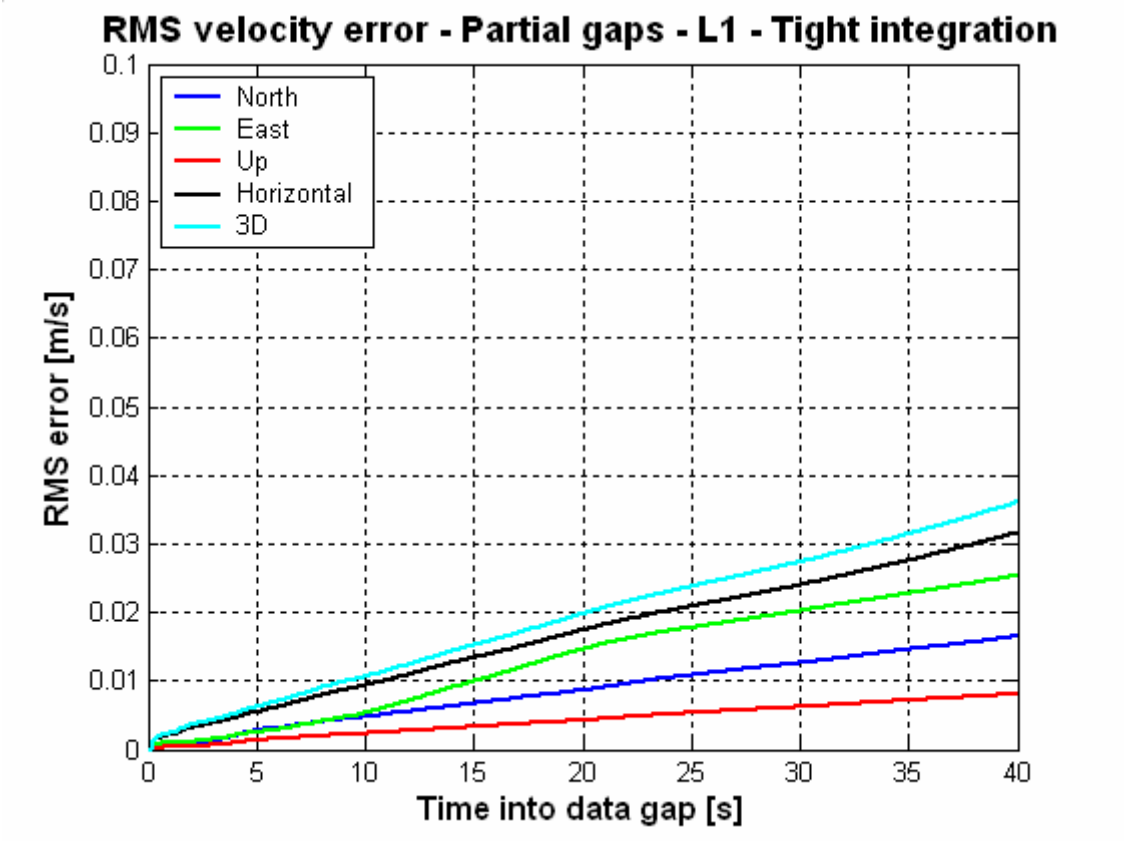

Figure 7.12: RMS velocity error during partial gaps and using L1 carrier phase measurement and tight integration

7.6 Attitude accuracy

Finally the attitude accuracy can be seen in figure 7.13 (next page). The attitude accuracy is split up in roll, pitch and azimuth RMS errors. As the test area mainly was flat, most of the angle rotation would occur as changes in azimuth. This can clearly be seen in figure 7.13 as the error in azimuth therefore becomes larger than similar ones from pitch and roll. For azimuth the RMS attitude error is growing up to around 0.03 degrees for complete gaps up to 40 seconds while it's only about 0.01 degrees for roll and pitch. If we compare these values with the specifications for the gyroscopes from table 2.1 (1 deg/hr which is similar to 0.01 degrees in 40 seconds) the performance is similar for the pitch and roll but worse for the azimuth.

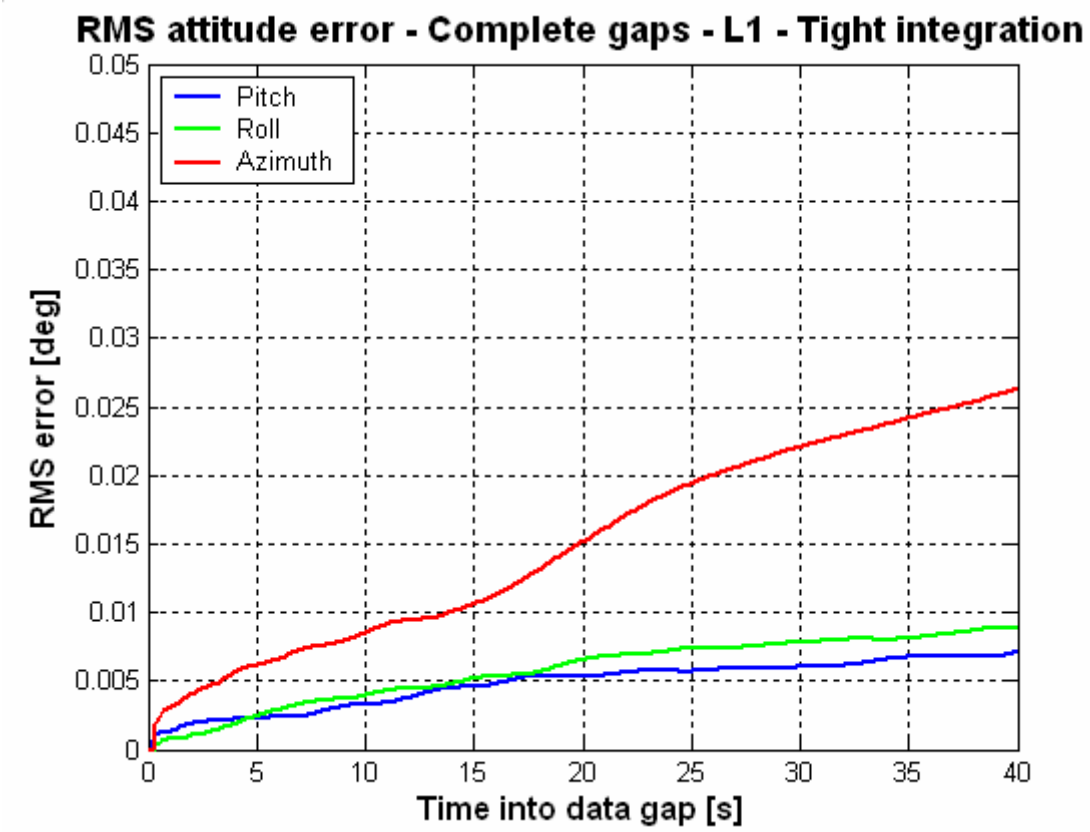

Figure 7.13: RMS attitude error during complete gaps and using L1 carrier phase measurement and tight integration

7.7 Time to fix ambiguity after outage

The previous part of the data analysis has mainly been analyzing the performance during either complete or partial gaps. Another important thing is the ability to recover after the gaps and determine correctly fixed ambiguities. This is important in order to get high accurate position updates from the GPS as the GPS solution provides most of the accuracy to the integrated INS and GPS solution (Petovello, 2003). Figure 7.14 (next page) shows the average time to fix the ambiguities after complete gaps with use of different integration methods. The loose integration with seeding refer to the use of the INS-derived position to help fix the ambiguity. It can be seen that for all gaps the INS can help fix the ambiguity faster than with only loose integration. The time can be reduced even more with use of tight integration. Figure 7.15 (next page) shows the time to fix the ambiguities as functions of the gaps duration (only gap 1). The biggest advantage of using tight integration or loose integration with seeding is seen for small gaps less than 10 seconds. No significant difference can be seen for larger gaps. Similar figures can be made for gap 2 to 5 but in general they show the same tendency as for gap 1.

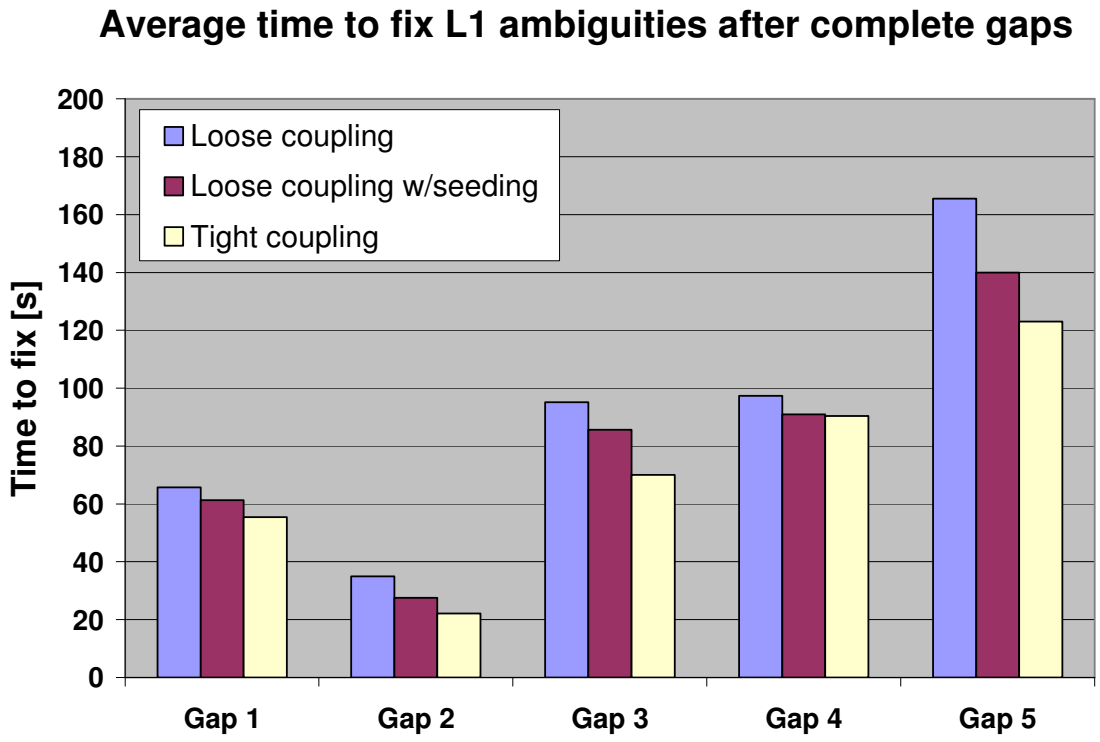

Figure 7.14: Average time to fix L1 ambiguities after complete data gap using different integration methods

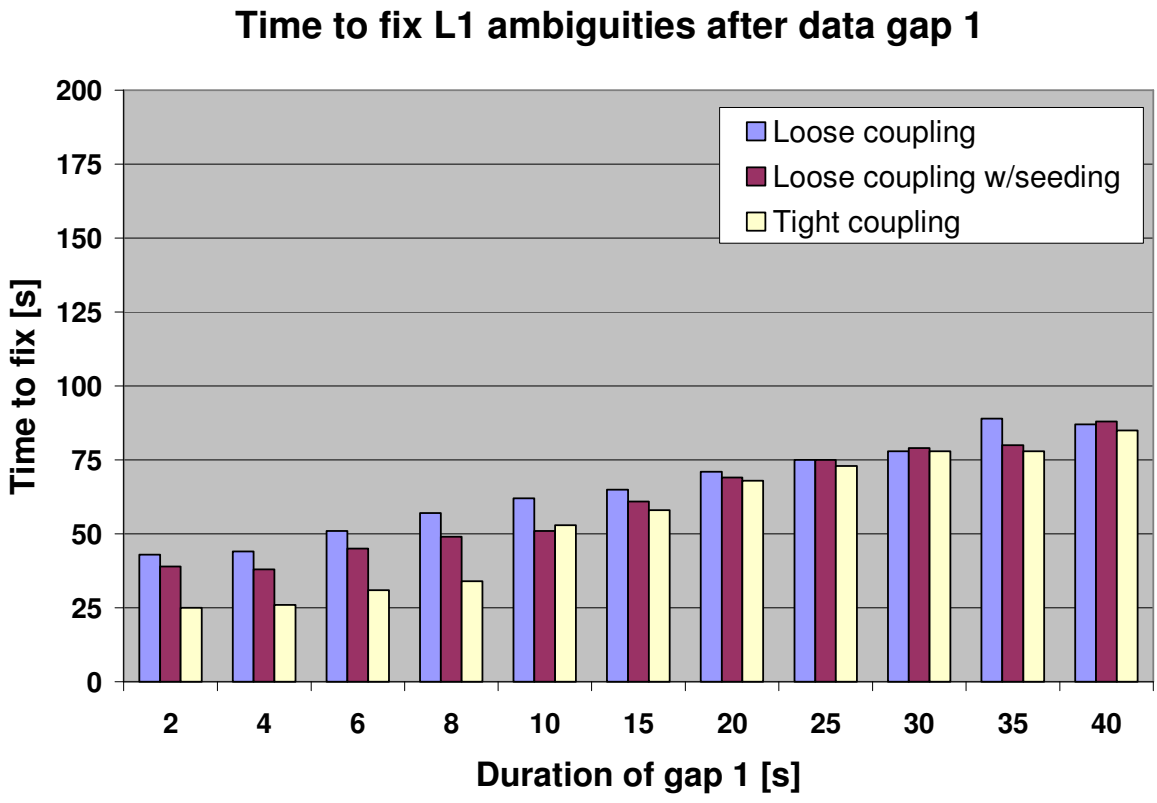

Figure 7.15: Average time to fix L1 ambiguities after complete data gap 1 using different integration methods

7.8 Accelerometer and gyroscope bias

The final part of the data analysis looks at the computed accelerometer and gyroscope bias from SAINT™. The biases were calculated for each epoch (every second) and were another sign for the performance of the integrated system. Table 7.5 shows the gyroscope bias as an average at different epochs for all five gaps. It can be seen that there is no significant difference between the calculated biases during the gaps. This is due to the relatively small gap period of only 40 seconds. In stead there is a larger difference between the bias at the beginning and the end of the dynamic mode. The changes in bias for the Z-gyroscope (the one that mainly show the azimuth rotation from turns as the area is relatively leveled) is up to 0.5 deg/hr for the entire dynamic period (about 30 minutes). It should be remembered that the specifications for the IMUs gyroscope bias were 1 deg/hr (see table 7.1). For most of epochs will the average bias therefore be under the specification level.

Average gyroscope bias [deg/hr]	**Without gap**		**With complete gap**			
	End of alignment	*End of dynamic mode*	*Before gap*	*20 sec. in gap*	*40 sec. in gap*	*End of dynamic mode*
X-gyroscope	0.116	0.255	0.320	0.320	0.317	0.255
Y-gyroscope	1.172	0.899	1.104	1.106	1.106	0.899
Z-gyroscope	0.065	0.595	0.533	0.548	0.550	0.596

Table 7.5: Average gyroscope bias with or without complete gap using L1 carrier phase measurements and tight integration

Similar average biases for the accelerometers can be calculated at different epochs as shown in table 7.6. The same tendency is seen as the only large changes in bias occur over long time and not within the 40 seconds gaps. Again the specifications for the IMUs accelerometer bias were 1000 µg and during no epoch this level was crossed.

Average accelerometer bias [µg]	**Without gap**		**With complete gap**			
	End of alignment	*End of dynamic mode*	*Before gap*	*20 sec. in gap*	*40 sec. in gap*	*End of dynamic mode*
X-accel.	347	593	565	565	565	593
Y-accel.	436	657	697	697	697	658
Z-accel.	796	705	759	759	759	705

Table 7.6: Average gyroscope bias with or without complete gap using L1 carrier phase measurements and tight integration

8 Conclusion

Different conclusions can be drawn upon this dissertation. In general it has shown the basic about INS and GPS together with different integration methods and estimation techniques. All the theory was necessary in order to develop a small software program that was able to perform an integration of the raw INS and GPS measurements.

MATLAB program

The MATLAB program turned out to have a couple of bugs which turned out to be impossible to find (at least in limited amount of time). This was not part of the original plan so a backup plan was needed. Instead the data were processed by a complete INS and GPS program that was used at a latter stage. The problem with the new program was that it required a key in order to work. This key was not available in Denmark so only the old processed data could be used in the data analysis.

Data analysis

The main objectives of the data analysis was to assess the integrated systems performance hereby determine the position and velocity accuracy during data outages and under different conditions. The simulated gaps showed that the stand alone INS performance was capable of providing sub meter level position accuracy for complete gaps lasting up to almost 40 seconds. (Petovello, 2003) showed only a maximum of about 20 seconds for the same IMU. During partial gaps the performance was generally improved by a factor 1.5-2. The analysis showed further that using tight integration instead of loose, the position accuracy could be improved especially for partial gaps. Finally the use of L1 compared to WL were investigated and it showed that due to more measurement noise on the WL, L1 was to prefer.

Hence use of the INS solution (for a tactical grade IMU) with tight integration and L1 phase measurements would result in almost the same level of accuracy after 40 seconds of complete gaps than for the differential GPS code solution.

For the velocity accuracy the same tendency were seen with better accuracy using tight instead of loose integration and using L1 instead of WL. For the attitude accuracy the azimuth error tended to be the largest (compared to roll and pitch) due to the vehicle movement and flatness of the test area.

The ability for the integrated system to resolve its ambiguities to fixed values after a data outage was investigated. It showed that the use of tight integration instead of loose reduced the time to fix ambiguities after gaps, but mainly for small gaps with duration under 10 seconds. The use of loose integration with seeding could also reduce the time compared to only loose integration, but not as much as the tight integration.

All in all is the main conclusion of this dissertation that the use of integrated INS and GPS can result in better accuracy and performance for navigation systems that operates in areas where the line of sight to the satellites sometime is blocked for shorter periods. Further investigations could therefore compare different types of IMUs in order to determine the level (grade) of which navigation system that can be used for different navigation applications.

9 References

All references used in this dissertation are shown below sorted alphabetically by the primary author's last name.

Britting, K.R. (1971)

"Inertial Navigation Systems Analysis", Wiley-Interscience, New York

Dueholm, K. and M. Laurentzius (2002)

"GPS", Ingeniøren Bøger, Denmark.

El-Sheimy, N. (2006)

"Inertial Techniques and INS/DGPS Integration", ENGO 623 Course Notes, Department of Geomatics Engineering, The University of Calgary, Canada.

Gelb, A. (1974)

"Applied Optimal Estimation", The Massachusetts Institute of Technology Press, USA.

Godha, S. (2006)

"Performance Evaluation of Low Cost MEMS-Based IMU Integrated With GPS for Land Vehicle Navigation Application", , MSc Thesis, Department of Geomatics Engineering, The University of Calgary, Canada, UCGE Report 20239.

Jekeli, C. (2000)

"Inertial Navigation Systems with Geodetic Applications", Walter de Gruyter, USA.

Julier, S.J. and J.K. Uhlmann (2004)

"Unscented Filtering and Non-Linear Estimation" Proc. of the IEEE, Vol. 92, No. 3, March 2004.

Lachapelle, G. (2005)

"Advanced GPS Theory And Applications", ENGO 625 Course Notes, Department of Geomatics Engineering, The University of Calgary, Canada.

Misra, P. and P. Enge (2001)

"Global Positioning System – Signal, Measurements and Performance", Ganga-Jamuna Press, USA.

Petovello, M.G. (2003)

"Real-Time Integration of a Tactical-Grade IMU and GPS for High-Accuracy Positioning and Navigation", Ph.D. Thesis, Department of Geomatics Engineering, The University of Calgary, Canada, UCGE Report 20173.

Shin, E.-H. (2001)

"Accuracy Improvement of Low Cost INS/GPS for Land Applications", MSc Thesis, Department of Geomatics Engineering, The University of Calgary, Canada, UCGE Report 20156.

Shin, E.-H. (2005)

"Estimation Techniques for Low-Cost Inertial Navigation", Ph.D. Thesis, Department of Geomatics Engineering, The University of Calgary, Canada, UCGE Report 20219.

Stenseng, L. (2002)

"Analyse af GPS og INS navigation i forbindelse med laserskanning", MSc Thesis, Geofysisk Afdeling, Københavns Universitet, Denmark

Titterton, D.H. and J.L. Weston (2004)

Strapdown Inertial Navigation Technology, 2nd Edition, IEE Radar, Sonar and Navigation series 17.

Tsui, J. B.-Y. (2005)

"Fundamentals of Global Positioning System Receivers", 2nd Edition. John Wiley & Sons, USA.

Wei, M. and K.P. Schwarz (1990)

"A Strapdown Inertial Algorithm Using An Earth-Fixed Cartesian Frame", Journal of The Institute of Navigation, Summer 1990, Vol. 37, No. 2.

Weston, J.L. and D.H. Titterton (2000)

"Modern inertial navigation technology and its application", Electronics & Communication Engineering Journal, April 2000.

Appendices

A Ambiguities for reference trajectory during alignment and dynamic mode